

*Ministry of Higher Education
And Scientific Research
University of Kerbala
College of Engineering
Mechanical Engineering Department*



***EXPERIMENTAL AND NUMERICAL
STUDY OF TWO-PHASE FLOW IN THE
RIBBED DIVERGENT \ CONVERGENT
RECTANGULAR DUCT***

*A Thesis
Submitted to the
Mechanical Engineering Department
at the University of Kerbala in a Partial Fulfillment of
the Requirements for the Degree of Master of Science in
Mechanical Engineering*

By

Ali Abdalaimma Hassan AL-Genaby

(B.Sc. University of Babylon 2004)

Supervisors

Assist. Prof. Dr. Abbas Sahi Shareef

Prof. Dr. Riyadh S. Saleh Al-Turaihi

2019 A.D.

1440 A.H.

بِسْمِ اللّٰهِ الرَّحْمٰنِ الرَّحِیْمِ

وَلَا تُدْرِكُهُ الْبَصَرُ وَلَا هِيَ تَدْرِكُهُ
وَلَا هِيَ كَالَّذِينَ تَدْرِكُونَ الْبَصَرَ وَرَبُّهَا
بِصَرٌ لَّا تُحِيطُ بِشَيْءٍ وَلَا هِيَ كَالَّذِينَ
يُقَدَّرُونَ

فِي رُبِّكَ نَزْمٌ مِّمَّا يَنْزَلُ الْأَنْجُمُ
لِلَّائِمَّةِ

صدق الله العظيم

سورة النجم آية ﴿39-41﴾

Linguistic Certification

I certify that this thesis entitled “**Experimental and Numerical Study of Two-Phase Flow in the Ribbed Divergent Rectangular Ducts**” that wrote by (Ali Abdalaimma Hassan AL-Genaby), has prepared under my linguistic supervision. Its language has amended to meet the style of the English language.

Signature: 

Name: Assist. Prof. Dr. Ahmed A. A. Al-Moadhen

Title: Linguistic Advisor

University of Kerbala – College of Engineering

Date: 18/11/2018

Supervisors Certification

We certify that this dissertation entitled " **Experimental and Numerical Study of Two-Phase Flow in The Ribbed Divergent \Convergent Rectangular Duct**" was prepared by (Ali Abdalaimma Hassan) and had been carried out completely under my supervision at the University of Kerbala, Mechanical Engineering Department in partial fulfillment of the requirements for the degree of Master Science in Mechanical Engineering.



Signature:

Assist. Prof. Dr. Abbas Sahi Shareef
Mechanical Engineering Department
University of Kerbala

Date: 7/2/2019



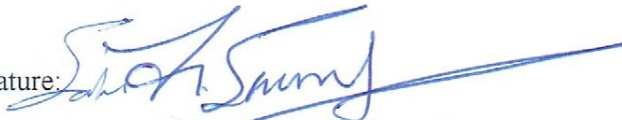
Signature:

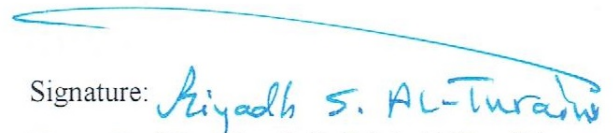
Prof. Dr. Riyadh S. Saleh Al-Turaihi
Mechanical Engineering Department
University of Babylon


Date: 12/2/2019

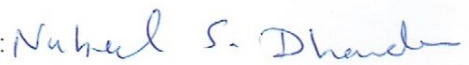
Examination Committee Certification


We certify that we have read the thesis entitled “**Experimental and Numerical Study of Two-Phase Flow in The Ribbed Divergent \Convergent Rectangular Duct**”, and as an examining committee, examined the student (**Ali Abdalaimma Hassan**), in it is content and in what is connected with it, and that in our opinion it meets the standard of a thesis for the degree of Master of Science in Mechanical Engineering.

Signature: 
Name: Assist. Prof.Dr. Abbas Sahi Shareef
Date: 7 / 2 / 2019
(Supervisor)

Signature: 
Name: Prof.Dr. Riyadh S. Saleh Al-Turaihi
Date: 10 / 2 / 2019
(Supervisor)


Signature: 
Name: Assist. Prof.Dr. Khaled A. AL-Farhany
Date: 7 / 2 / 2019
(Member)


Signature: 
Name: Dr. Nabeel S. Dhaidan
Date: 11 / 2 / 2019
(Member)

Signature: 
Name: Prof.Dr. Najim A. Jassim
Date: 10 / 2 / 2019
(Chairman)

Approval of Mechanical Engineering
Department

Approval of Deanery of the College of
Engineering / University of Kerbala

Signature: 
Name: Dr. Hazim Umran Alwan
(Head of Mechanical Engineering Dept.)
Date: 12 / 1 / 2019

Signature: 
Name: Assist. Prof. Dr. Laith Shakir Rasheed
(Acting Dean)
Date: 13 / 2 / 2019

Dedication

To the one walked with me step by step (my wife).

To the joy of my life (my baby Abbas).

To those who provide me constant support(my mother and my sisters).

To those who gave me help, courage, and strength(my friends).

ALI 2019

Acknowledgments

Full achievement of any project cannot be achieved without thanking those who made it possible. First and foremost I thank Allah for where I am and for giving me the strength to keep going.

I would like to express my deep thanks and sincere gratitude to my supervisors **Assist. Prof. Dr. Abbas Sahi Shareef** and **Assist. Prof. Dr. Riyadh S. Saleh Al-Turaihi** for their assistance, guidance, encouragement and endless help throughout the steps of this work.

I am grateful to **Mr. Hussein H. Rashid** of mechanical engineering laboratories at Babylon University for the help he gave me during the experimental work.

I sincerely thank all the staff of the Mechanical Engineering Department of the University of Kerbela and Babylon for their support and teaching.

My sincere thanks also go to **Miss. Sarah Hasan Oleiwi** at the University of Babylon who helpfully answered to all my questions, especially with regard to the ANSYS program.

I am also thankful to all who helped me directly or indirectly to complete this work.

Abstract

Two-phase flow in the ribbed divergent\convergent rectangular duct for two cases: upward vertical and inclined was studied in this thesis. There are two working fluids used in this instigation, water and air. Experimental and numerical studies were performed to test the influence of increased air and water discharges on the pressure distribution and differential pressure through the divergent\convergent section. Also, the effect of increasing the divergent/ convergent angle on the pressure difference across the divergent/convergent section was studied. All sets of the experimental data in this study are obtained by using a pressure transducer and visualized by a video camera. Water inlet discharges used were between (5-20 L/min), and air discharges were between (5.833-16.666 L/min). Two testing channels with divergent\convergent angles (10 and 15 degrees) were used. The results indicated that the pressure along the testing channel raised as water and air discharge increased. For the divergent section, it was observed that; as the divergence opening angle increased, the pressure recovery decreased. While in the case of the convergence section, the pressure drop increased when the convergence angle increased. Computational fluid dynamics for a three-dimensional model was simulated with ANSYS FLUENT 18 depending on the operating condition obtained experimentally and governed by equations of volume of fluid (VOF) for Eulerian multiphase flow model and turbulence RNG model. A numerical study was conducted to study the effect of ribs on the flow behavior and pressure recovery. In the case of ribs absence, it was noted that; the value of the recovery of the pressure across the divergence section was higher than the case of ribs presence by (8.333%). An agreement was observed between the experimental and numerical values of pressure with a maximum deviation

rate of (9 %). also, a similarity was observed in the flow behavior between experimental and numerical work.

Table of Contents

<u>Subject</u>	<u>Page</u>
Abstract	I
Table of contents	III
Nomenclature	VII
Chapter One-Introduction	1-7
1.1. Overview	1
1.2. Flow patterns	2
1.2.1. Flow patterns in vertical systems	3
1.2.2. Flow patterns in inclined systems	4
1.3. Flow patterns map	4
1.4. Pressure drop	5
1.5. Void fraction and liquid hold up	6
1.6. Objectives of this work	6
1.7. Publications and submitted papers	7
Chapter Two - Literature review	8-17
2.1. Vertical flow	8
2.2. Inclined flow	10
2.3. Horizontal flow	11
2.4. The Scope of this work	16
Chapter Three – The experimental work	18-31
3.1. The setup components of the two-phase flow experiment.....	20
3.1.1. The water tank	20
3.1.2. The water centrifugal pump	20
3.1.3. The water flow meter	20
3.1.4. Air compressor	22
3.1.5. Air flow meter	22
3.1.6. Testing section	23

3.1.7. Pressure sensors	24
3.1.8. Pressure interface	26
3.2. Cases of study of experimental work	27
3.3. Phases used in the experimental work	29
3.3.1. Continuous phase	29
3.3.2. Dispersed phase	29
3.4. Experimental procedure	29
3.5. Design considerations	30
3.6. The error analysis	31
Chapter Four–Numerical Analysis	32-43
4.1. Basic models of two-phase flow	32
4.2. The physical parameters	33
4.2.1. The velocity	33
4.2.2. Mass flux	34
4.2.3. Reynolds number	35
4.3. The geometry model	35
4.3.1. The geometry	35
4.3.2. The mesh	37
4.4. The boundary conditions	39
4.4.1. Inlet boundary condition	39
4.4.2. Wall boundary condition	39
4.4.3. Outlet boundary condition	39
4.5. Problem assumptions	40
4.6. Properties of the two-phase flow	40
4.7. Simulation model	40
4.8. Governing equations	40
4.9. The turbulence model	41
4.10. The simulation steps	43
4.11. The convergent criteria	43

Chapter Five – Results and Discussions	44-97
5.1. Program validation	44
5.2. Two Phase Flow through divergent section of the vertical and inclined position	46
5.2.1. Experimental results	46
5.2.1.A. Influence of water and air discharges on the pressure profile	46
5.2.1.B. Effect of water and air discharges and opening angle on the recovery pressure	52
5.2.2. The numerical results	55
5.2.2.A. Pressure contour	55
5.2.2.B. Velocity vector	60
5.2.3. Comparison between experimental and numerical results ..	62
5.2.3.A. Effect of water and air discharge on pressure profile	62
5.2.3.B. The influence of water and air discharge on the flow behavior	65
5.2.4. Visualization and flow patterns maps	71
5.3. Two- phase flow through convergent section for vertical and inclined position	75
5.3.1. Experimental results	75
5.3.1.A. Effect of water and air discharges on pressure Profile	75
5.3.1.B. Effect of water and air discharges and convergence angle on the drop pressure	80
5.3.2. Numerical Results	83
5.3.2.A. The pressure contour.....	83
5.3.2.B. The velocity vector	88
5.3.3. Comparison between experimental and numerical results	89

5.3.3.A. Effect of water and air discharge on pressure	
Profile	89
5.3.3.B. Influence of water and air discharge on the flow	
behavior	92
5.4. Numerical study of effect the ribs the pressure recovery	96
Chapter Six – Conclusions and Recommendations	133-134
6.1. Conclusions	98
6.2. Suggestions for future works	98
References	100- 103
Appendix A	1-A- 2-A
Appendix B	1-B - 2-B

Nomenclature

Latin Symbols		
Symbol	Description	Units
A	Cross-sectional area	m ²
D _h	Channel hydraulic diameter	m
D	Diameter of air pipe	m
g	Acceleration of gravity; Standard values = 9.80665	m/s ²
P	Pressure	N/m ²
S	Source term	
Q	Volume flow rate	m ³ /s
Re	Reynolds number	dimensionless
U	velocity	m/s
v	Velocity field	m/s
p	Wetted perimeter of the channel	m
w	Width of channel	m
h	Height of channel	m
G	Mass flux	Kg/m ² s
F	Body force	N

Greek Symbols		
Symbol	Description	Units
ΔP	Pressure drop	Pa
μ	Dynamic viscosity	kg/m. s
ϵ	Turbulent dissipation rate	m ² /s ³
α	Volume fraction	dimensionless
ρ	Mass density	kg/m ³
κ	Turbulent kinetic energy	m ² /s ²

Symbol	Description
in	inlet
q	Phase
m	Mixture
n	Number of the Phases
X , y	Variables Coordinate

Abbreviations	
Abbreviation	Description
ANSYS	Analysis of System
CFD	Computational Fluid Dynamics
CFX	Computational Fluid Xerography
RNG	Re-Normalization Group
SST	Shear Stress Transport Model
VOF	Volume of Fluid

CHAPTER ONE

INTRODUCTION

CHAPTER ONE

INTRODUCTION

Introduction

1.1. Overview

Two-phase flow is defined as two-phase different flow simultaneously in the same place like gas and liquid, gas and solid, two dissimilar liquids or liquid and solid. The most complex of these types is the flow of gas -liquids due to the compressibility and deformation of both phases. Two-phase flow can often be used in chemical or mechanical engineering applications, oil wells, power generation, reactors, boilers, condensers, evaporators and combustion systems [1]. The existence of geometrical singularities in channels such as divergence, convergence and bends may greatly impact the behavior of two-phase flow and thus the resulting pressure can be dropped.

Therefore, it is an important subject of studying in the applications that relate to safety valves. The studies of the two-phase flow in straight pipe existing in the literature are numerous. In contrast, the study of two-phase flow in the divergence, convergence, bends and other types of singularities are rather sparse. The purpose of studying these geometries is to find how these geometrical accidents influence the two-phase flow patterns and pressure distribution. Especially, the comprehension of the flow in these singularities can lead to a better design of safety systems[2]. Two-phase flow can be classified by Naji[3] as:

- According to the phase matter:
 1. Two-phase, one-component. (e.g. water-steam flow)
 2. Two-phase, two-components. (e.g. water-gas flow)
- According to the external wall state:
 1. Adiabatic flow (e.g. generally gas- liquids flow)
 2. Heating flow (e.g. pipes in the boiler)

3. Cooling flow (e.g. pipes in the condenser)

- According to the inclination of the pipe which carries the flow:
 1. Horizontal flow.
 2. Vertical flow. (Upwardly or downwardly).
 3. Inclined flow. (Upwardly or downwardly).

Two-phase, two components (air-water), adiabatic and vertical and inclined upward flow are the cases under consideration in the present study.

The manufactured ducts or pipes with ribs are widely used. The ribs in channels contribute to increase the mass and heat transfer and produce flow circulation which leads to increase turbulence [4]. In the present work, the ribs are used to create strong turbulence intensity inside the divergence section by breaking the laminar-sub layer leading to rapid mixing between the phases.

The employ of numerical simulation has increased in recent years. Numerical predications of the behavior of two-phase flow become more necessary. The development of computational codes for the simulation of two-phase flows relies heavily on the physical understanding of the two-phase flow phenomena, such as phase distribution, interfacial structure development, bubble interactions, two-phase flow turbulence, boiling and condensation, etc. To gain insight into these phenomena and to further enhance the capabilities of numerical simulation, accurate information and a clear about the flow should be provided [5].

1.2. Flow Patterns

When liquid and gas flow simultaneously in a pipe, spatial arrangement of liquid and gas occur due to difference in fluid properties (density and viscosity), pipe orientation and other forces acting in the two-phase flow. This spatial or geometric reorganization of the liquid and gas phase in the pipe is termed flow pattern [6]. Guess of flow patterns is a

central problem in two-phase flow in pipes. Design parameters such as pressure drop and mass, momentum and heat transfer are strongly dependent on the flow pattern. Hence, in order to accomplish a reliable design of gas-liquid systems such as pipe lines, boilers and condensers, an a priori knowledge of the flow pattern is needed [7]. In the present work, upward vertical and inclined flows were studied. Therefore, the flow patterns of these types of flows will be mentioned.

1.2.1. Flow Patterns in Vertical Systems

At low gas discharges, the gas phase begins to rise through the continuous liquid such as small and separate bubbles, and this flow is known as bubble flow. Whenever the gas discharge increases, the smaller bubbles tend to coalesce and form bigger bubbles. At suitably high gas discharges, the agglomerated bubbles become big sufficient to occupy nearly the complete pipe cross section. This type of bubbles is called Taylor bubbles. Liquid slug separates between these bubbles, which usually contain smaller gas bubbles, and this type of flow pattern is called slug flow. With continuing to increase gas discharge, the shear stress between the liquid film and Taylor bubble increases, then producing a collapse of the liquid film and the bubbles. This leads to making a churning motion for the fluids. Therefore, this flow is called a churn flow. The very high gas discharge causes the entire gas phase to flow through the core of the channel. Some liquid phase is entrained in the gas central as droplets, while the remainder of the liquid flows between the tube wall and the gas core. This type of flow is called annular flow as show in Figure 1.1.

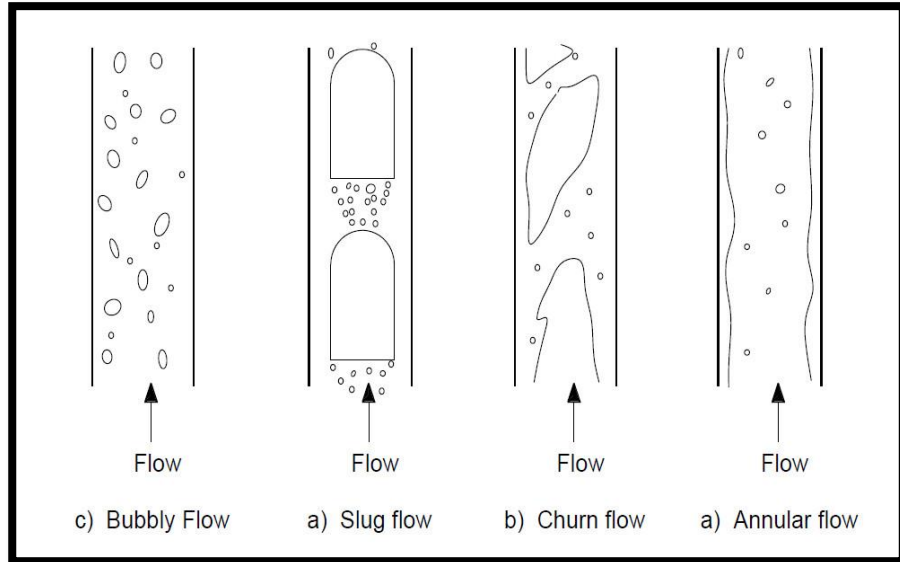


Figure 1.1: Flow patterns in the vertical upward flow.

1.2.2. Flow Patterns in Inclined Systems

Flow patterns noted in upward inclined systems are extremely like to those noted in vertical upward flow, particularly for near-vertical systems. It involves bubbly, slug, churn and annular. As shown in Figure 1.2.

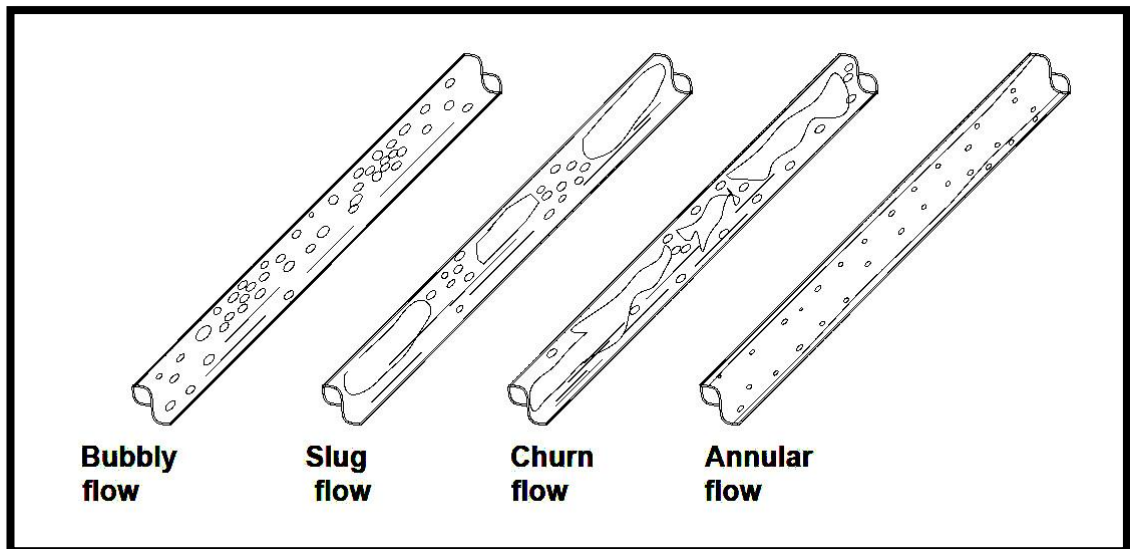


Figure 1.2: Flow patterns in inclined pipes.

1.3. Flow Patterns Map

To predict which of the flow pattern exist in available flow conditions in the flow pattern series, many investigations draw maps to locate that by depending on the flow conditions. These maps of flow patterns are described by using a chart that has many lines to separate the

consequent flow pattern. Otherwise, maps are described by a set of equations called "Flow pattern Transitions". The difference between various maps is due to their specification, some for a single inclination angle, while the other is for the whole range of inclination angles. Hewitt and Roberts flow maps [8] is used for vertical upward two-phase flow as shown in Figure 1.3.

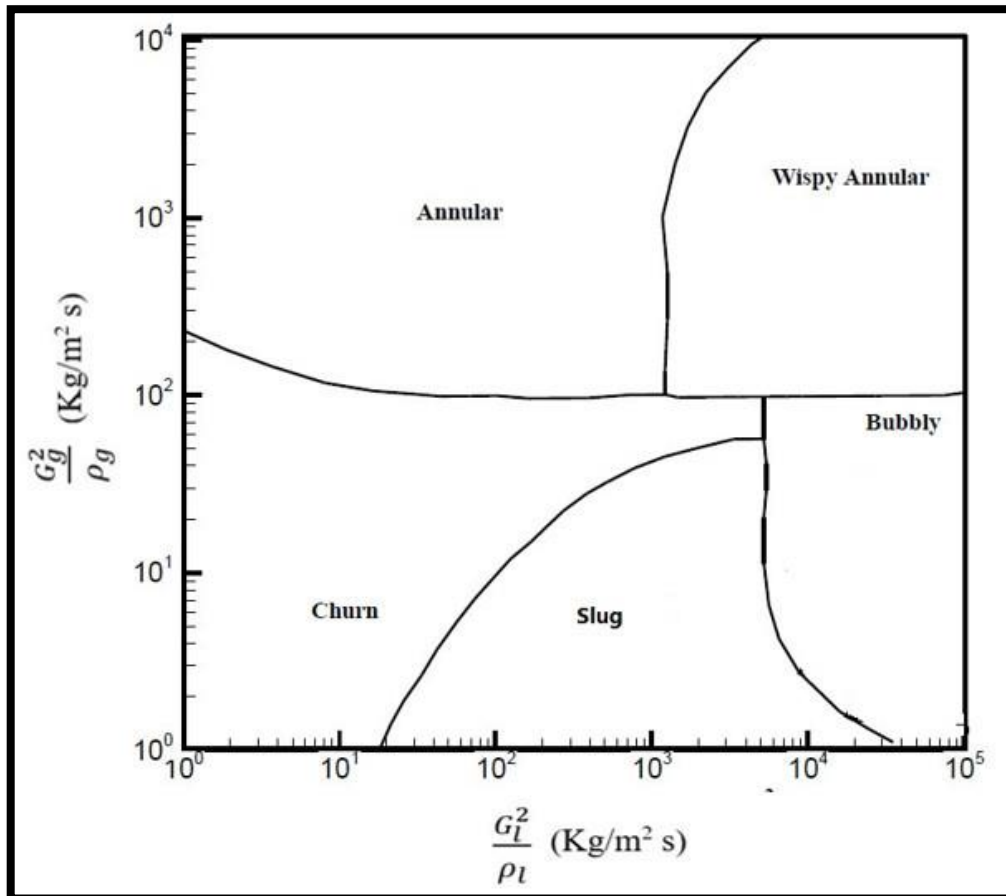


Figure 1.3: Hewitt and Roberts flow maps[8]

1.4. Pressure Drop

The pressure drop in the system is a main variable to determine the pumping capacity of a given flow. For that reason, the pumping ability should be suitably compatible with the system requests. Therefore, it is significant to identify as accurately as possible the value of pressure drop. A significant part of this pressure drop happens along vertical channels, and it becomes mainly significant when the pipes are lengthy as detailed by

Perez [9]. The pressure drop happens because of many factors including gravitational, frictional and acceleration drops. Pressure drop that results from friction is considered more problematic and expressed as a function of the friction factor.

1.5. Void Fraction and Liquid Hold Up

One of the main problems encountered in any study of two-phase (gas-liquid) flow is the void fraction. It means the volumetric ratio of the channel section occupied by the gas to the volume of the channel section. Generally, void fraction is expressed by a fraction various between zero and unity. Thome [10] concluded that it is the key physical value for determining numerous other important parameters, such as the density and viscosity of two-phase, finding the relative average velocity, the primary significance for guessing flow patterns transitions, pressure drop, and heat transfer. On the other hand, the volumetric ratio of the pipe section which occupied by the liquid phase to the pipe section is usually known as the liquid hold up.

1.6. The Objectives of This Work

The main objective of this work is to investigate an experimentally and numerically the impact of water, air discharge and the opening angle on the pressure profile and recovery pressure across ribbed divergence section. It have been done for two cases; vertical and inclined duct. Also, This study presented the effect of water, air discharge and convergence angle on the pressure profile and drop pressure across ribbed convergence section. The experimental results extended by numerical results which are obtained from the ANSYS program.

1.7. Publications and Submitted Papers

The following is a list of the author's publications and submitted articles relating to the present thesis.

Conference Publications

R. S. Al-turaihi, A. S. Shareef, and A. Abdalaimma, "A Numerical study of Two-Phase flow through a Rectangular Duct with a Convergence Ribs," vol. 8, pp. 610–619, 2019.

Submitted Articles

A. S. Shareef, R. S. Al-turaihi and A. Abdalaimma, "Experimental and Numerical Study of Two Phase Flow (Air-Water) in Ribs Divergent Rectangular Duct". 2009

CHAPTER TWO

LITERATURE REVIEW

Literature Review

The aim of this chapter is to highlight the previous experimental and numerical investigations, about the two-phase flow; especially the flow of type of gas-liquid will be introduced. Many researchers studied the flow behavior and pressure drop through smooth and ribbed channel. The previous studies in this chapter were classified according to flow orientation: vertical, inclined and horizontal flow.

2.1. Vertical Flow

Xu[11] investigated experimentally an adiabatic co-current two-phase flow of water and air in vertical rectangular conduits. A testing section was used with dimensions of 12 mm in width, 260 mm in length, and different gaps of 0.3, 0.6 and 1 mm. A video camera was used to observe flow patterns. They found that, the flow pattern in the conduits with the gaps of 1.0 and 0.6 mm was correspondent to those achieved in conduits with medium dimensions. It can be classified into bubbly, slug, churn and annular flow. While the conduit with the gap of 0.3 mm, the flow configurations were different from the typical flow configurations in conduits with medium dimensions and in the conduits with the gaps of 0.6 and 1 mm. The bubbly flow was never been detected even at very low gas flow velocity.

Noora[12] studied experimentally the two-phase flow (water-air) through the vertical pipe. The experimental study was aimed to investigate the flow patterns by using a camera and measuring the pressure at five locations by using pressure sensors. The experimental results showed that; for bubble and slug flow, pressure gradient, and pressure drop were proportional with the superficial velocity of water and inversely with the superficial velocity of air. The annular flow, pressure gradient and pressure drop are directly proportional with the superficial velocity of air and water. The experimental results were compared with several theoretical correlations

and could be observed that the correlation of Lockhart and Martinelli[13] was the closest to the results of the pressure drop for the bubble flow. While Steinhagen and Heck[14] correlation gave a good prediction of the results of slug and annular flow.

The two-phase flow in a vertical diverging pipe section for a progressive and sudden enlargement have been investigated by Anupriya and Jayanti[15]. The divergent angles for progressive enlargement were used with (8 and 15) degrees. The area ratios were (1.5 and 2.0) with a range of water and air flows rate used so that the annular flow was prevails in the upstream section. Their study showed that the pressure recovery was strong at downstream of the expansion in all cases. Recovery pressure was significantly delayed if air flow rates are much lower than those required to form an annular flow.

Brankovic and Currie[16] made one of the first attempted to numerically simulate a dilute bubbly flow through an area expansion. An Eulerian description for liquid flow and a Lagrangian formulation for the gas bubble movements have been utilizing. For the experimental study, a Laser Doppler Anemometry was used to measure the bubble and liquid velocity. The results showed that the agreement of mean velocity was excellent between experimental and numerical results of downstream. However, the agreement was not good near the entrance of the separation area. As the predicted void fraction profiles were found to be exceedingly flat relative to the data.

Koichi and Kenji[17] studied the vertical gas-liquid flow in a round tube with an axisymmetric sudden expansion. Bubble deformation and slug break up were reported due to a strong shear layer generated just above the expansion. Another interesting observation was a noticeable pick in void

fraction distribution near pipe walls downstream of the expansion for various operational conditions.

For bubbly flows with high void fractions, Behzadi et al.[18] modified the standard Eulerian approach in two-phase flow to account for inter-phase forces in dense gas-liquid mixtures. They also proposed a modified version of k- ϵ turbulence model which was able to predict gas bubbles interaction with the liquid eddies more efficiently and they successfully simulated the bubbly flow through a sudden expansion.

Sakr et al.[19] extended the work of Behzadi et al.[18] by considering various turbulence models. It was concluded that SST (k- ω) turbulence model produces the most accurate results for the two-phase flow across sudden expansions.

Ahmadpour et al.[20] simulated two-phase flows (air-water) in a smooth gradual divergence with three different area of ratio (0.43, 0.5, and 0.65) and five different of opening angle (5, 15, 30, 45, and 90). A turbulence model k- ϵ was employed. The influence of Reynolds number, volumetric fraction and divergent angle on pressure profile was studied. This study showed that; by increasing the Reynolds number and volumetric fraction, the liquid increases the recovery of pressure. While the recovery pressure decreased by increasing the area ratio and the opening angle. Secondary recirculating flow with high turbulent intensity was observed for high divergent angles of the expansion due to flow separation.

2.2. Inclined Flow

Abed and Al-Turaihi[21] studied experimentally the flow pattern and pressure drop of gas-liquid flow in inclined pipe. The diameter of test section is 50 mm, and overall length of 4 m. The inclination angle of the test section is 30°. Air and water are used as working fluids. A video

camera recording and pressure transducer sensor with interface are used to study flow regimes and pressure drop through test section. The flow regime and pressure fluctuating across pipe depending on superficial liquid and gas velocities. Also, it noted that the pressure decreases with distance along pipe when gas superficial velocity increased and also increased liquid superficial velocity.

Naji[22] developed explicit correlations to predict the liquid holdup of two-phase flow in the inclined pipe. The comparison was conducted with several previous studies. The comparison showed that there correlation was semi-correspondence with correlation by Taitel-Dukler[23] model. It displayed that the suggested correlation had best performance than the others due to its adoption of the effect of the inclination. In addition, it showed that the amount of the liquid holdup in horizontal flow was higher than the amount of the liquid in inclined flow because of the inclination effects.

Kumer[24] performed numerical simulation for water-oil two-phase stratified flow in the horizontal and inclined pipes by using the volume of fraction (VOF) approach and RNG $k-\epsilon$ turbulence model. The angle of inclination was ranged from $\pm 50^\circ$, 0° , to $\pm 10^\circ$ from the horizontal. The selected models have successfully predicted the flow pattern, local phase fraction, slip ratio, pressure drop, turbulent kinetic energy and turbulent energy dissipation rate.

2.3. Horizontal Flow

Aloui and Souhar[25] investigated experimentally bubble flow in a horizontal rectangular sudden enlargement. The cross-section of upstream and downstream of the enlargement was 55 x 44 mm and 5 x 100 mm, respectively. The void fraction and the pressure of downstream of the enlargement for a semi-symmetric bubble flow were studied. The results

showed that when volumetric qualities were low, the bubble flow became asymmetrical. However, when the void fractions were about 10%, the bubble flow became practically symmetrical. Moreover, it was observed that the highest void fraction was in the recirculation region. The local void fraction reduced gradually when one moves farther from the singularity along the axis of the enlargement in the main flow.

For sudden area restrictions in small channels, the corresponding pressure drop values, the two-phase flow pattern, and the accurate empirical correlations were reported by Abdelall et al. and Chen et al.[26] The testing was carried out with deionized water and air. The smaller and larger inner diameters tubes were (0.84) and (1.6) mm, respectively. The two-phase flow pressure changes caused by enlargement were significantly lesser than the predictions of the homogeneous flow model and showed a significant velocity slip at the vicinity of the flow area change. The closest acceptability obtained between experimental and theoretical results was found at the assumption of the slip ratio of $S = (Q_L/Q_G)^{1/3}$.

Mugradich[27] studied experimentally the effect of mixing ratio between the gas and the liquid in two-phase flow in a horizontal tube with and without rotating disk which made the flow eddying. The water was used as a liquid phase and the air as the gas phase. The tube was made of glass to observe flow patterns. The results showed that different flow patterns could be obtained by changing the mixing ratio. It also showed the increase in the pressure drop by (40%-60%) in case of using the rotating disk.

Chen et al.[28] examined the evolution of two-phase flow pattern with the mixture quality downstream of a sudden expansion in a small channel. The inlet tube is a round tube with 3 mm diameter while the expansion is of rectangular shape having aspect ratios of 3x6 or 3x9 mm. A new liquid-jet flow pattern was observed for low values of the quality, which reduces the

pressure difference across the area expansion. This work was complemented by Wang et al.[29] who presented a comprehensive evaluation of available pressure correlations for the aforementioned two-phase flow.

Ahmed et al.[30] based on a series of experiment on oil-air flow through horizontal sudden expansions, developed a general formulation for pressure recovery across the sudden expansion accounting for wall shear stress, the losses in recirculation zone and void fraction (flow pattern) changes. It was observed that this formula improved the prediction of the pressure recovery because this formula took into account all the relevant parameters. Also, it gave a good prediction for the flow pattern map of Taitel and Dukler[23] .

Ahmed et al.[31] extended their previous work by providing detail measurements on local characteristic of the two-phase flow. Particularly, it was concluded that the liquid turbulence intensity is higher in the immediate vicinity of the sudden expansion and reduces with axial distance. Also, the results showed that, as the flow approached sudden enlarged, the void fraction increased. The reason for the sudden increases in a void fraction at the enlargement section was due to the separation of gas in the recirculation region.

Rogero[5] performed an experimental investigation for intermittent flows in horizontal tubes in order to attain a thorough physical understanding of the internal structure of two-phase flow regimes. The differences between the slug and the plug flow were explained and the effect of a slug void fraction on the flow characteristics and the behavior of the dispersed bubbles in the slug body were examined.

Gas-liquid flows through smooth expansions (a divergent section with a constant slop) were studied thoroughly by Kourakos et al.[2] In addition to presenting axial pressure profiles for various area ratios, the effect of

volumetric void fraction on the pressure changes across the singularity was quantified. A modified correlation was provided for pressure difference.

Takashi et al.[32] studied the influence of a sudden enlargement on the flow pattern of two-phase flow (air-water) in rectangular millimeter-scale channel. Four different heights (0.19, 0.5, 1 and 2) mm were used for different expansion ratio (5, 2.5, 1.67 and 1.25) for every height. The superficial velocities of water were between (10 to 80) cm/s and superficial velocities of air were between (5 to 80) cm/s. The flow regimes were classified generally into the following four types:

- (1) The flow regime was not affected by a sudden enlargement. Bubbly, slug, annular flows were involved in this type. This type often occurs in small expansion ratios.
- (2) The recycling area appeared immediately after the sudden enlargement. The recirculation zone was observed at high expansion ratios for ($h = 2.00$, 1.00 and 0.50) mm at high expansion ratios.
- (3) The configuration of the air cavity after the sudden enlargement and a water jet enter through it. This type occurred in a low water flow rate, high air discharge, and high expansion ratio.
- (4) A split occurs for each bubble toward sideways direction immediately after the sudden enlargement. This type was observed in the small channel height at ($h = 0.19$) mm.

Ansari and Arzandi[4] studied experimentally the flow map of air-water two-phase flow using ribbed and smooth horizontal rectangular channels to illustrate the influence of ribs height on the regime boundaries. There were three ribs with heights (1, 2, and 4) mm were used; the rib pitch and width were (50) mm and (10) mm respectively. The ribs were located in the channel at three different locations: in the lowest wall, the upper wall, and

both in the lowest and upper wall. They found that; the position of the ribs in the channel did not influence the type of the flow regimes, but the regime boundaries were shifted to the lower gas velocities due to the presence of the ribs. It was concluded that the effect of the ribs when positioned on both the lowest and upper wall was clearer than in other cases. As well as, it was observed that by increasing the rib height, the hydrodynamical started to be instable at lower fluid velocities.

Eskin and Deniz[33] investigated experimentally the pressure drop for two-phase flow in adiabatic horizontal channel with smooth divergence. The smaller and larger tube diameters were (40) mm and (50) mm respectively. Flow rates of air were (30, 50 and 60) L/min while the flow rate of air was constant at (3) L/s. Measurements of the pressure were carried out at four regions: injector, upstream, expansion section and downstream pipes. In order to obtain a two-phase flow, the injector was used to inject the air into the water. Two injectors with different distribution holes were used: an in-line injector and a circular injector. Their study showed that when the in-line injector was used, the pressure recovery caused by expansion was higher.

For bubbly flow pattern, the numerical simulation of a two-phase turbulent flow through sudden expansions/contraction was carried out by Roul et al.[34]. They relied on the two-phase Eulerian-Eulerian scheme with the $k-\varepsilon$ model of turbulence. It was shown that the calculated value of pressure changes across sudden expansion/contraction by the numerical method was in a near perfect agreement with experimentally measured data. Moreover, it was concluded that; the use of the mixture model instead of the homogenous model (which neglects the velocity slip at the gas-liquid interface) is a necessity to acquire an admissible numerical simulation of the multiphase flow.

Abadie et al.[35] investigated the effect of fluid properties and operating conditions on the generation of gas–liquid Taylor flow in micro channels. The results showed that, when the flow rate ratio of liquid and gas increases, the length of the slug and bubble increases. A numerical study of the hydrodynamic properties of the two-phase flow in the channel and small tubes was also carried out. As the results of numerical simulations were found to be in relatively good agreement with the experiments despite their 2D nature.

Deniz and Eskin[36] studied numerically the two-phase flow in the adiabatic horizontal pipe with smooth divergence. The commercial software, FLUENT was used for modeling the system. The numerical results were validated and compared with the experimental results, which were previously obtained. In their study, the coalescence between the bubbles was neglected and the diameter of the bubbles was assumed to be constant. For numerical simulation of the two-phase flow, RSM turbulence model was selected because this model gave results closer to the experimental results. This study showed that a numerical simulation provided well agreement with the experimental results. Also, it showed that experimental and numerical profiles for local void fraction downstream and upstream the expansion were similar and could approach each other when the flow progress.

2.4. The Scope of This Work

After reviewing the previous researches, it was noticed that there is no comprehensive study of the effect of the ribs in the two-phase flow. Therefore, the present work is aimed to study the effect of adding ribs in the divergence\contraction section and study the behavior of the flow. In this work, two-phase flow in ribbed divergent\convergent rectangular ducts has been studied by using air and water as working fluid. The experimental

testing channel was photographed to show the flow behavior. The pressure was measured from the testing channel experimental rig by using four pressure sensors at four different points along the testing channel. The values were compared with the pressure values of a CFD model that was modeled with the experimental boundary conditions.

The Experimental Work

This chapter will explain a detailed description of the experimental system that used to study the two-phase flow in the ribs divergent/convergent duct. It is configured in the fluid laboratory of the Mechanical Engineering Department in the College of Engineering at Babylon University. A schematic diagram of the system is shown in Figure (3.1). There is a rigid frame to support the testing pipe and prevent vibration and can be noticed in figure (3.2). All experiments were carried out at conditions of the ambient laboratory, i.e., the temperature range was (19-23) C° and the pressure was (1) bar.

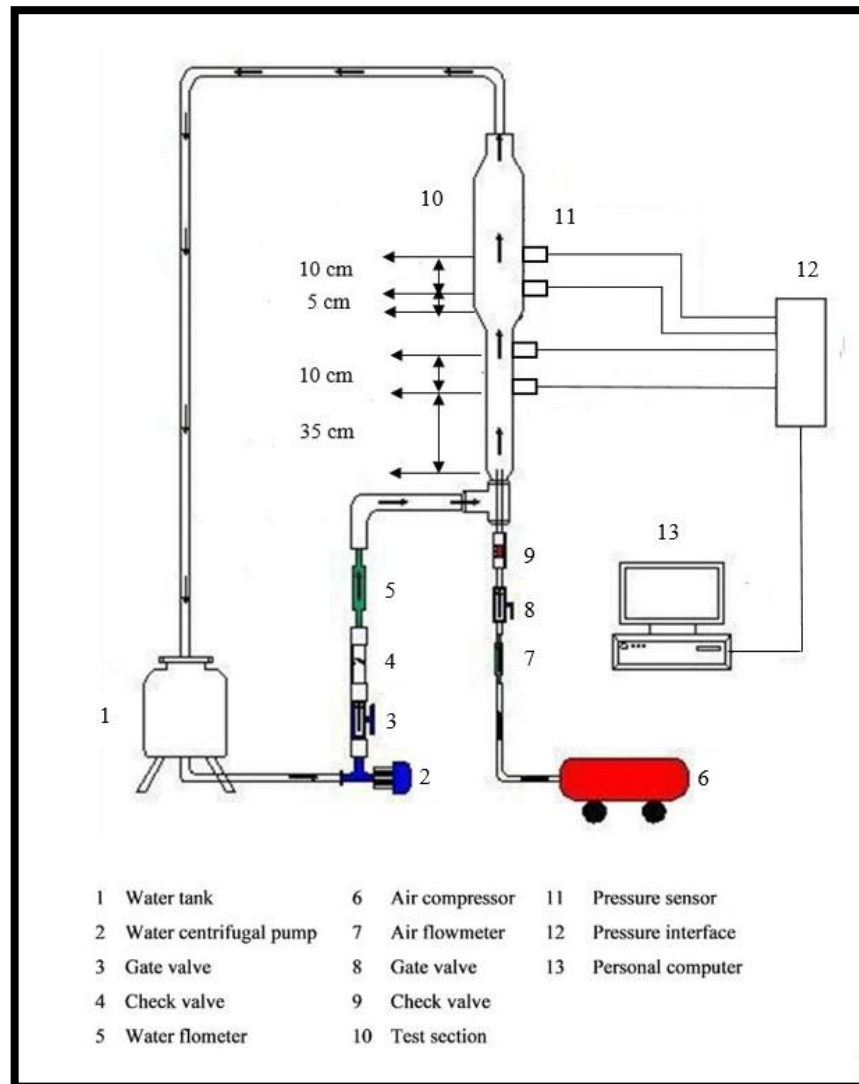


Figure (3.1): Schematic of the Experimental system

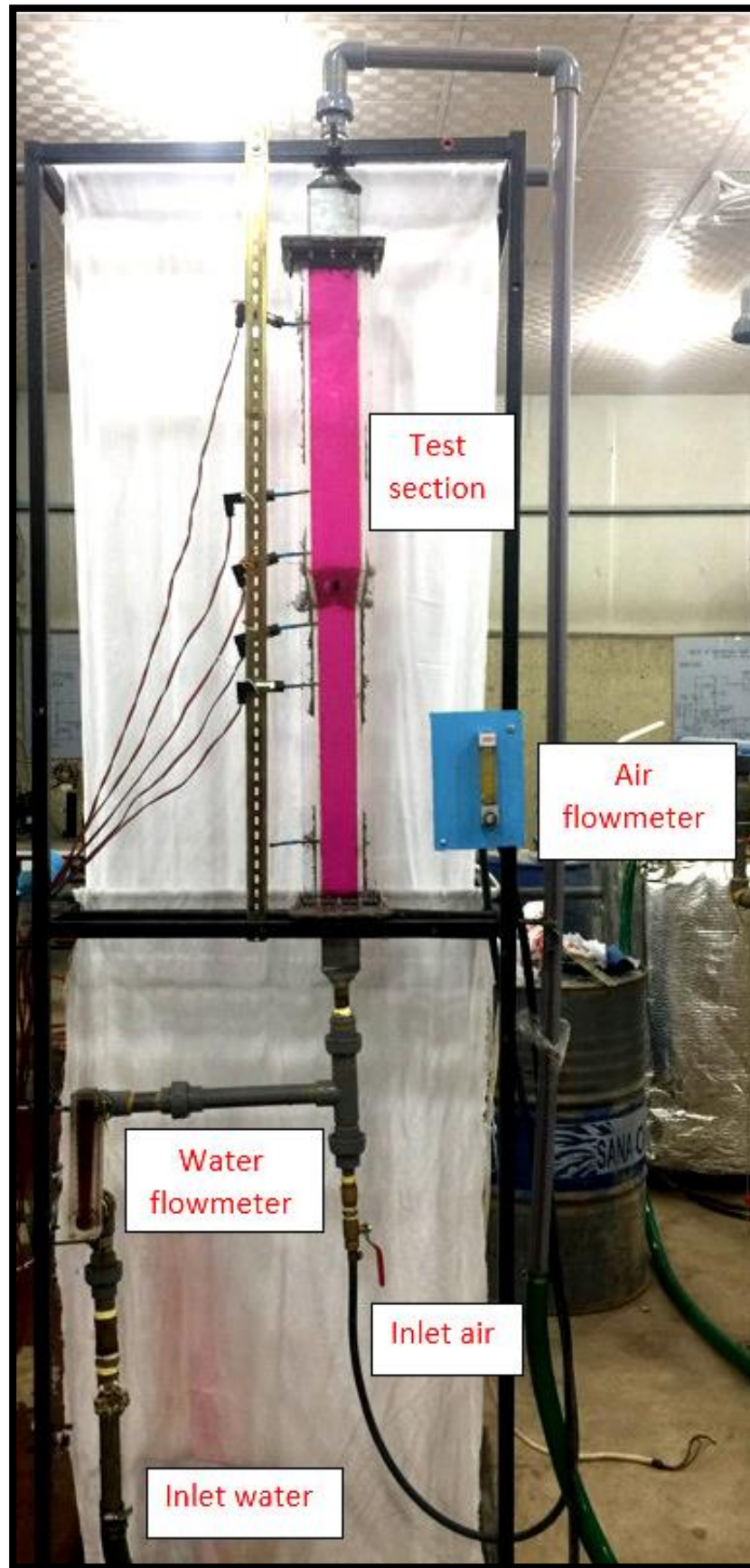


Figure (3.2): Experimental Rig for the two-phase flow

3.1. The Setup Components of the Two-Phase Flow Experiment

The experimental rig, which was utilized to do the experimental tests of the two-phase flow in a divergence/convergence rectangular channel, comprised of the following parts:

- 1-Water tank
- 2-Water centrifugal pump
- 3-Water flow meter
- 4-Air compressor
- 5-Air flow meter
- 6-Testing section
- 7-Pressure sensors
- 8-Interface device
- 9-Personal computer
- 10-Normal video camera

These parts will be explained in the next subsections.

3.1.1. The Water Tank

The water reservoir has a capacity of (500) liters, with dimensions of (1 m x 1 m x 0.5 m). It is made of stainless steel metal and covered with a rock wool to keep the temperature of the water. Potassium Permanganate is added to water tank in order to the water is coloured, to appear the air bubble more clearly.

3.1.2. The Water Centrifugal Pump

A centrifugal pump is used to pump water into the test channel. It has a maximum discharge of (480 L/min), (1.5 kW) power, voltage of (220 volt), a maximum head of (5 m) and 1410 rpm.

3.1.3 The Water Flow meter

A flow meter is used to control and measure the water quantity by liters/minute (L/min) that entered into the testing section. It has values of

flow rate range from (5) to (35) L/min. Figure (3.3) shows the water flow meter.

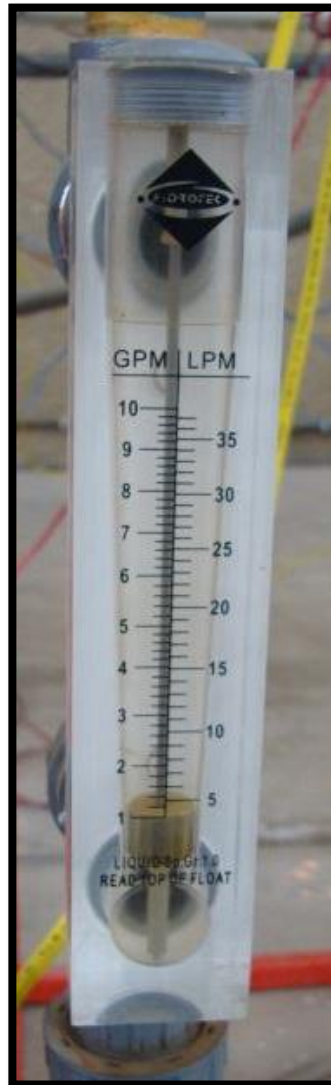


Figure (3.3): The Water Flow Meter

The water flow meter was calibrated by using a scalar container filled with the water coming out from the testing pipe at a specific flow rate. The time of the water to reach a specific point on the container was recorded. This process was repeated for five times and the values are represented in a curve with the flow meter values as shown in figure (3.4).

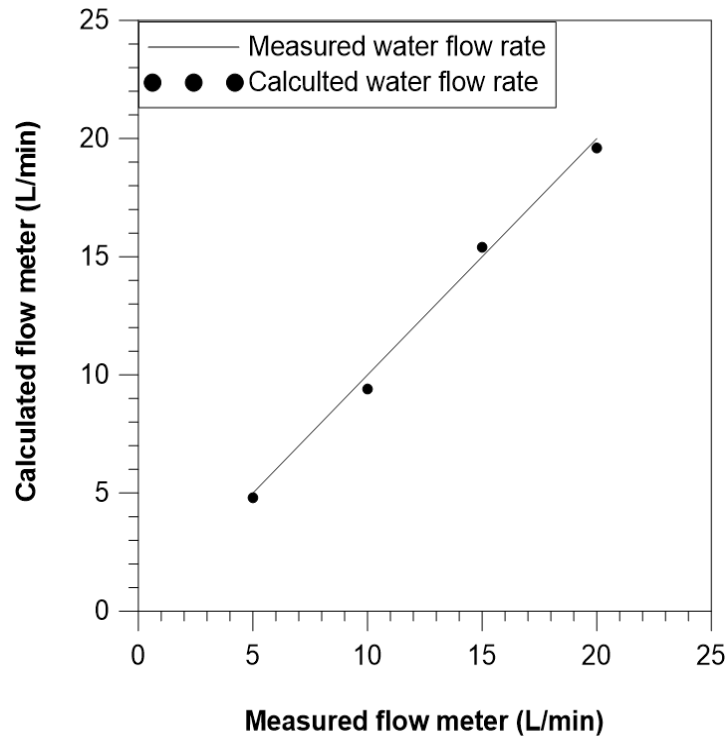


Figure (3.4): Calibration of the Water Flow Meter

3.1.4 Air Compressor

The air compressor is used to raise the air pressure, which is used as a gas in two-phase flow. It was designed by Ingersoll-Rand company type (WELDED AIR RECEIVER –BS 5169 IIIE). This compressor is the type of a positive displacement machine. It contains crankshaft that moves the piston for supplying gases at high pressure with a connecting rod.

3.1.5 Air Flow Meter

The air flow meter has a flow rate range from (350) to (3500) l/hour as shown in figure (3.5). It is utilized to govern the discharge of air that enters the testing channel. A flow meter consists of a tube, which is made of a pure material with a float that is exerted by a drag force of the flow and gravity. The air flow meter has been calibrated as shown in Appendix A.



Figure (3.5): Air Flow Meter

3.1.6. Testing Section

In this work, two testing sections were used for opening angles (15) and (10) degrees. The cross-sectional area for each testing sections was $(2 \times 6) \text{ cm}^2$ before the divergence section with a length of (0.5) m long, while the section area was $(2 \times 8) \text{ cm}^2$ after the divergence section with a length of (0.5) m as shown in figure (3.6). The testing sections were manufactured of transparent glass (Perspex) with thickness is (1) cm. The divergence section of both testing sections has four ribs, two ribs on each side with dimensions of $(0.5 \times 0.5 \times 2) \text{ cm}^3$ as shown in figure (3.7). The testing sections consist of four holes in different locations. The pressure sensors are fixed inside each hole in order to measure the pressure of two-phase flow inside the channels.

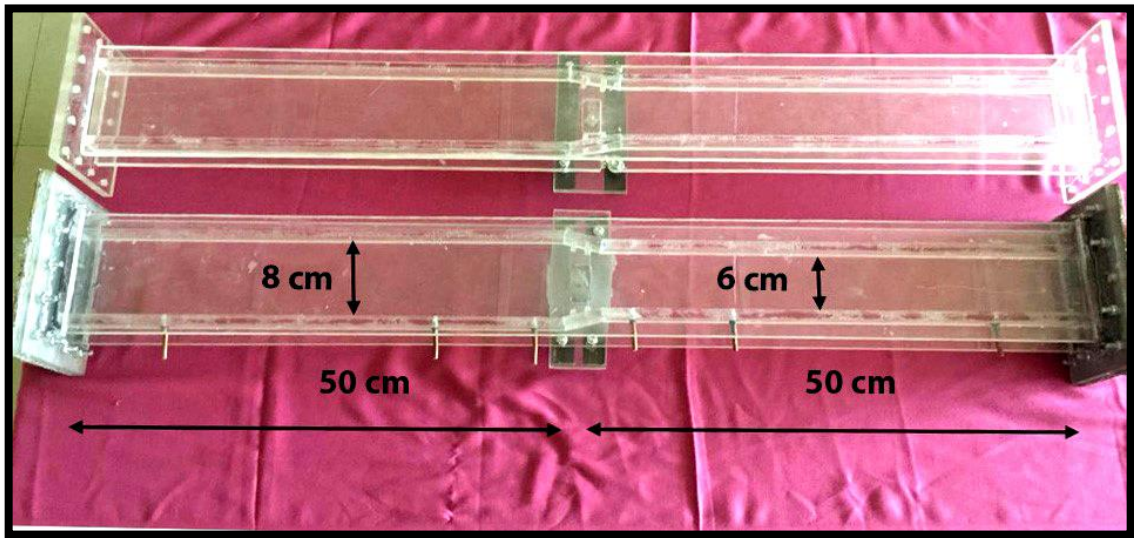


Figure (3.6): Testing Section

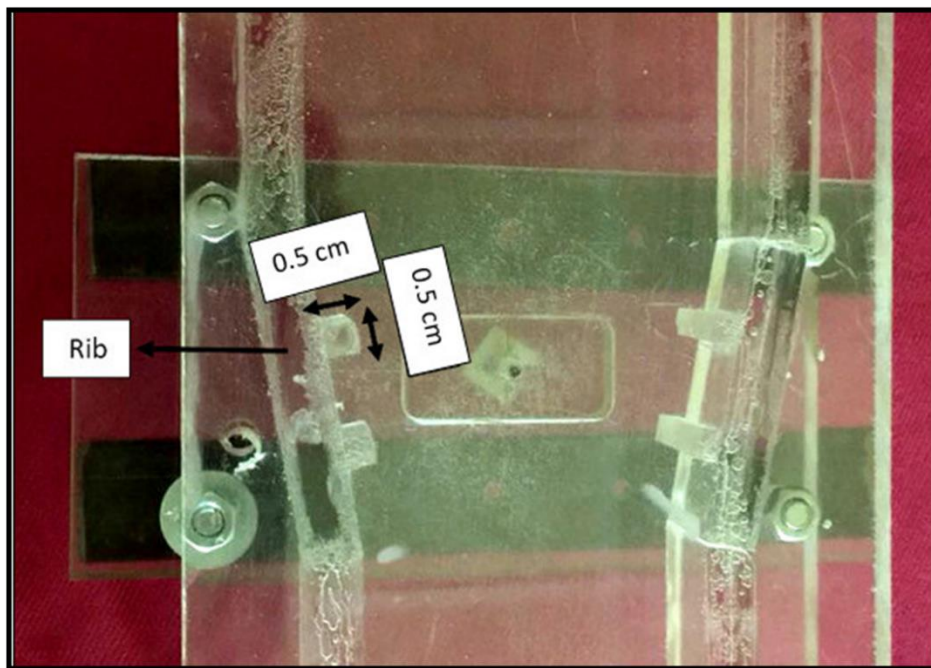


Figure (3.7): Ribs with Their Dimensions

3.1.7. Pressure Sensors

Four pressure transducer sensors are mounted along the pipe to measure the pressure with a range from (0) to (1) bar as shown in Figure (3.8). The specifications of the pressure sensors can be shown in Table (3.1).



Table (3.1): Specification of the Pressure Sensor

Operating pressure range	(0 to 1) bar
Sensor Output	Current (4 to 20 mA)
Hysteresis	0.5%
Body Material	Stainless Steel
Pressure Sensor Type	Piezo resistive Transmitter
Operating Temperature	(-20°C to +80°C)
External Diameter	17mm
External Length	Height = 76mm

A U-tube manometer was used to calibrate the pressure measuring system. The difference in the pressure between the first and the last tap was measured with the pressure sensor and with the manometer at the same time and for the same values of flow rate. The comparison between the values is shown in Figure (3.9).

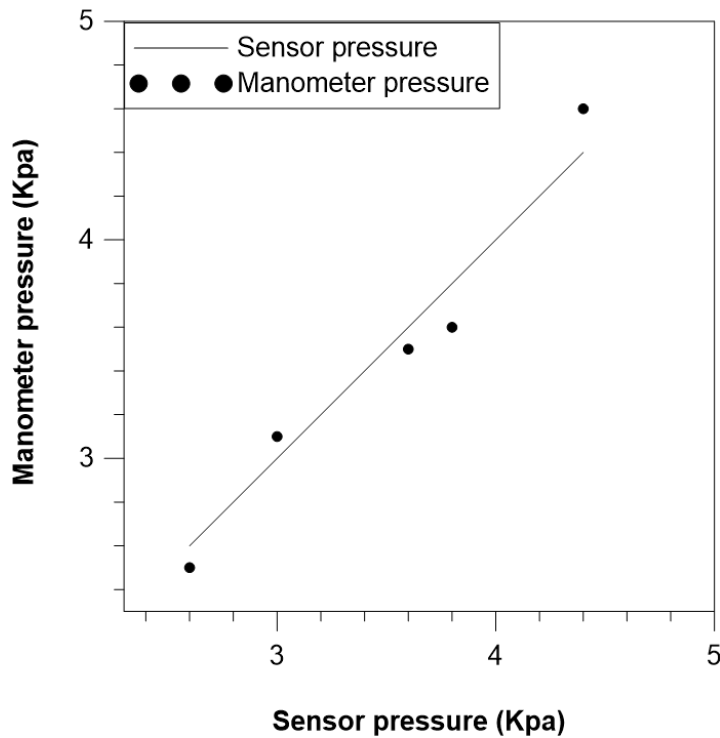


Figure (3.9): Calibration of the Pressure Sensor

3.1.8. Pressure Interface

A pressure interface was used to connect the pressure sensor with the personal computer and it can be seen in Figure (3.10). The generated voltage signal (analog) from a pressure sensor is converted into a digital signal via the interface that can be read through the DaLi08 program running by the computer. The data logger interface has a technical specification shown in Table (3.2).



Figure (3.10): The Pressure Interface

Table (3.2): Specification of the pressure interface

Supply Voltage	5 V AC \pm 5%		
Environmental temperature	Operation range(-10 to 50)C°		
Accuracy	\pm 2%		
Weight	87gr		
Dimensions	Width:72m	Height:112m	Depth:26m
Power consumption	1W		

3.2. Cases Study of the Experimental Work

Two testing sections were used with opening angles (15) and (10) degrees and can be shown in figure (3.11). Each testing section has been fixed in two positions: vertical position and an inclined position with an angle of 60 degree in related to the horizon. Each position has been studied in the case of diverge and converge as shown in figures (3.12) to (3.15).

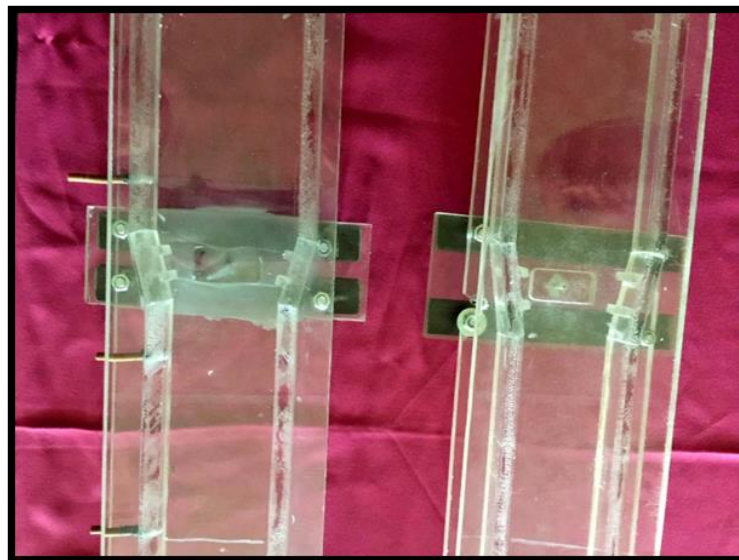


Figure (3.11): Divergence Sections with Different Opening Angle

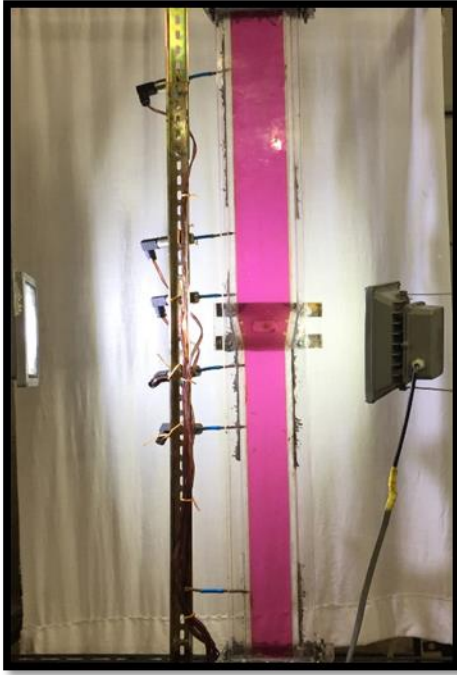


Figure (3.12):vertical diverge
Testing section

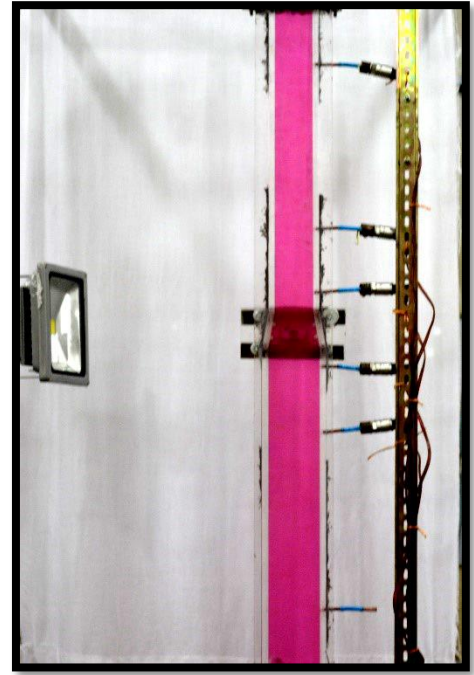


Figure (3.13):vertical converge
Testing section



Figure (3.14):inclined diverge
Testing section

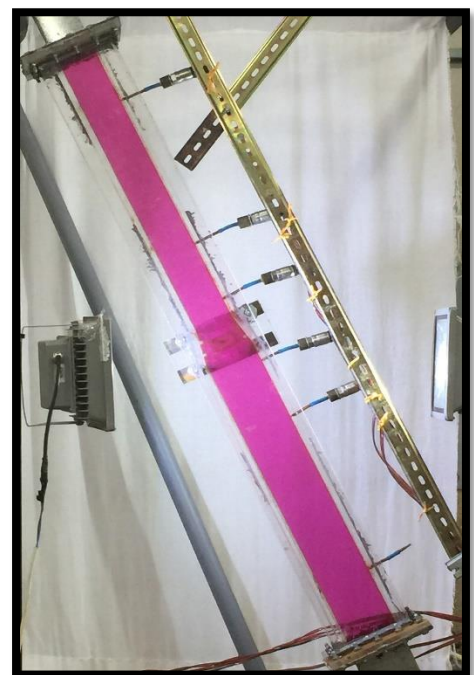


Figure (3.15):inclined converge
Testing section

3.3. Phases Used in the Experimental Work

3.3.1. Continuous Phase

The continuous phase that utilized for the experimental work was liquid water at ambient conditions. It was pumped to the testing channel from the tank by the water pump and regulated by water flow meter.

3.3.2. Dispersed Phase

The air was the dispersed phase at ambient conditions. The air was pumped by an air compressor and regulated by using an air flow meter and then mixed with water from the bottom of the testing channel.

3.4. Experimental Procedure

After building the system and installing all the measuring devices, the system was operated several times to ensure that there was no leak or any mistake in operating. In this work, one hundred and eighteen experiments were performed. All the tests carried out by taking different amounts of discharged water and different amounts of discharged air, as shown in Table (3.3) and Table (3.4).

1. Run the water centrifugal pump to push the water from the water tank. Then the water valve was opened until set the first flow rate to (5) L/min.
2. Turn on the air compressor and then open the air valve until the volume rate in the flow meter reached the first value (5.833) L/min.
3. The water and air mixture entered from the bottom of the testing channel.
4. The pressure begging measured by the pressure sensors, where it can be read through computer software. The image of the two-phase flow motion was taken by the normal digital camera.
5. Repeat above procedure with new discharges of water until complete the entire water discharges.

Table (3.3): Values of work conditions used in experiments for diverge and converge vertical cases

Water discharge (L/min)	Air discharge (L/min)
5	5.833
10	8.333
15	10.833
20	13.333
	16.666

Table (3.4): Values of work conditions used in experiments for diverge and converge inclined cases

Water discharge (L/min)	Air discharge (L/min)
5	5.833
15	10.833
20	16.666

3.5. Design Considerations

Considerations of this study were depending on the previous study. Applications of two-phase flow are in chemical or mechanical engineering applications for that was selected two-phase water and air. The cross-

sectional area of the duct and the opening angle was chosen depending on Ahmedpour [20]. Where the hydraulic diameter was equivalent to the circular pipe diameter, which used in the work of Ahmedpour[20] was calculated. A wide range of water and air discharges were selected, only the values of the discharges which make the dominant flow are slug flow were selected. The discharge that makes the flow of a type of churn flow are not selected because high fluctuation occurs in the flow.

3.6. The Error Analysis

The error analysis is necessary in order to decide if the result is adequate for its intended purpose and to ascertain if it is consistent with other similar results. A more precise method of error analysis in experimental results has been presented by Ronald and Richard [37]. (Appendix B) .

CHAPTER FOUR

NUMERICAL ANALYSIS

Numerical Analysis

Ansys FLUENT 18.0 has been used in this work to simulate and analyze the flow characteristics of two-phase flow (water-air) through the test channel. The effect of the water and air discharge and the opening angle on the pressure profile and differential pressure are studied, also the air volume fraction of the two-phase flow was also performed. To understand such a system, computational fluid dynamics can be used as it is an effective tool in predicting the behavior of the flow.

The simulation done similar conditions in the experiments. The solution in FLUENT divide into four parts; Physical model geometry, Mesh Generated, Set-up physical model, and the post process [38]. In ANSYS FLUENT 18, the Euler-Euler models of multiphase are classified into three models: volume of fluid (VOF), mixture, and Eulerian. In the present work, two-phase flow through ribs divergent/convergent rectangular duct will be modeled using VOF model with several parameters depending on variables of experiments work.

4.1. Basic Models of Two-Phase Flow

There are two models of two-phase flow

1. Homogeneous flow model: In this approach, the two-phase flow is assumed to be a single-phase flow having pseudo properties arrived by suitably weighting the properties of the individual phases.
2. Separated flow model: In this approach, the two phases of the flow are considered to be arterially segregated. One different sets of basic equations can be written for each phase. Alternatively, the equations may be combined. The information about the area of the channel occupied by each phase and about the frictional interactions with the channel wall or between the phases is inserted into the basic

equations, either from separate empirical relationships or on the basis of simplified models of the flow.

4.2. The Physical parameters

4.2.1. The Velocity

The velocities were estimated for water and air to know the range of velocities which could be used. The discharge was read immediately from the flow meter and employed to compute the velocity according to Eq. (4.1) [3], which gives the values as shown in Table (4.1).

$$Q = UA \quad \dots\dots\dots (4.1)$$

Where

U = velocity (m/s).

Q = discharge (m³/s).

A = Cross-sectional area (m²).

$$A_{\text{air}} = \pi/4 D_{\text{pipe}}^2 \quad \dots\dots\dots (4.2)$$

$$A_{\text{water}} = (wxh) - A_{\text{air}} \quad \dots\dots\dots (4.3)$$

Where

w = width of the duct

h = height of the duct

Table (4.1): Velocities of water and air

Water flow rate (L/min)	Water velocity (divergence case)(m/s)	Water velocity (convergence case) (m/s)	Air flow rate (L/min)	Air velocity (m/s)
5	0.0777	0.04448	5.833	0.761
10	0.1554	0.088968	8.333	1.088
15	0.2331	0.13335	10.833	1.414
20	0.3108	0.17792	13.333	1.7409
			16.666	2.1756

4.2.2. Mass Flux (G)

Mass flux for water and air was calculated for the purpose of calculating the term $\left(\frac{G^2}{\rho}\right)$ which used for drawing the flow map as shown in Table (4.2).

Table (4.2): Table of values of $\frac{G^2}{\rho}$

Air flow rate (L/min)	$\frac{G^2}{\rho}$ air	Water flow rate (L/min)	$\frac{G^2}{\rho}$ water
5.833	0.706	5	6.015
8.333	1.44	10	24.0447
10.833	2.4377	15	54.1439
13.333	3.6921	20	96
16.666	5.762		

4.2.3. Reynolds Number

Reynolds number can be found by the Eq. (4.4), which gives the values as shown in Table (4.3).

$$Re = \frac{\rho U D_h}{\mu} \quad \text{..... (4-4)}$$

for water

$$D_h = \frac{4A}{P} \quad \text{..... (4-5)}$$

Where

P is wetted perimeter = $\pi D_{\text{pipe}} + 2(w+h)$

Table (4.3): Reynolds Number

Q_{water} L/min	Re_{water} (divergence case)	Re_{water} (convergence case)	Q_{air} L/min	Re_{air}
5	1855	1181	5.833	661
10	3711	2362	8.333	945
15	5567	3540	10.833	1229
20	7423	4724	13.333	1513
			16.666	1891

4.3. The Geometrical Model

4.3.1. The Geometry

The software SOLIDWORKS 2013 is used to construct the geometry of testing section in three-dimension, by drawing the front view of testing channel on the X-Y plane. The extrude order was given for geometry to obtain the 3D structure. A circle with a diameter of (0.00126) m was drawn inside a rectangle in the bottom surface of the structure, so that the circle

represented entry of the air into the testing channel and the remaining area represented entry of the water as shown in Figure (4.1). All sides of the structure were set to be adiabatic walls. The bottom surface of the testing channel was drawn in order to be the entry points of the air and water into the testing section, while the top surface represented the outlet flow. The surface body of geometry was fixed as a fluid.

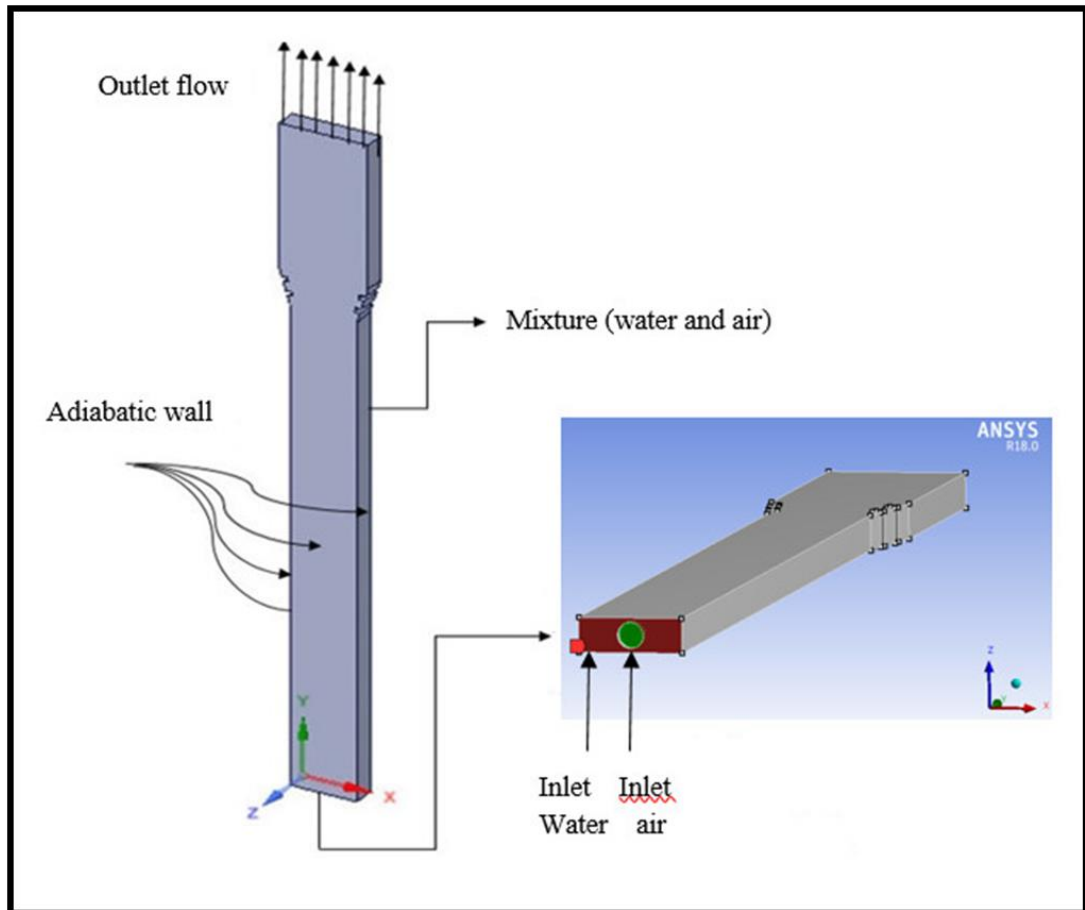


Figure (4.1): Problem Description

Description of two-phase flow geometry can be observed from the figure (4.2 a) to (4.2d) of the testing channel for all cases.

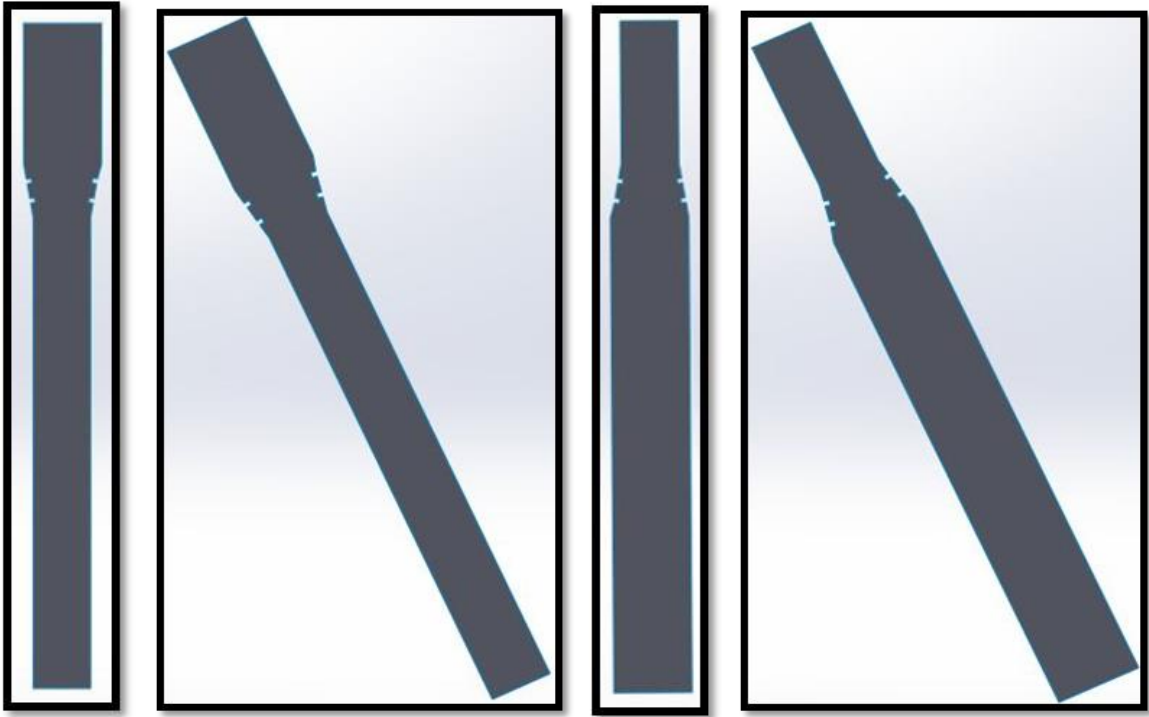


Figure (4.2a)

Figure (4.2b)

Figure (4.2c)

Figure (4.2d)

Figure (4.2): Geometry of test channel for all cases

4.3.2. The Mesh

After sketching the geometry, many attempts were made using the ANSYS meshing to mesh the domain. Many types of meshes, and choosing the suitable type of mesh is depended on some parameters such as flow field, geometry, and complexity. The size and type of mesh have a main impact on the CPU (central processing unit) time requisite, the accuracy of the solution, and convergence rate [39]. In this work, the geometry of the testing pipe was divided into elements. A Quadrilateral grid type was chosen by employed ANSYS workbench 18, where the bigger and lesser size of elements was (1) mm, because the results are fixed at these values of mesh size as shown in Figure (4.3). The range of number of nodes is (1013502-1156722), while the range of elements is (949600-1071760). Figures (4.4) show the mesh of the two-phase flow in the divergence section with 10 and 15 degrees.

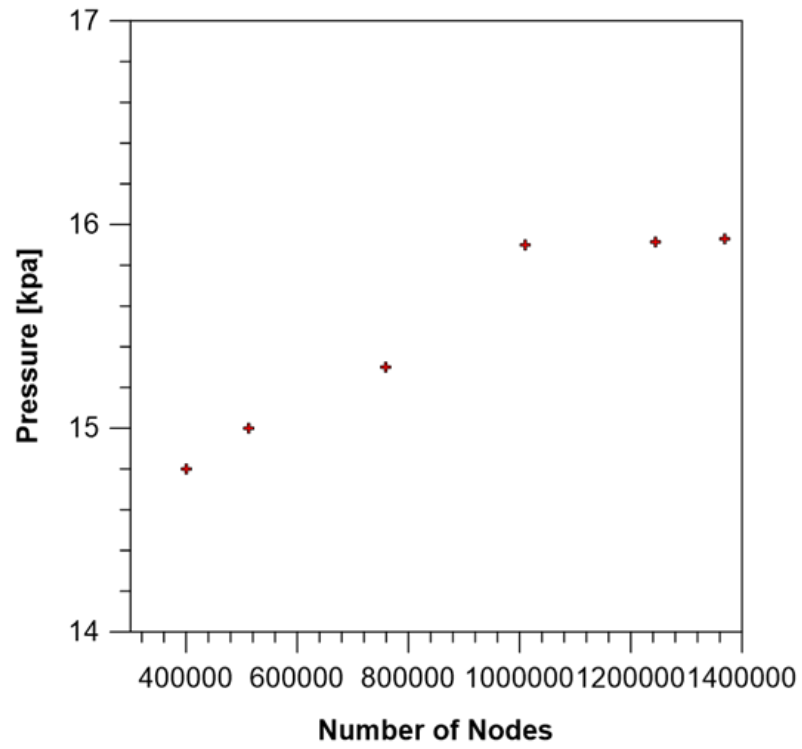


Figure (4.3). Test of number size of mesh

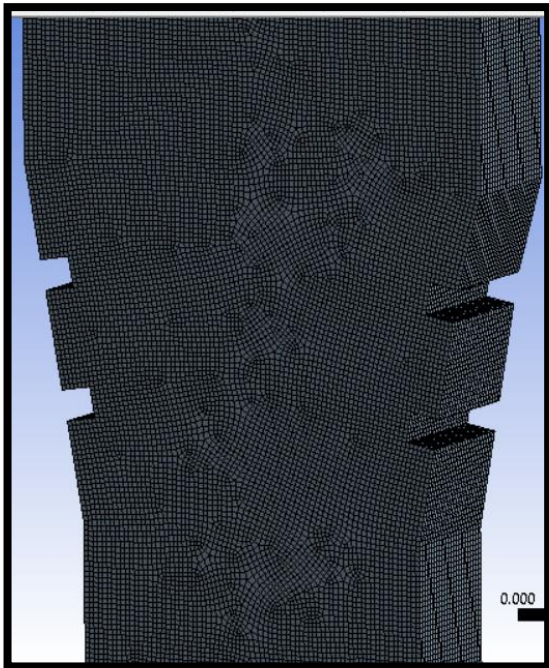


Figure (4.4a): The mesh of divergence with 10 degree

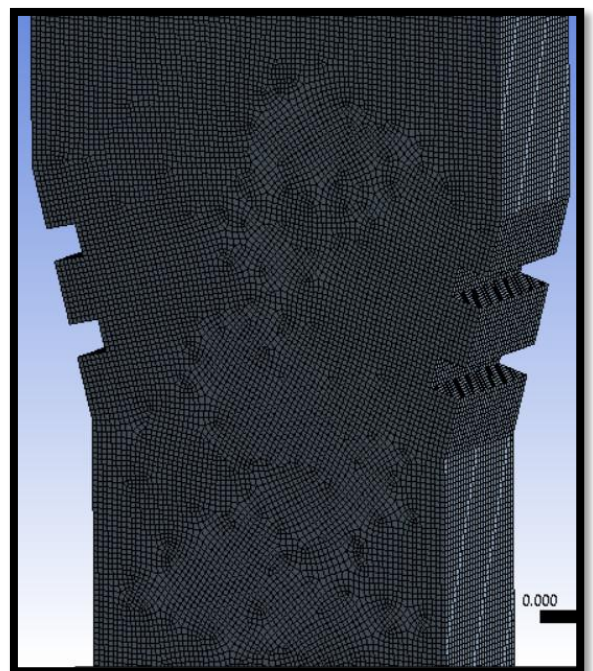


Figure (4.4b): The mesh of divergence with 15 degree

4.4. The Boundary Condition (B.C)

The fluids that used in this study were water and air; which had been used as the primary and secondary phase, respectively. Boundary conditions used for this model are explained in the following subsections:

4.4.1. Inlet B.C.

The inlet boundary condition used in this study was the superficial velocity of the air and the water entering the testing channel from the lowest surface of the channel. The superficial velocity of the air and water were taken from the experimental work with values of (0.0777 - 0.3108) m/s and (0.761 - 2.1756) m/s, respectively.

4.4.2. Wall B.C.

All the portions of the channel wall were set to be an adiabatic wall.

4.4.3. Outlet B.C.

The upper surface of the channel represented to the exit end and it was set to be the outlet of the flow.

To control the simulation and get the convergent solution, the under-relaxation factors have been setup as shown in Table (4.4).

Table (4.4): The under relaxation-factor

Variable	Relaxation Factor
Pressure	0.3
momentum	0.7
Volume Fraction	0.5
Turbulent Kinetic energy	0.8
Turbulent Dissipation Rate	0.8

4.5. Problem Assumption

In order to simulate the two-phase flow through the duct in a geometrical model, the follow assumed to be a turbulent flow, three-dimensional space, unsteady flow, pressure-based solver, incompressible flow.

4.6. Properties of the Two-Phase Flow

The properties of working fluid of the two-phase flow are shown in Table (4.5)

Table (4.5): Properties of the Two-phase Flow

Property at temperature (19-23) c°	Water	Air
Density (kg/m ³)	998.49-997.63	1.204-1.194
Viscosity (kg/m.s)	0.001028-0.000933	1.825e-05 – 1.873e-05

4.7. The Simulation Model

The Eulerian-Eulerian multiphase model was used with a volume of the fluid model (VOF) where the viscous model was RNG k-epsilon (ϵ), to simulate the two-phase flow in the testing channel.

4.8. The Governing Equation

The volume of fluid model solves the volume fraction and conservation of momentum equations for all phases. This model is more suitable and accurate for the present work. Value of the domain is modeled as 3-D, according to the boundary conditions of mixture internal flow and by pressure-based solver that calculating the solution. The momentum equation is solved by depending on variables such as phase volume fractions, and properties: density (ρ), and viscosity (μ) [40].

4.8.1. The Volume Fraction Equation

The evolution of the q^{th} fluid in a system on (n) fluids is governed by the transport equation:

$$\frac{\partial \alpha_q}{\partial t} + \vec{v} \cdot \nabla \alpha_q = \frac{S_{\alpha_q}}{\rho_q} \quad \dots\dots\dots (4-6)$$

With the following constraint

$$\sum_{q=1}^n \alpha_q = 1 \quad \dots\dots\dots (4-7)$$

For each cell, the properties of the mixture like mixture density and dynamic viscosity are depended on the volume fraction of all phases as given by equation (3-3).

$$\rho = \sum \alpha_n \rho_n ; \mu = \frac{\sum \alpha_n \rho_n \mu_n}{\sum \alpha_n \rho_n} \quad \dots\dots\dots (4-8)$$

4.8.2 The Momentum Equation

A single momentum equation is solved throughout the domain, and the resulting velocity field is shared among the phases. The momentum equation is dependent on the volume fractions of all phases through the properties: density (ρ) and dynamic viscosity (μ)

$$\frac{\partial}{\partial t} (\rho \vec{v}) + \nabla \cdot (\rho \vec{v} \vec{v}) = -\nabla p + \nabla \cdot [\mu (\nabla \vec{v} + \nabla \vec{v}^T)] + \rho \vec{g} + \vec{F} \quad \dots\dots (4-9)$$

Where \vec{v} is the velocity field and \vec{F} is a body force.

4.9. The Turbulence Model

In this work, the turbulence RNG mixture model was used to simulate the two-phase flow, which used with swirl flow. The two-equation for RNG model are; the kinetic energy equation (4-10), and dissipation equation (4-11).

$$\frac{\partial}{\partial t}(\rho_m K) + \nabla \cdot (\rho_m \vec{V}_m K) = \nabla \cdot \left(\frac{\mu_{t,m}}{\sigma_k} \nabla K \right) + G_{K,m} - \rho_m \epsilon \quad \dots\dots(4-10)$$

$$\frac{\partial}{\partial t}(\rho_m \epsilon) + \nabla \cdot (\rho_m \vec{V}_m \epsilon) = \nabla \cdot \left(\frac{\mu_{t,m}}{\sigma_\epsilon} \nabla \epsilon \right) + \frac{\epsilon}{K} (C_{1\epsilon} G_{K,m} - C_{2\epsilon} \rho_m \epsilon) \quad (4-11)$$

Where k is the turbulent kinetic energy, ϵ is the rate of turbulent dissipation, G is the energy, and σ is the number of turbulent Prandtl for K and ϵ . The density and the velocity of the mixture can be found by using Equations (4-12) & (4-13), respectively.

$$\rho_m = \sum_{i=1}^N \alpha_i \rho_i \quad \dots\dots\dots(4-12)$$

$$\vec{V}_m = \frac{\sum_{i=1}^N \alpha_i \rho_i \vec{V}_i}{\sum_{i=1}^N \alpha_i \rho_i} \quad \dots\dots\dots(4-13)$$

The turbulent viscosity ($\mu_{t,m}$) and kinetic energy ($G_{k,m}$) of the mixture (air-water) can be calculated by the equations (4-14) & (4-15), respectively.

$$\mu_{t,m} = \rho_m C_m \frac{k^2}{\epsilon} \quad \dots\dots\dots(4-14)$$

$$G_{K,m} = \mu_{t,m} \left(\nabla \vec{V}_m + (\nabla \vec{V}_m)^T \right) : \vec{V}_m \quad \dots\dots\dots(4-15)$$

The model constants are shown in Table (4-6).

Table (4-6): Model Constants

Model constant	Value
C_m	0.0845
$C_1 - \epsilon$	1.42
$C_2 - \epsilon$	1.68
σ_k	1
σ_ϵ	1.3

4.10. The Simulation Steps

For two-phase flow modeling by using a dynamic computer fluid model, the following steps were implemented:

- 1- SOLIDWORK used to configure the model geometry.
- 2- ANSYS Workbench 18 used to generate the mesh of two-phase field.
- 3- Choosing a model (VOF).
- 4- Specify the definition of material.
- 5- Choosing phases and boundary conditions.
- 6- Obtain the initial solution.
- 7- The solution was run with a maximum iteration (5000) and time step was 0.1 sec.
- 8- The results of the pressure and the air volume fraction were extracted.

4.11. Convergent Criteria

Every numerical basis solution contains errors. The key is to know how those errors are big and whether the numerical results are acceptable in the engineering applications. In the present study, the numerical convergence was accepted as it was completed when the residual error reached as shown in Table (4.7).

Table (4.7): Residual error for the tested case.

Equations	Continuity	X- Velocity	Y- Velocit y	Z- Velocity	k	E	Volume Fraction
Residual Error	10^{-5}	10^{-4}	10^{-4}	10^{-4}	10^{-4}	10^{-4}	10^{-4}

Results and Discussion

In this chapter, a description of the experimental results and the numerical results that extracted from a system of two-phase flow (water and air) in divergence/convergence ribbed rectangular duct will be explained. Comparison between experimental results and computational fluid dynamics results has been made in order to study and investigate the two-phase flow characteristics.

The effect of increasing water discharge from (5) L/min to (20) L/min, air discharge from (5.833) L/min to (16.666) L/min for two opening angles (10 and 15) degree on the pressure distribution and pressure difference were studied. The experimental and numerical pressure results were drawn together in order to compare between them. Furthermore, the two-phase flow was recorded by video camera, and converted into a series of images, and then compared with images for the corresponding contours, which were estimated numerically.

5.1. Program Validation

To verify the numerical code, the calculated axial profile of the pressure is compared with the numerical results of the previous study made by Ahmedpour [20] about the two-phase flow (water and air) through sudden and graduated smooth divergence circular vertical channel. The parameters was Reynolds number (Re_L)= 1.8×10^5 , volumetric void fraction (β)=20%, surface area ratio (σ)=0.43 and different opening divergence angle (90, 15 and 5) degree as shown in figure (5.1). A good agreement was detected between the numerical results of pressure study and the numerical results of Ahmedpour [20] with an average maximum percentage error of (12.8) %. These results have validated the accuracy of the numerical code.

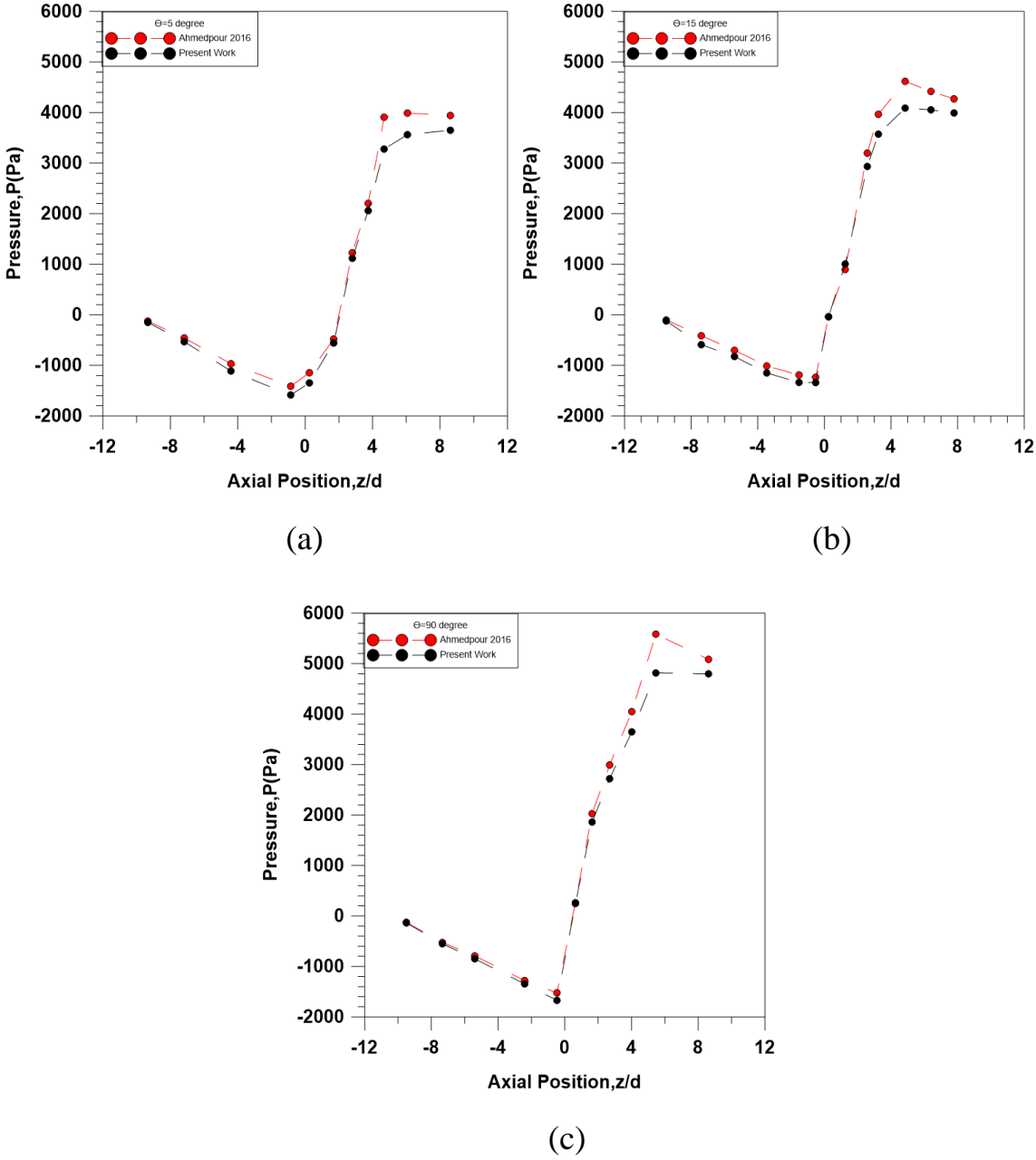


Figure 5.1: The validation of the numerical code with the numerical results of Ahmedpour[20]

5.2. Two-Phase Flow through Divergence Section of the Vertical and Inclined Position

5.2.1. Experimental Results

5.2.1. A. Influence of Water and Air Discharge on the Pressure Profile

Figures (5.2) to (5.5) show the effect of increasing water and air discharge on the experimental results of the pressure profile at four different points along the testing channel. From these figures, it can be noted that the value of the mixture pressure is decreased as the flow progress. When the mixture reached the divergence section, the pressure value began to increase. At the downstream of the divergence section, the pressure value will decrease again. It can be seen that the pressure profile increased when the water or air discharge increased because the volume of the testing channel was constant, so any increasing in the amount of water or air would increase the pressure over the walls of the channel.

Figure (5.2), explains the experimental results of the pressure profile for vertical testing channel with opening angle of (10) degree, with different air discharge (5.833,8.333,10.833,13.333 and 16.666) L/min for water discharge (5 and 20) L/min. When the water discharge increased from (5) to (20) L/min at the same location of the pressure transducer and constant air discharge (0.35 m and 5.833 L/min), respectively, the value of the pressure increased from (14.6) kpa to (16.7) kpa.

Figure (5.3), shows the experimental results of the pressure profile for vertical testing channel with opening angle (15) degree, with different air discharge for water discharge (5 and 20) L/ min. When the water discharge increased from (5) L/min to (20) L/min at the same location of the pressure transducer and constant air discharge (0.35 m and 5.833 L/min), respectively, the value of pressure increase from (14.9 to 17.2) kpa.

Figure (5.4) shows the experimental results of the pressure profile for inclined test channel with opening angle (10) degree, with different air discharge (5.833, 10.833 and 16.666) L/min for water discharge (5 and 20) L/min. When the water discharge increased from (5 to 20) L/min at the same location of the pressure transducer and constant air discharge (0.35 m and 5.833) L/min, respectively, the value of pressure increase from (16) kpa to (17.6) kpa.

Figure (5.5), shows the experimental results of the pressure profile for inclined testing channel with opening angle (15) degree, with different air discharge for water discharge (5 and 20) L/ min. As the water discharge increased from (5 to 20) L/min at the same location of the pressure transducer and constant air discharge (0.35 m and 5.833 L/min), respectively, the value of pressure increase from (15.6 to 18.3) kpa.

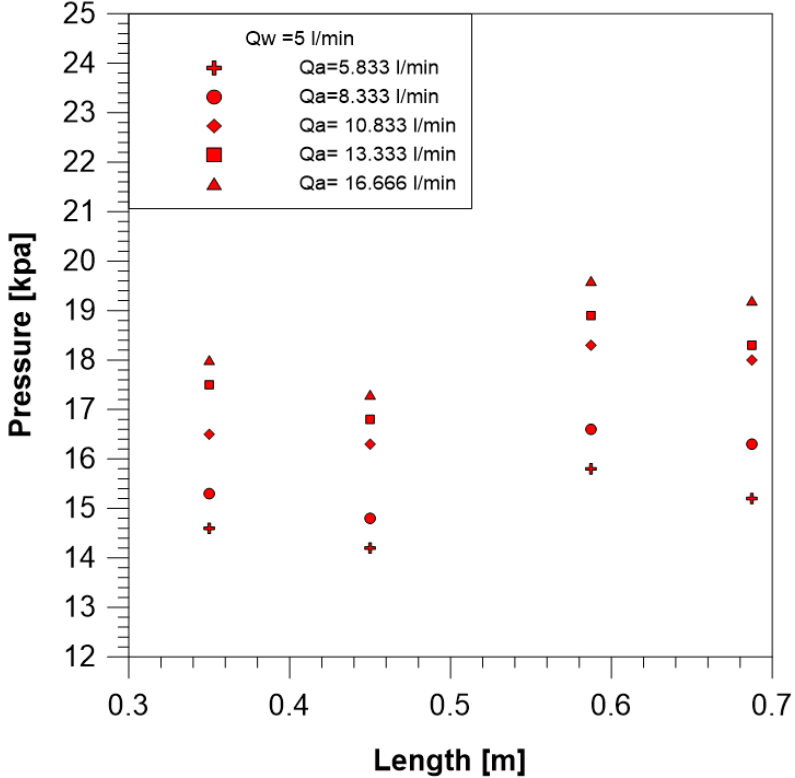


Figure (5.2a)

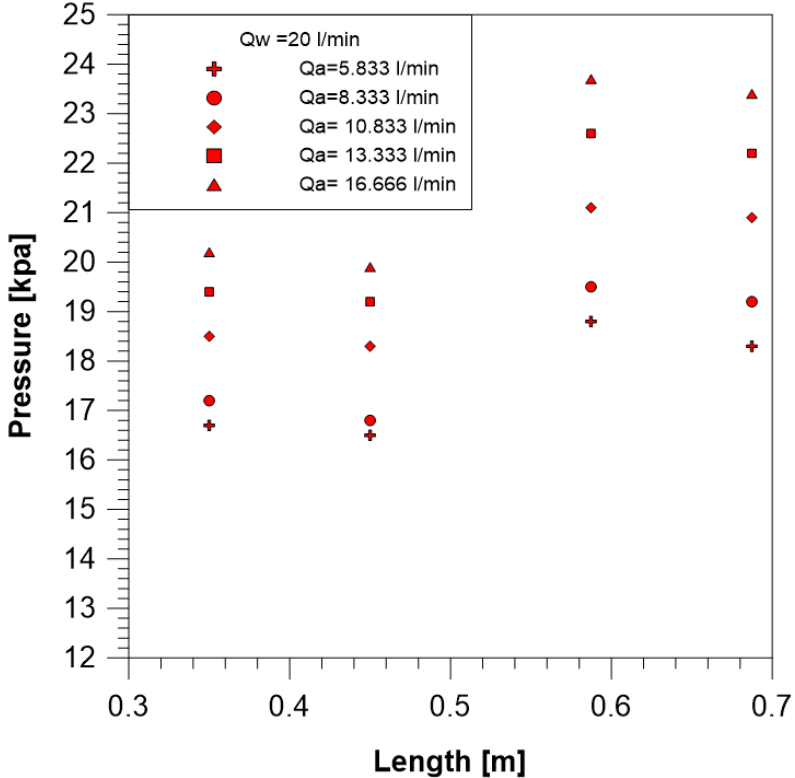


Figure (5.2b)

Figure (5.2): Effect water discharge on Pressure profile for opening angle 10 degree (vertical)

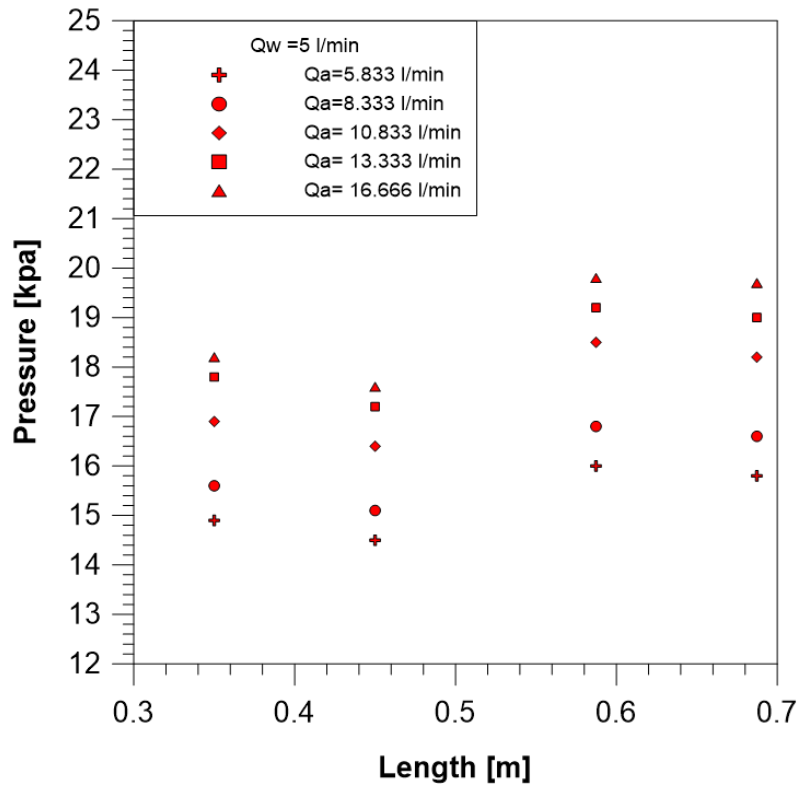


Figure (5.3a)

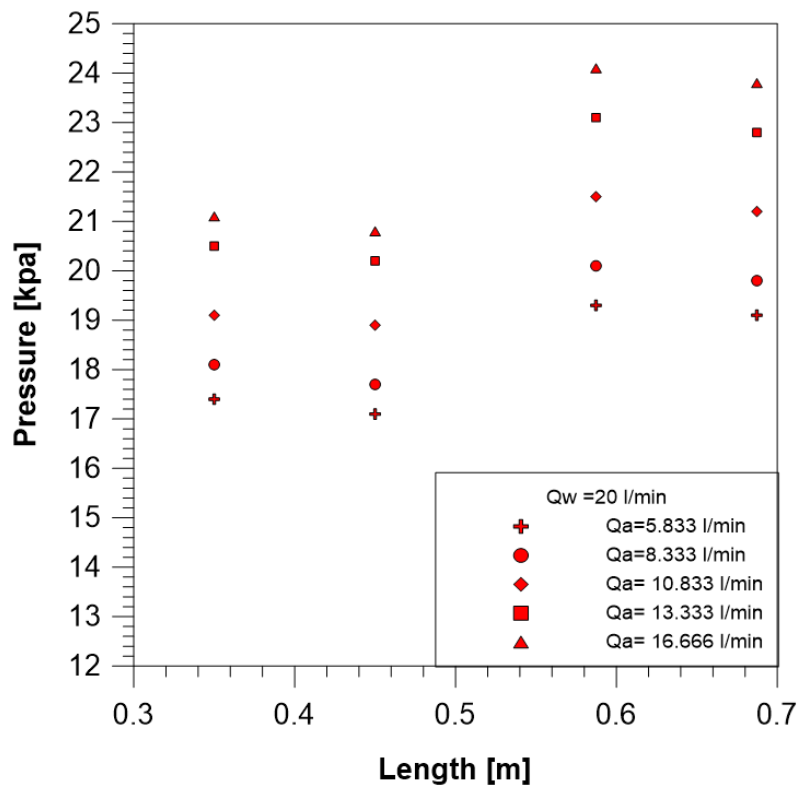


Figure (5.3b)

Figure (5.3): Effect water discharge on Pressure profile for opening angle 15 degree (vertical)

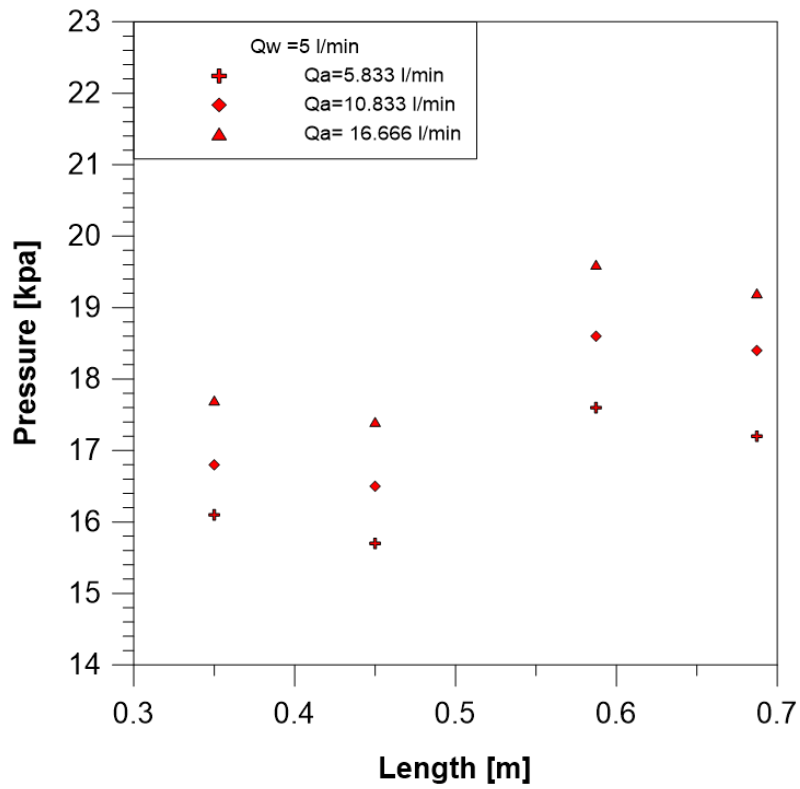


Figure (5.4a)

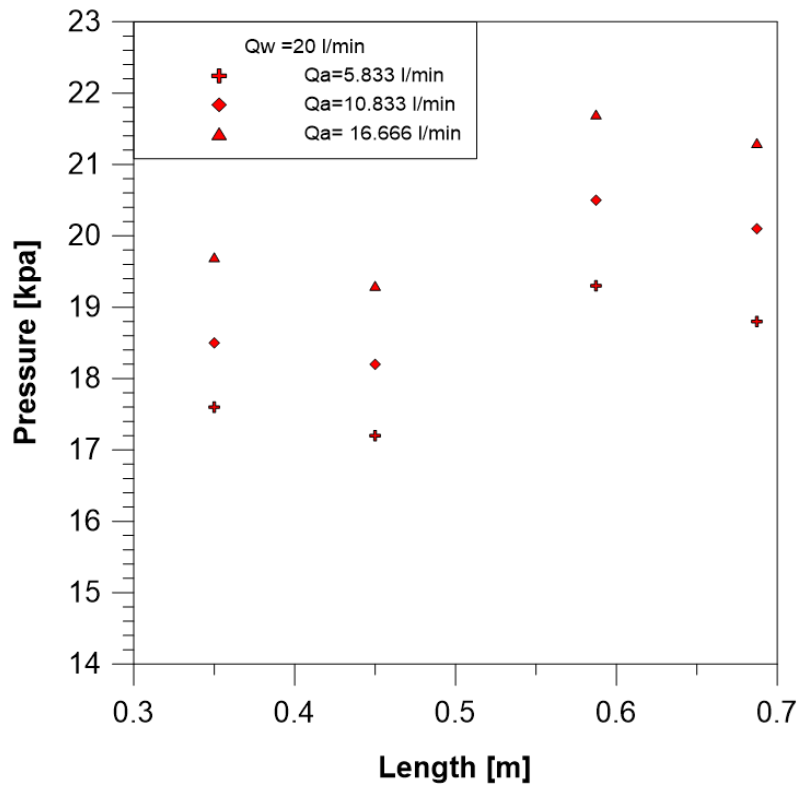


Figure (5.4b)

Figure (5.4): Effect water discharge on Pressure profile for opening angle 10 degree (inclined)

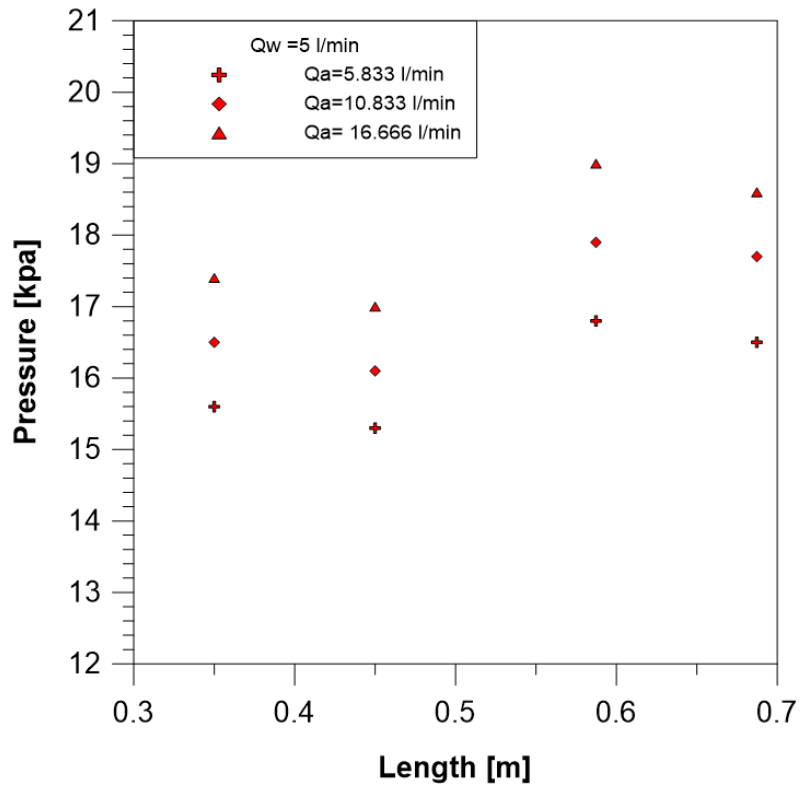


Figure (5.5a)

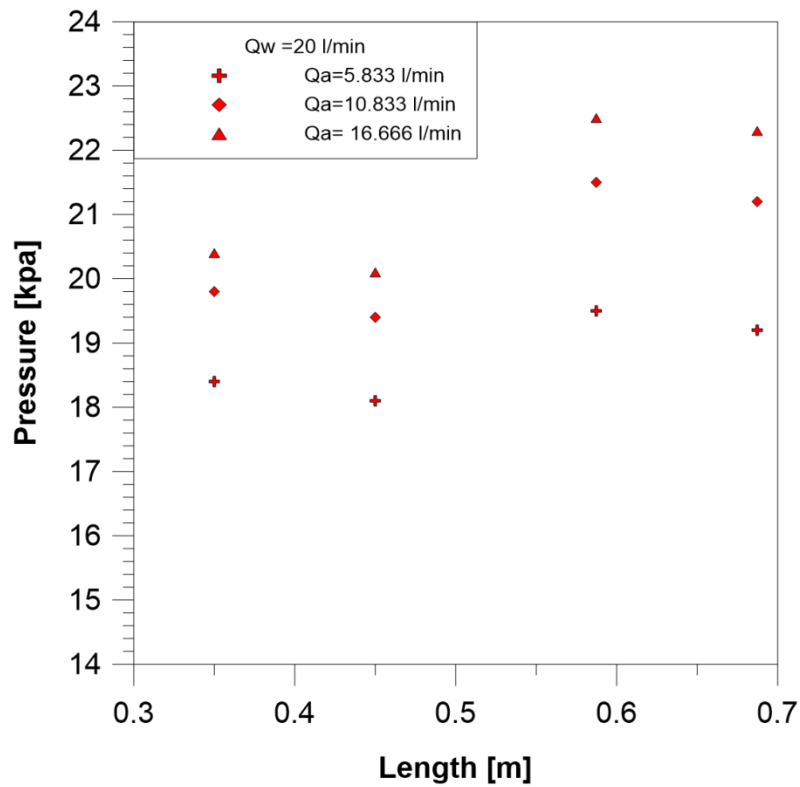


Figure (5.5b)

Figure (5.5): Effect water discharge on Pressure profile for opening angle 15 degree (inclined)

5.2.1. B. Effect of Water and Air Discharge and Opening Angle on the Recovery Pressure

Figures (5.6) to (5.9) show the experimental results of the mean recovery pressure through the vertical and inclined divergence section with different air and water discharge. It can be seen from these figures that the recovery pressure increase by increasing the discharge of air or water for both the (10) and (15) opening angles. Also, it was observed that the recovery pressure for the opening angle 15 is less than the recovery pressure at the opening angle 10 at the same air and water discharge. The reason was the presence of the additional flow area for the case of angle 15 degrees which produced more turbulence wherefore more eddies are generated this led to making the recovery pressure less than the case of opening angle of 10 degrees.

Figures (5.6) and (5.7) show the experimental recovery pressure through the vertical divergence section for opening angle (10 and 15) degree, respectively, with different air discharge for water discharge (5 and 20) L/min. As the air discharge increased from (5.833 to 16.666) L/min at a constant water discharge (5) L/min, the recovery value of the pressure increase from (1.6) kpa to (2.3) kpa for opening angle 10. For opening angle 15, the recovery value of the pressure increase from (1.5) kpa to 2.1) kpa.

Figures (5.8) and (5.9) show the experimental recovery pressure through the inclined divergence section for opening angle (10) and (15) degrees respectively with different air discharge for water discharge (5 and 20) L/min. As the air discharge increased from (5.833) to (16.666) L/min at a constant water discharge (5 L/min), the value recovery pressure increase from (1.9 kpa to 2.3 kpa) for opening angle 10 degree, while the

recovery value of the pressure increase from (1.9) kpa to (2.1) kpa for opening angle 15 degree.

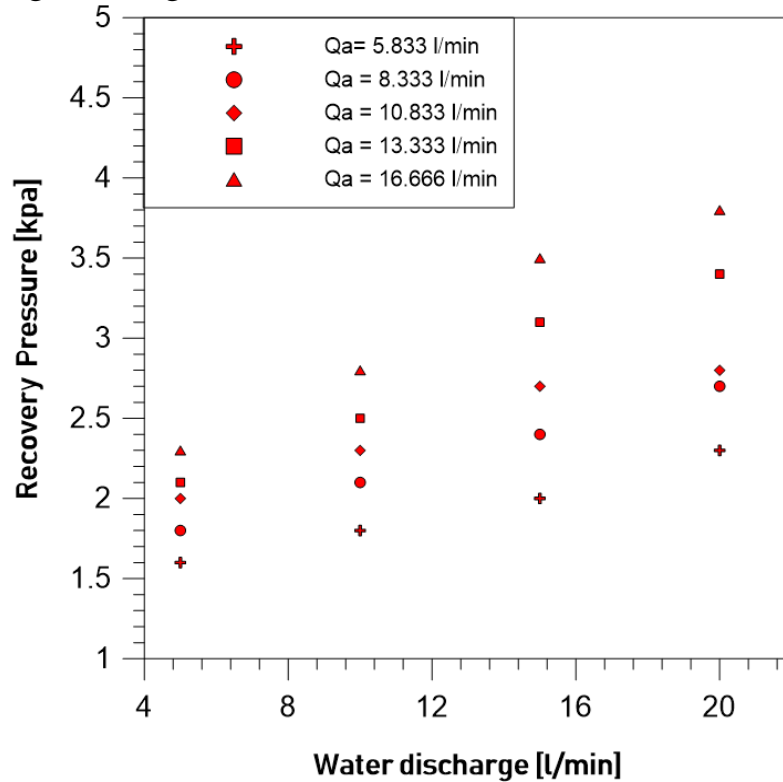


Figure (5.6): Recovery pressure for different values of Water discharge at opening angle 10 degree (vertical)

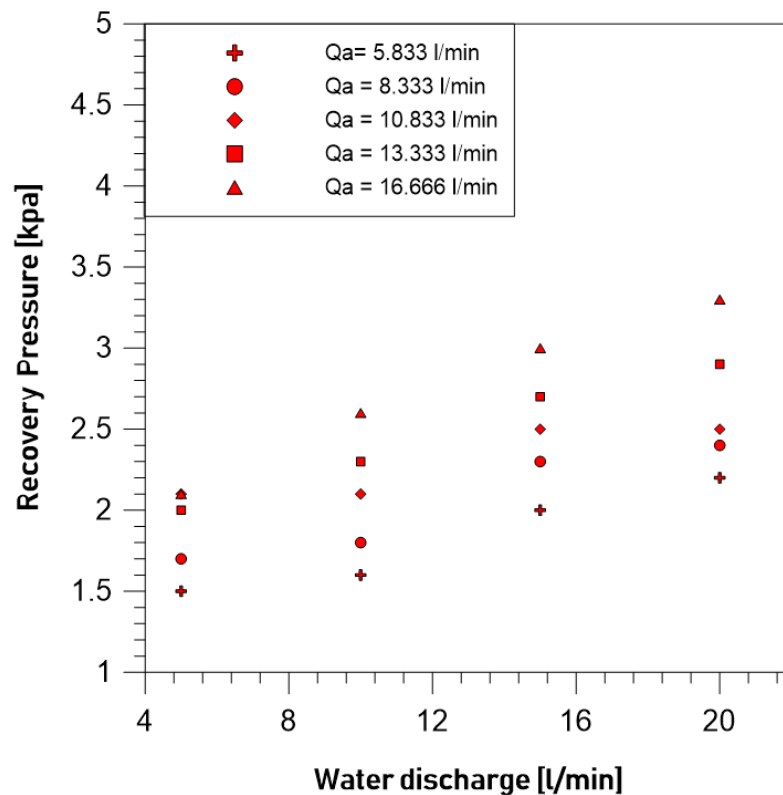


Figure (5.7): Recovery pressure for different values of Water discharge at opening angle 15 degree (vertical)

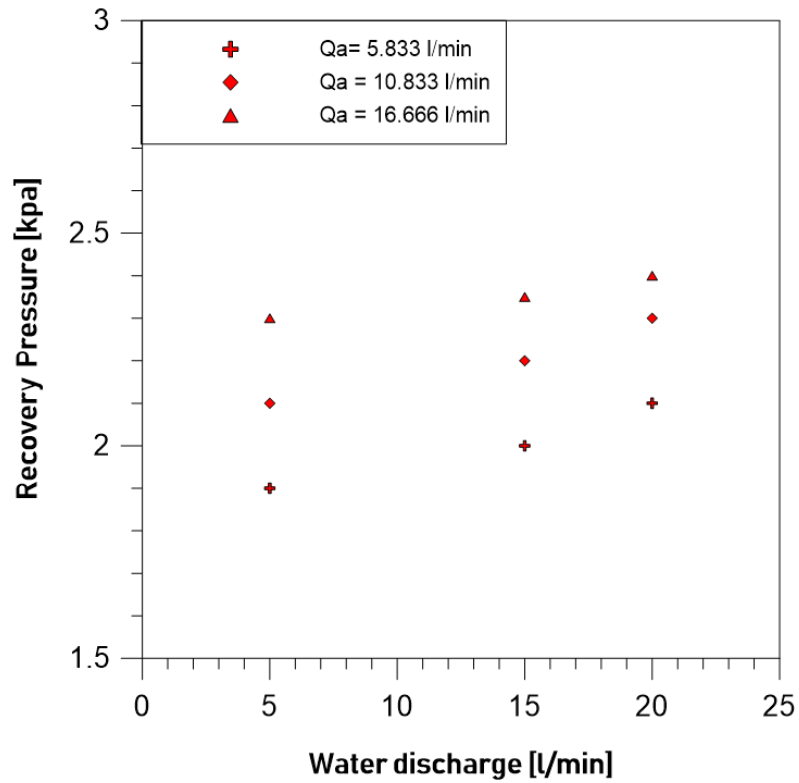


Figure (5.8): Recovery pressure for different values of Water discharge at opening angle 10 degree (inclined)

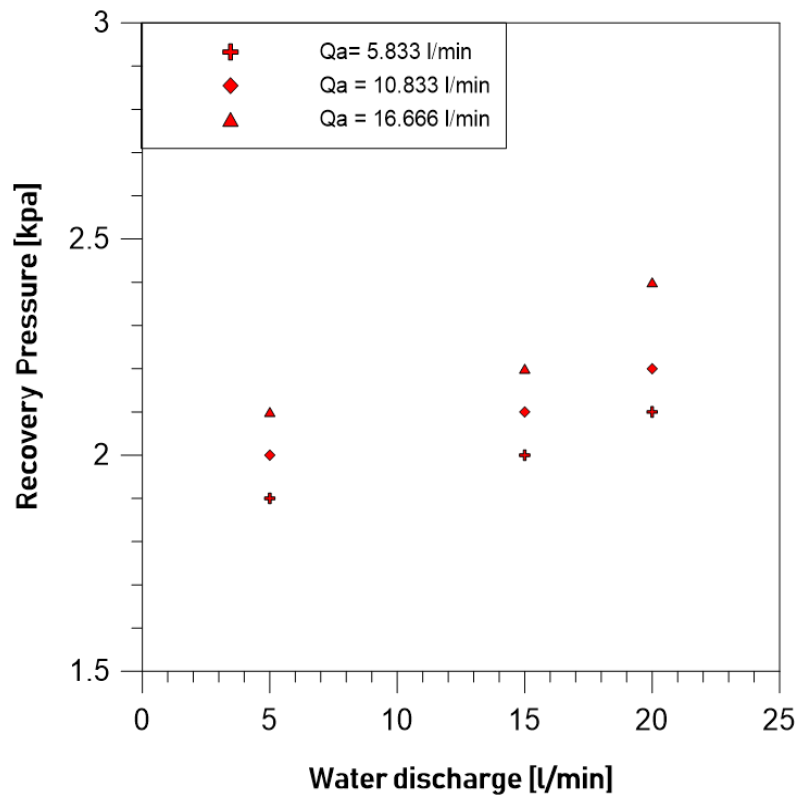


Figure (5.9): Recovery pressure for different values of Water discharge at opening angle 15 degree (inclined)

5.2.2. The Numerical Results

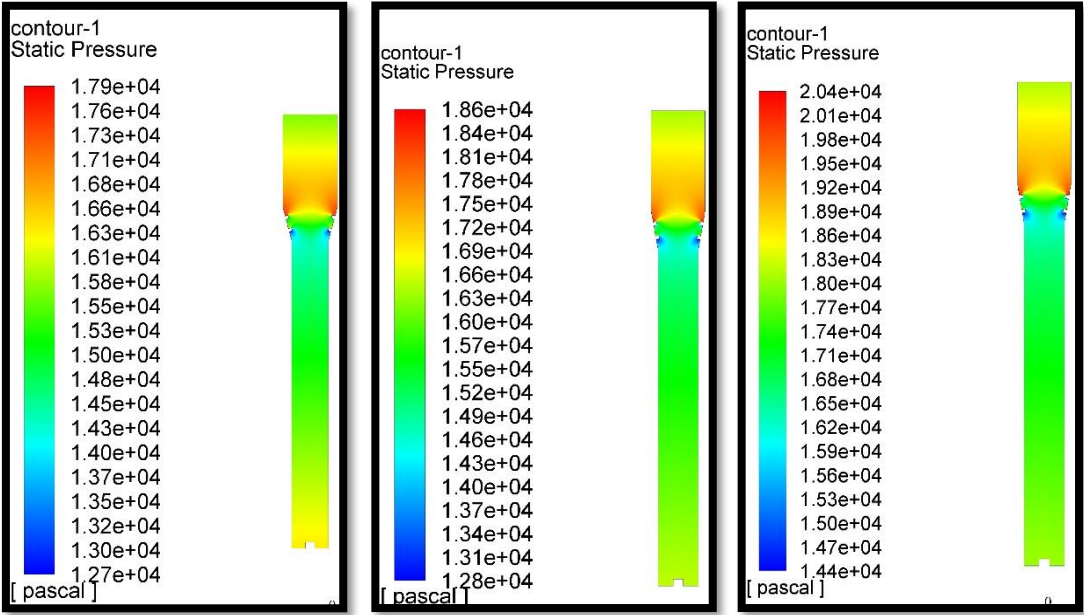
5.2.2. A. The Pressure Contour

The purpose of the numerical CFD is to study the pressure distribution and air volume fraction distribution through ribs divergence section for the vertical and inclined position. Like the experimental study, a region of the test was between pressure sensor (1) and sensor (4).

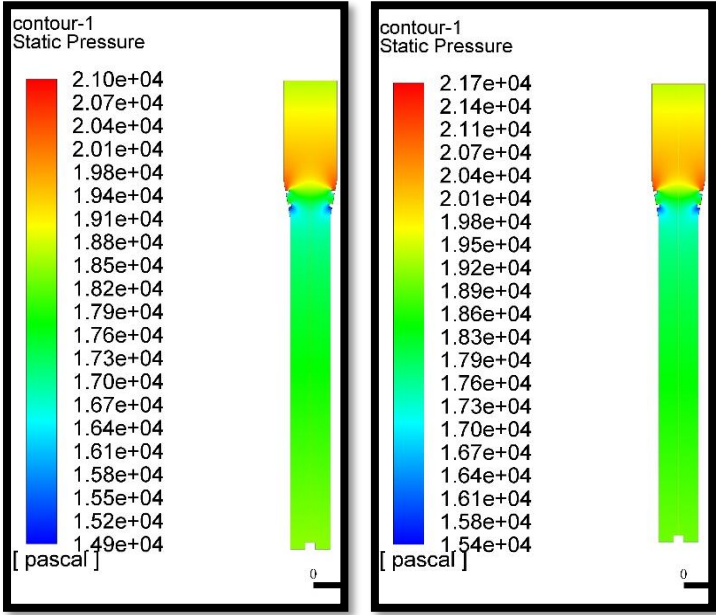
Figures (5.10) to (5.13) show the contours of pressure distribution for two-phase flow through vertical and inclined ribs divergence testing channel with opening angle 10 degrees at various values of water discharge (5,10,15 and 20) L/min. Also, each figure has five values of air discharge (5.833, 8.333, 10.833, 13.333 and 16.666) L/min.

These figures describe the contour of the pressure values, where the descending gradient of the pressure value before the divergence section. And at the divergence section, it could be observed that the ascending gradient of the pressure values was due to the increase of the flow area which led to reduce the velocity and increase the pressure values. After the divergence section, the pressure values began to descend gradually.

Also, it can be noted that the value of the pressure increase by increasing the values of air or water discharge due to the rise in the amount of flow mixture and thus increase the pressure on the walls of the channel.

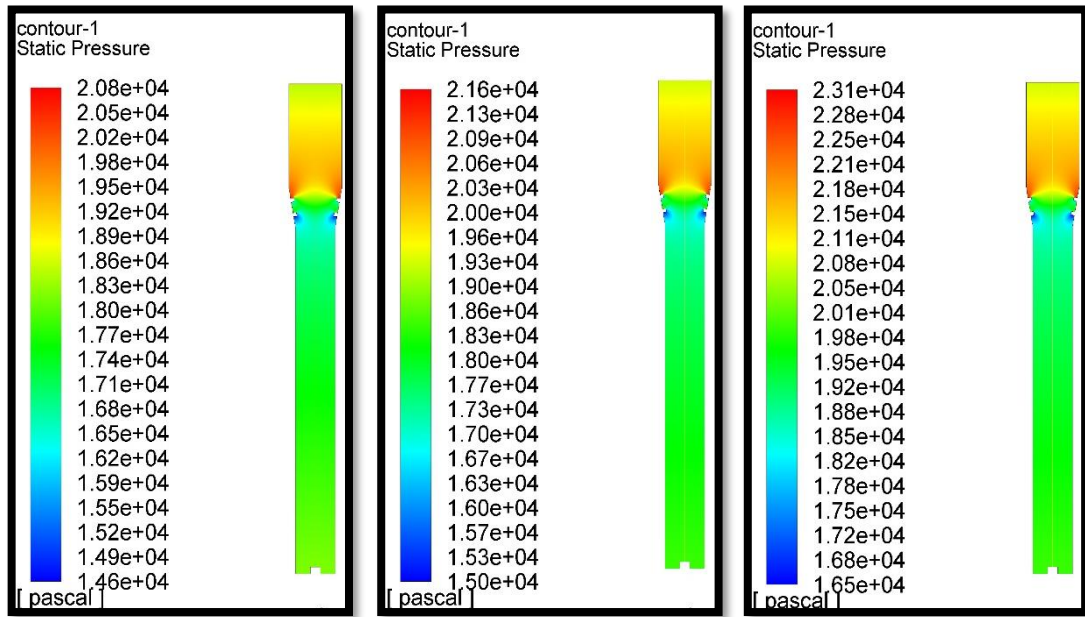


(a) $Q_{air} = 5.833$ (b) $Q_{air} = 8.333$ (c) $Q_{air} = 10.833$



(d) $Q_{air} = 13.333$ (e) $Q_{air} = 16.666$

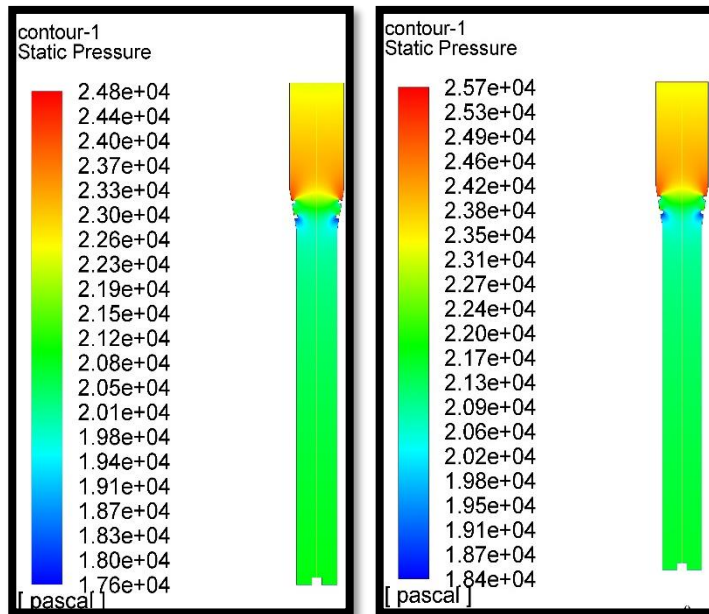
Figure (5.10): Influence of air discharge on pressure distribution at 5 L/min water discharge (opening angle 10 degree)



(a) $Q_{\text{air}} = 5.833$

(b) $Q_{\text{air}} = 8.333$

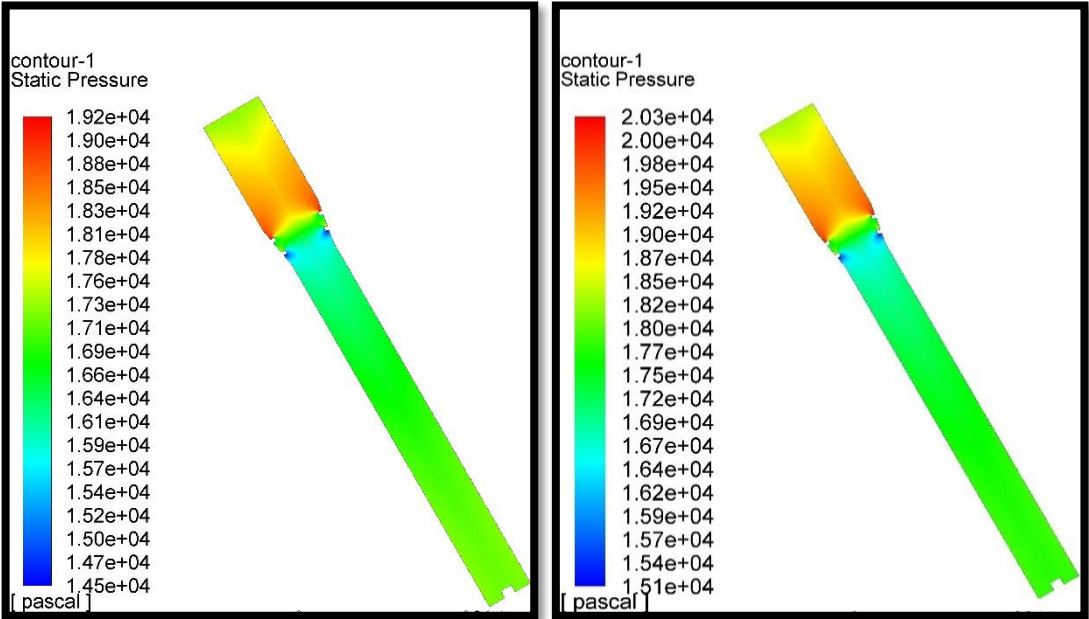
(c) $Q_{\text{air}} = 10.833$



(d) $Q_{\text{air}} = 13.333$

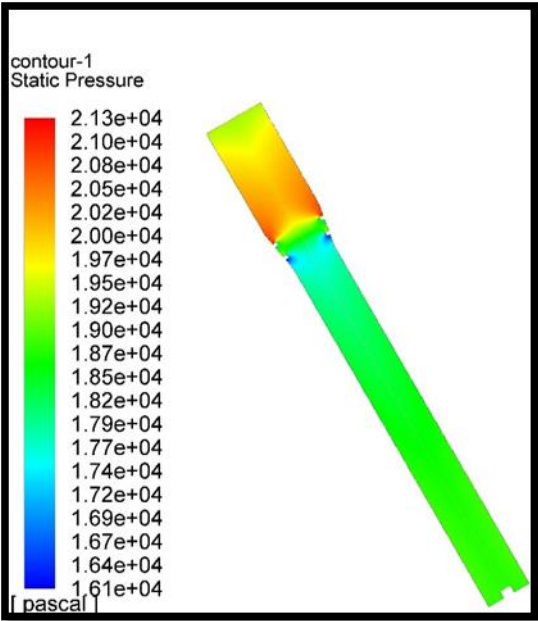
(e) $Q_{\text{air}} = 16.666$

Figure (5.11): Effect of air discharge on pressure distribution at 20 L/min water discharge (opening angle 10 degree)



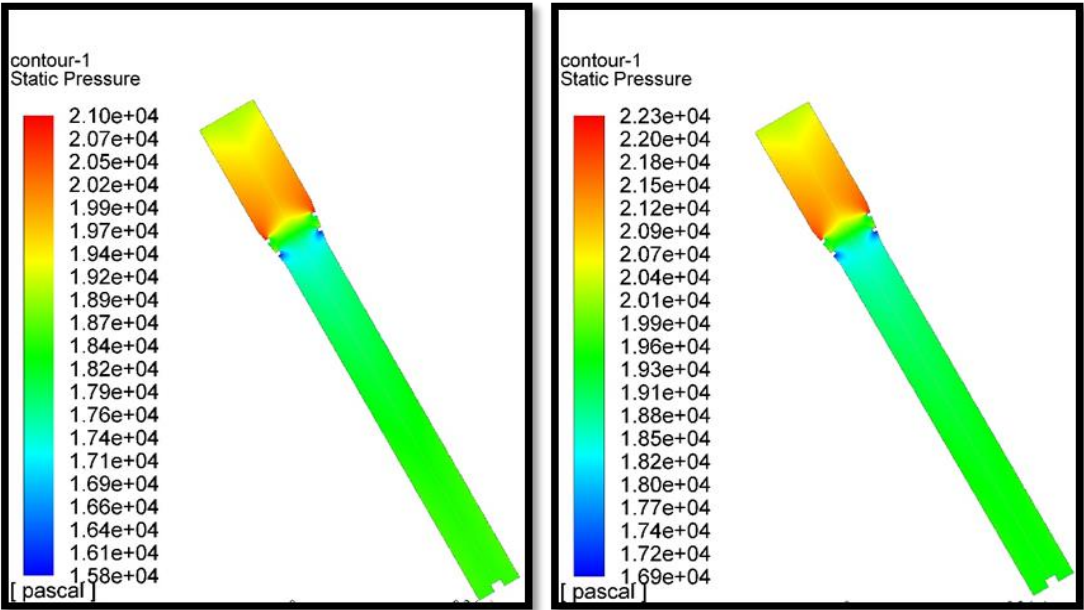
(a) $Q_{\text{air}} = 5.833$

(b) $Q_{\text{air}} = 10.833$



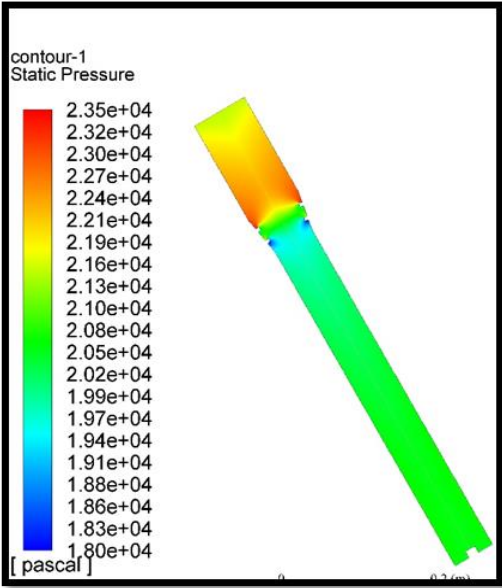
(c) $Q_{\text{air}} = 16.666$

Figure (5.12): Effect of air discharge on pressure distribution at 5 L/min water discharge (opening angle 10 degree)



(a) $Q_{air} = 5$

(b) $Q_{air} = 10.833$

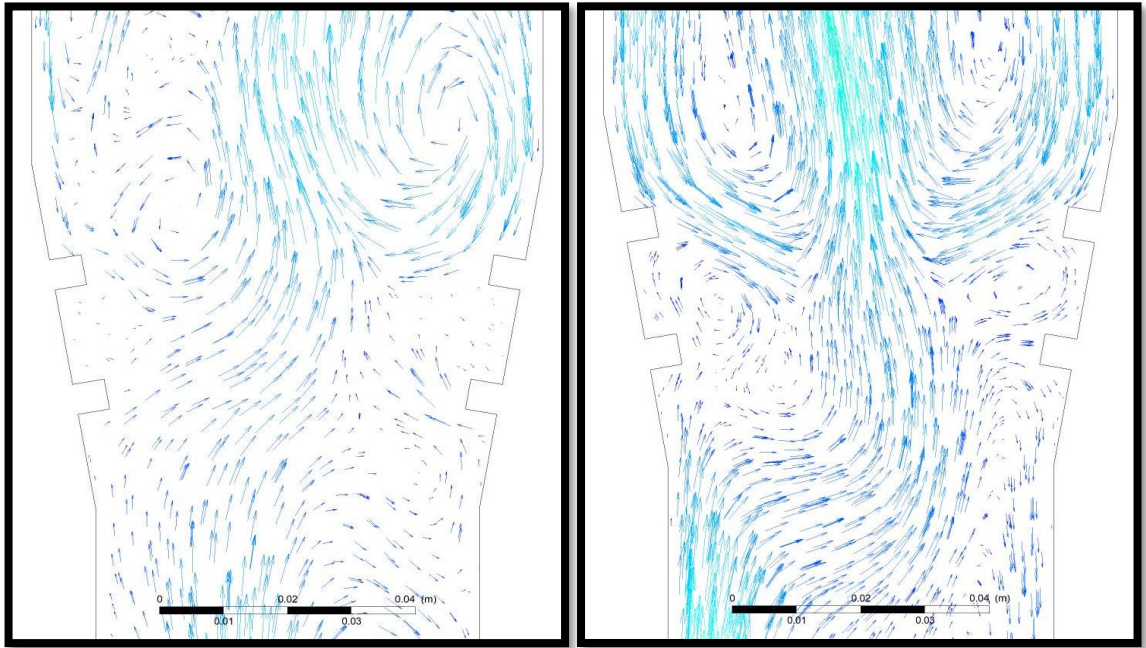


(c) $Q_{air} = 16.666$

Figure (5.13): Effect of air discharge on pressure distribution at 20 L/min water discharge (opening angle 10 degree)

5.2.2. B. Velocity Vector

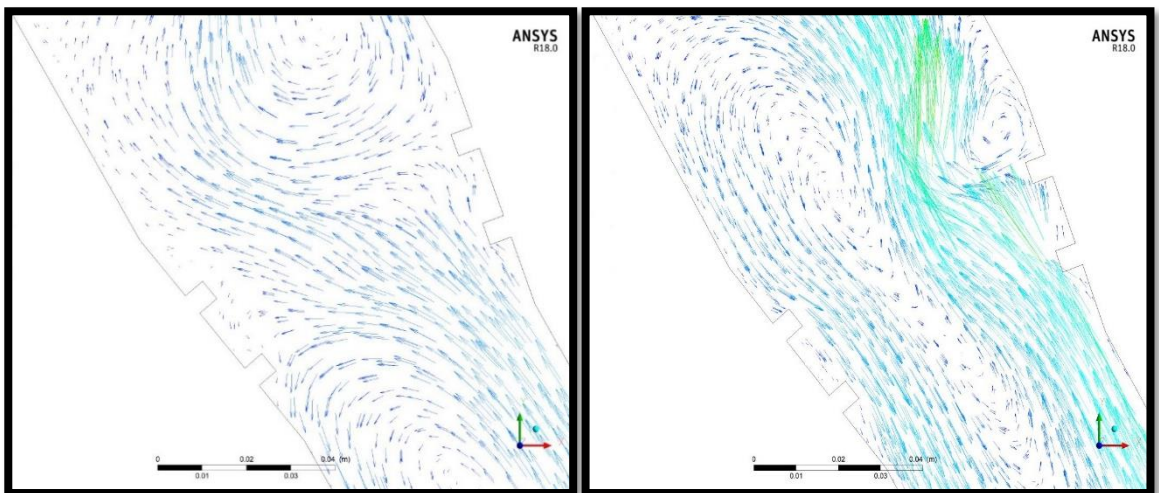
The figures from (5.14) to (5.17) represent the velocity vector for different cases, which indicates the direction of velocity. It can be noted from these figures that the velocity vector is affected by the turbulence of flow where it is formed as vortices, where the number and size of vortices have increased by increasing the turbulence of flow.



(a) $Q_{air}=5.883$ L/min

(b) $Q_{air}=16.66$ L/min

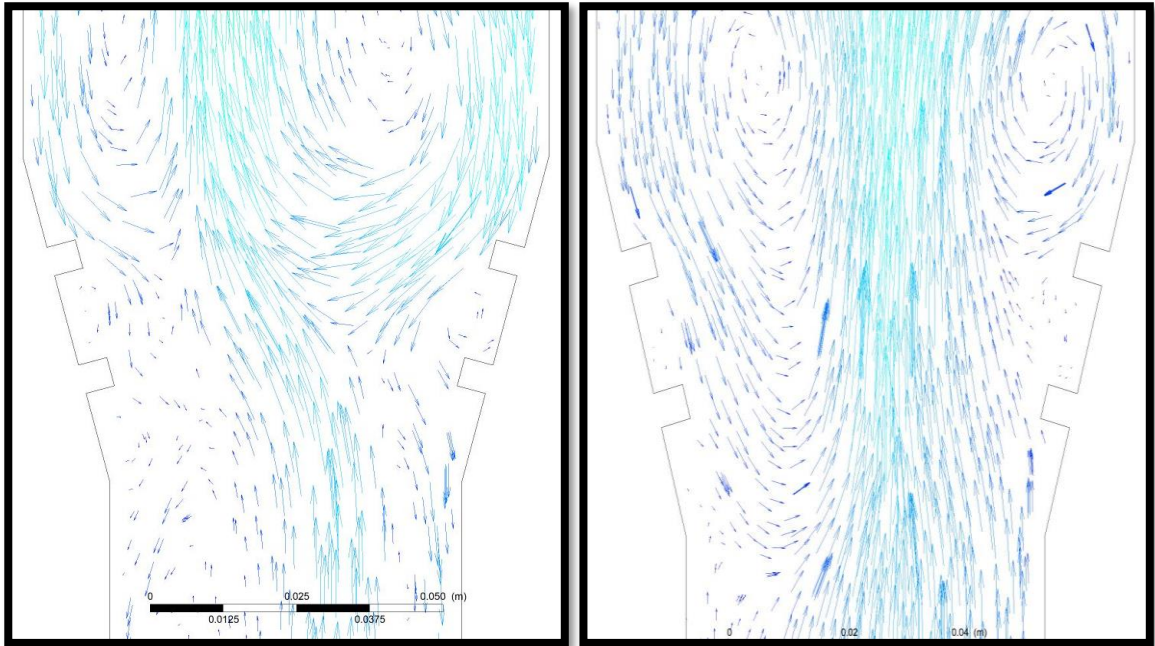
Figure (5.14): velocity vector at 5 L/min water discharge (opening angle 10 degree)



(a) $Q_{air}=5.883$ L/min

(b) $Q_{air}=16.66$ L/min

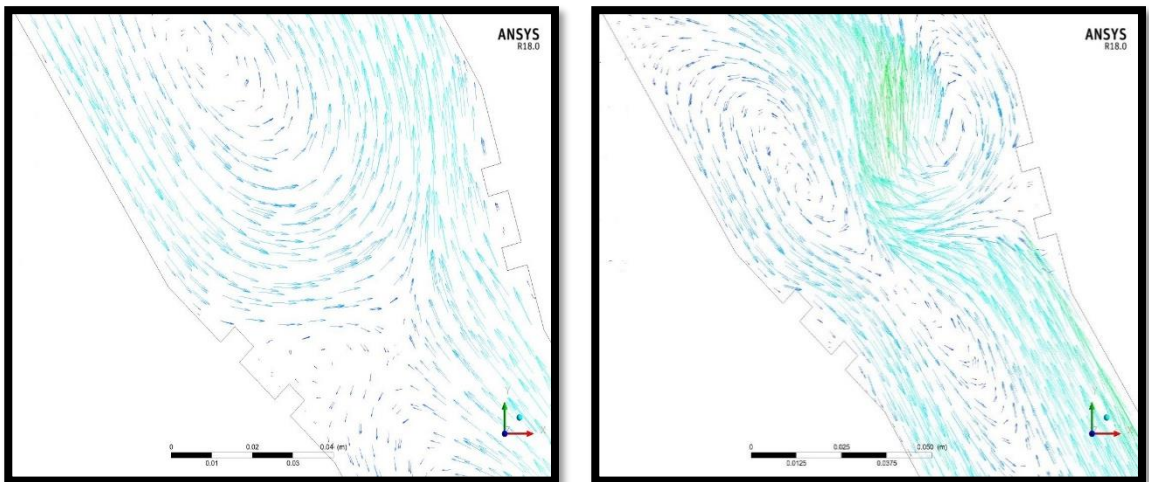
Figure (5.15): velocity vector at 5 L/min water discharge (opening angle 10 degree)



(a) $Q_{air}=5.883$ L/min

(b) $Q_{air}=16.66$ L/min

Figure (5.16): velocity vector at 5 L/min water discharge (opening angle 15 degree)



(a) $Q_{air}=5.883$ L/min

(b) $Q_{air}=16.66$ L/min

Figure (5.17): velocity vector at 5 L/min water discharge (opening angle 15 degree)

5.2.3. Comparison between Experimental and Numerical Results

5.2.3. A. Effect of Water and Air Discharge on the Pressure Profile

It was observed that the effect of increasing the discharge of air or water on pressure distribution was similar for both experimental and numerical works. Also, the values of experimental and numerical results were close and the maximum deviation was (7%). It was also observed that the numerical results were greater than the results of the experimental result due to neglect of several effects such as neglect of the turbulence caused by the pump and neglect of the effect of sharp edges of enter the air and water on the pressure and also neglect the friction between the phases.

Figures (5.18) to (5.31) demonstrate the comparison between the experimental and numerical results for the effect of increasing water discharge on the pressure profile at four different points along the vertical testing channel with opening angle (10) and (15) degrees for various values of air discharge.

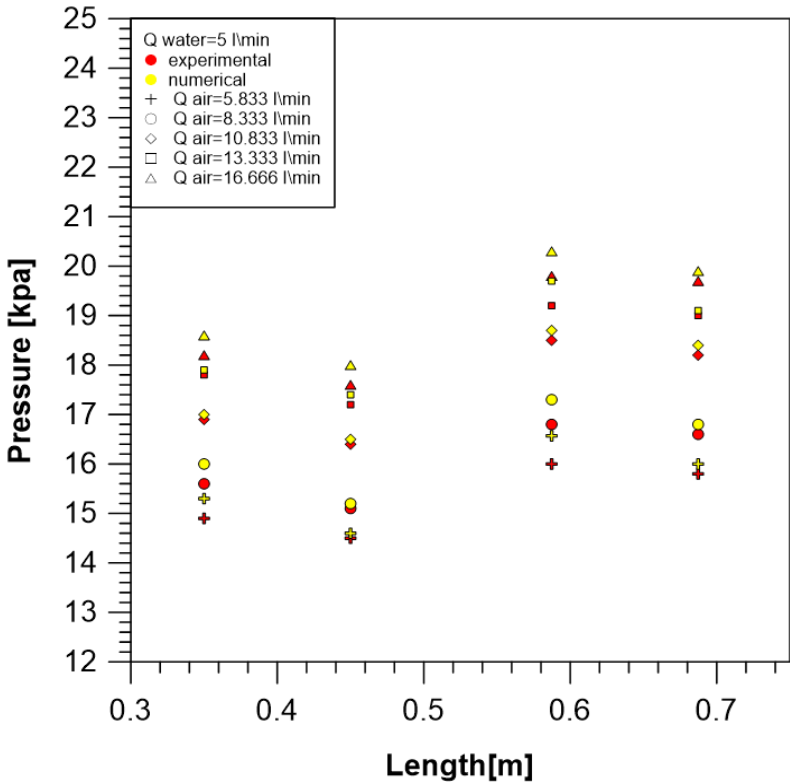


Figure (5.18 a)

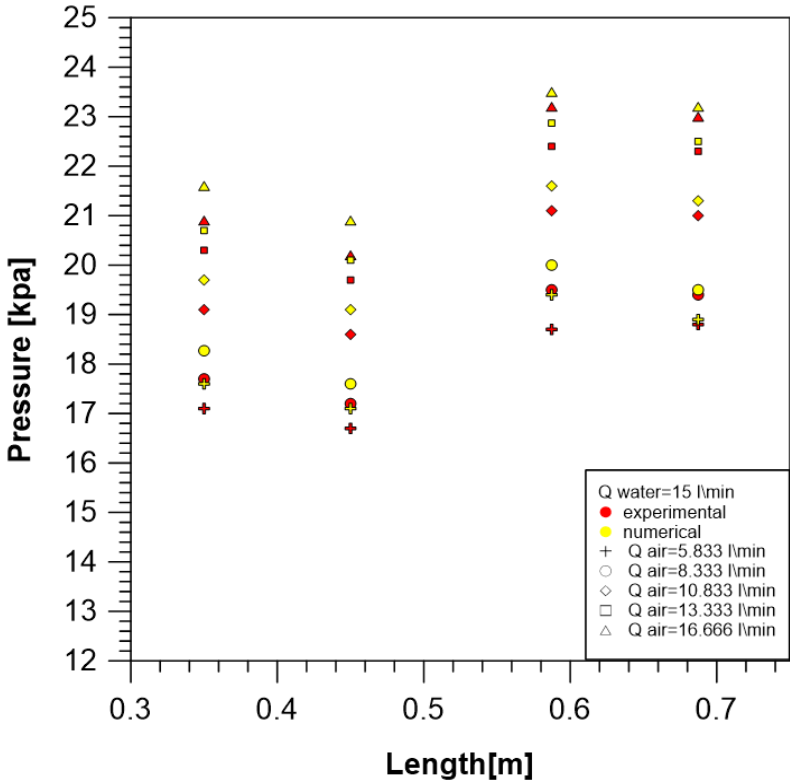


Figure (5.18 b)

Figure (5.18): comparison between the effect of water discharge in experimental And numerical pressure profile for opening angle 15 degree (vertical)

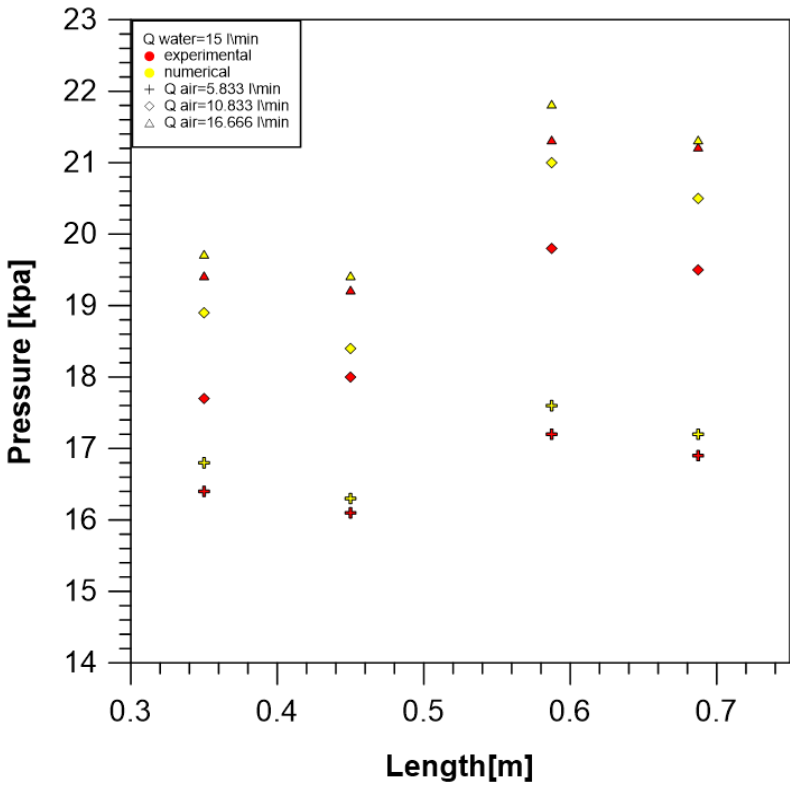


Figure (5.19 a)

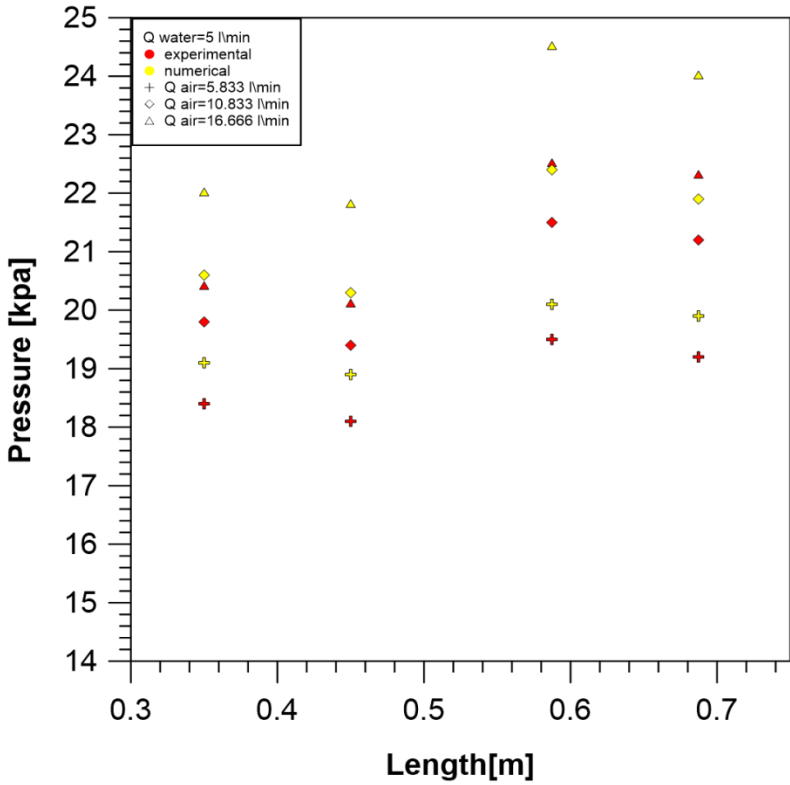


Figure (5.19 b)

Figure (5.19):comparison between the effect of water discharge in experimental And numerical pressure profile for opening angle 15 degree (inclined)

5.2.3. B. The Influence of Water and Air Discharge on The Flow Behavior

The effect of the water and air on the flow behavior are shown in figures (5.20) to (5.23). These figures show the experimental two-phase flow behavior through the photographs that were taken for the testing channel and compared them with the air volume fraction found numerically by ANSYS fluent 18. A close similarity was seen between the experimental and numerical images.

Figure (5.20) represents the experimental and numerical images for the two-phase flow behavior in the divergent ribs in a rectangular vertical duct for water discharge ($Q_w=5$ L/min) and air discharges ($Q_a=5.833$, 10.833 and 16.666) L/min, for the opening divergence angle of 10 degrees. The figure (5.20a), ($Q_a=5.833$) L/min shows that the number of bubbles was less and the volume of the bubble was small due to the low values of air and water discharges. Also, by increasing the air discharge, the volume and number of bubbles increase, when ($Q_a=10.833$) L/min as shown in figure (5.20b). When increasing the air discharge, the turbulence in flow and velocity of the vortex in the divergence section became higher as compared with low air discharge cases as shown in Figure (5.20c) at ($Q_a=16.666$) L/min.

Figure (5.21) shows the images for the two-phase flow at ($Q_w=20$) L/min and air discharges (5.833 , 10.833 and 16.666) L/min. This figure shows that the increase in the discharge of the water makes the flow unstable and increase in the turbulence. Also, it was observed that the eddies in the divergent section were stronger. Generally, the increase in the discharge of air or water led to an increase in the velocity of the bubbles and caused more turbulence in the flow, so it led to generate more bubbles. In addition, it was observed that the increase in water discharge had a

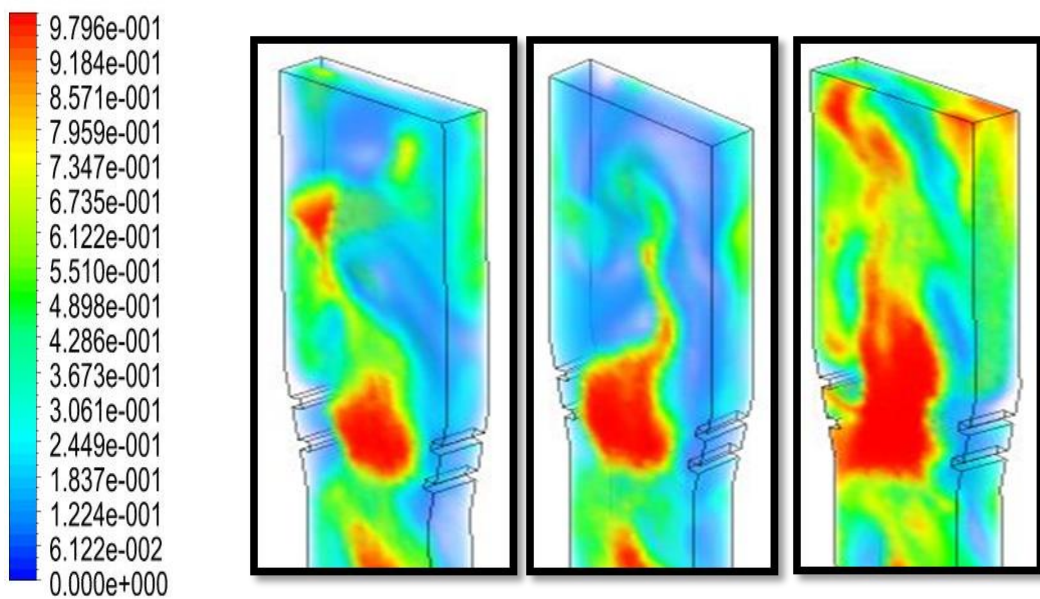
greater effect on the turbulence of flow than the increase in the discharge of air.

Regarding the inclined flow, the effect of an air and water discharge on the flow is similar to the vertical flow cases as shown in the figures from (5.22) to (5.23). Note that the bubbles tend to move towards the far wall of the channel from the inclination angle due to the influence of buoyancy force, which pushes the bubble to the far side of the channel.



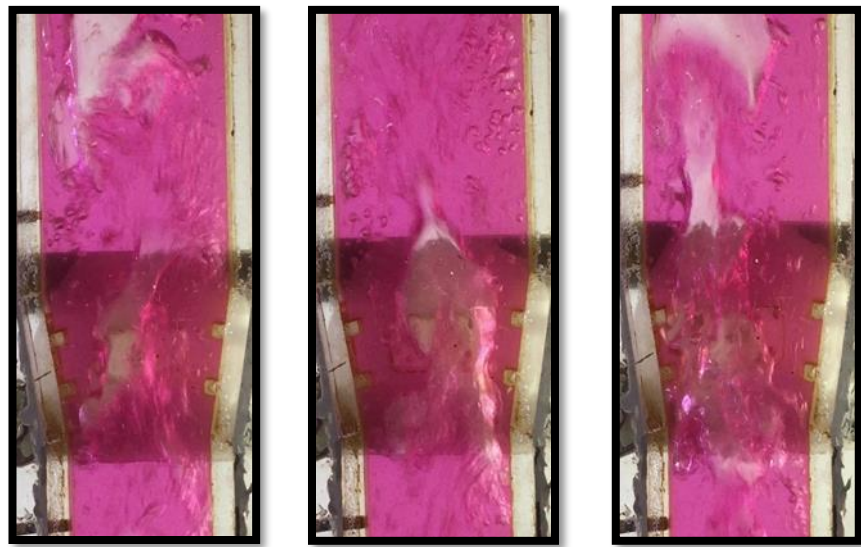
Experimental Q air (a) 5.833 (b) 10.833 (c) 16.666

Phase 2: Volume Fraction
Contour 1



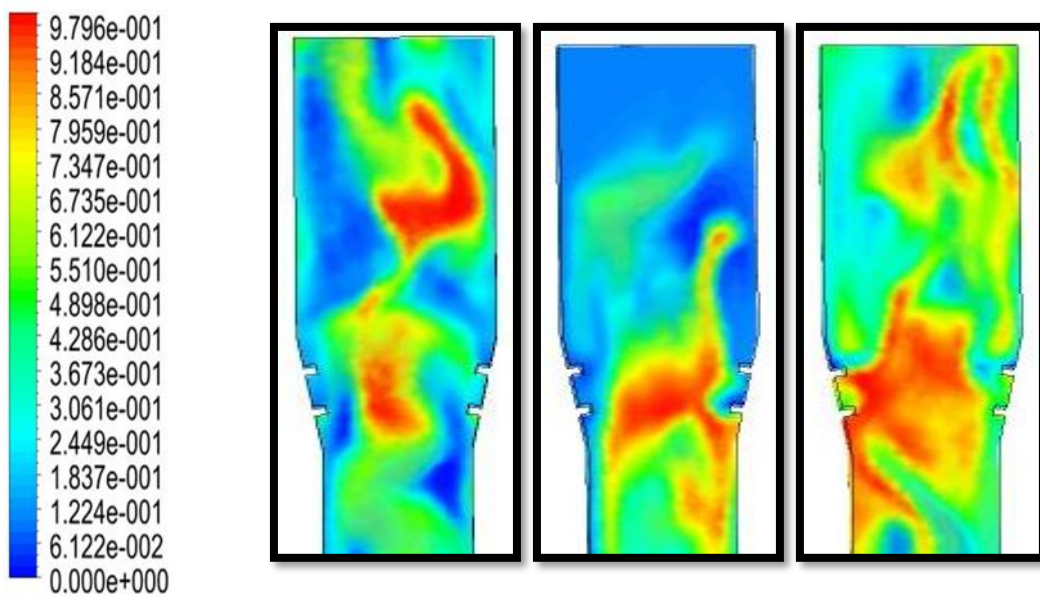
Numerical Q air (a) 5.833 (b) 10.833 (c) 16.666

Figure (5.20) A comparison between the experimental and numerical of effect of water and air discharge on the flow behavior at Q water =5 L/min



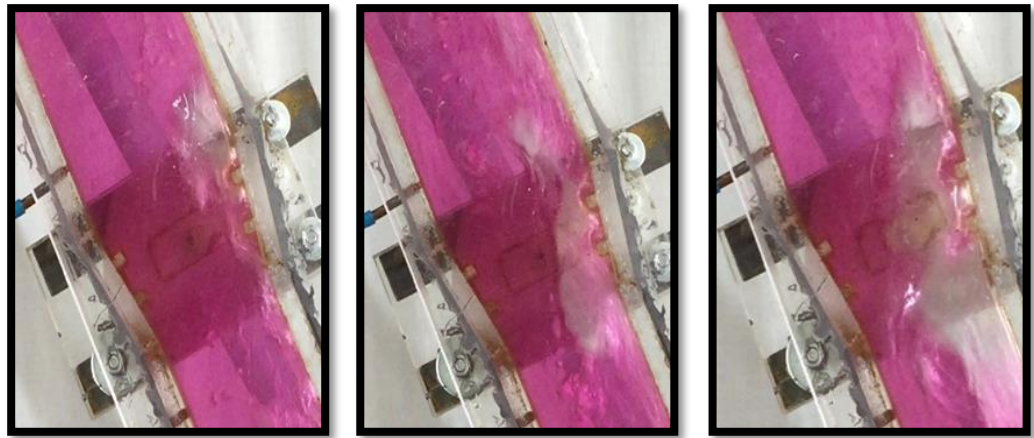
Experimental Q air (a) 5.833 (b) 10.833 (c) 16.666

Phase 2. Volume Fraction
Contour 1



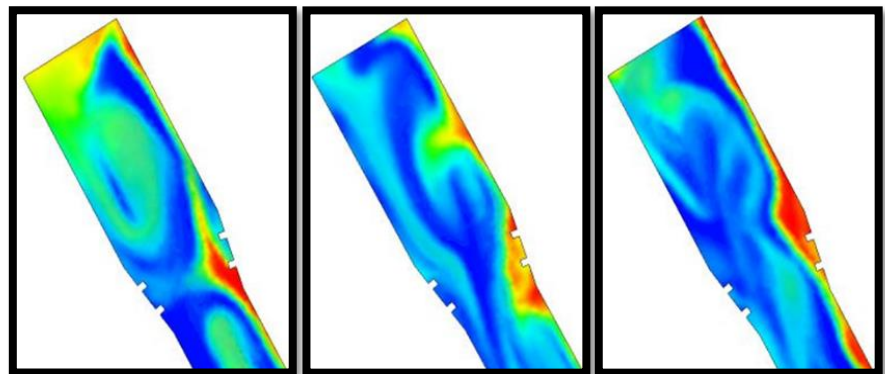
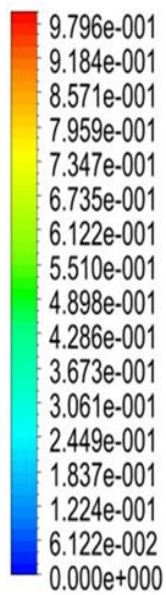
Numerical Q air (a) 5.833 (b) 10.833 (c) 16.666

Figure (5.21) A comparison between the experimental and numerical of effect of air discharge on the flow behavior at $Q_{\text{water}} = 20 \text{ L/min}$



Experimental Q_{air} (a) 5.833 (b) 10.833 (c) 16.666

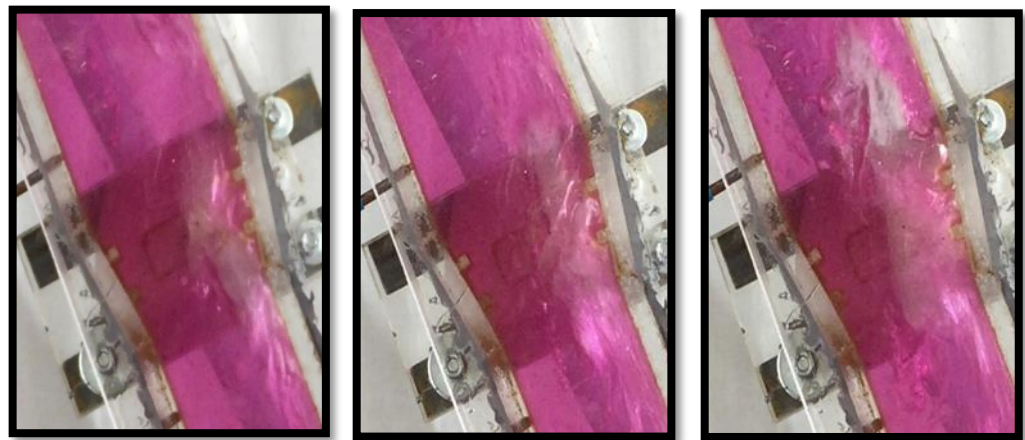
Phase 2: Volume Fraction
Contour 1



Numerical

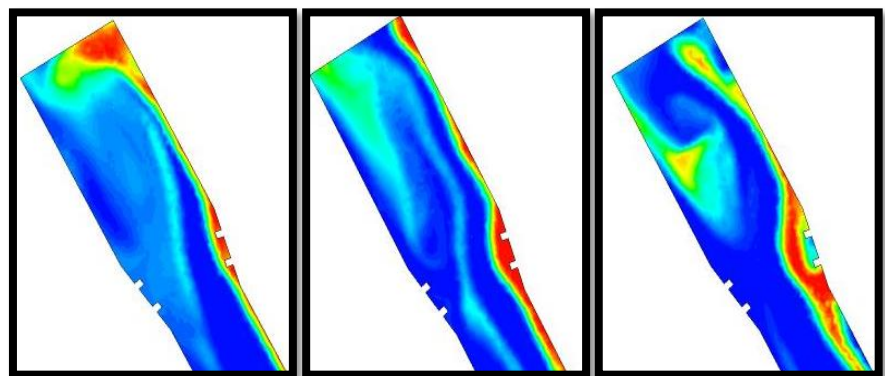
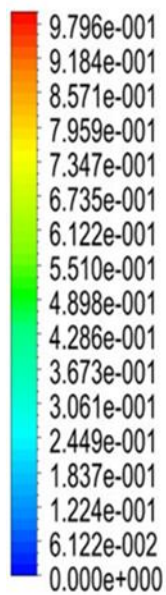
Q_{air} (a) 5.833 (b) 10.833 (c) 16.666

Figure (5.22) A comparison between the experimental and numerical of effect of air discharge on the flow behavior at $Q_{water} = 5 \text{ L/min}$



Experimental Q air (a) 5.833 (b) 10.833 (c) 16.666

Phase 2 Volume Fraction
Contour 1



Numerical

Q air (a) 5.833 (b) 10.833 (c) 16.666

Figure (5.23) A comparison between the experimental and numerical of effect of air discharge on the flow behavior at $Q_{\text{water}} = 20 \text{ L/min}$

5.2.4. Visualization and Flow Pattern Maps

By observing the flow during the vertical divergence testing section, it was observed that the current flow pattern at the downstream and upstream for the divergence section was a slug flow. While the flow pattern through the divergence section cannot be determined due to the high disturbance caused by the mixing of the phases made by the presence of the ribs, in particular when a high discharge of the air or water, as shown in Figure (5.24).

Figure (5.25) shows the flow pattern map at the upstream divergence testing channel. A common chart is the one proposed by Hewitt and Roberts [8] that has been established for vertical flow in pipes of the constant cross section. The flow map for upstream shows that the test cases that listed in (Table 4.2) are residing on the slug and churn, in contrast to the observation during the experiment that showed that the flow pattern was only a slug flow. This is because some experiment conditions of the present work do not correspond to the standard conditions of Hewitt and Roberts' [8] map.

For the inclined flow, the dominant flow pattern was the slug flow as shown in figure (5.26). In the present work, the proposed flow map by Barnea[41] has been used. Note that it achieved excellent prediction for present work as shown in figure (5.27), where it was noted that all points are located in the region of a slug.

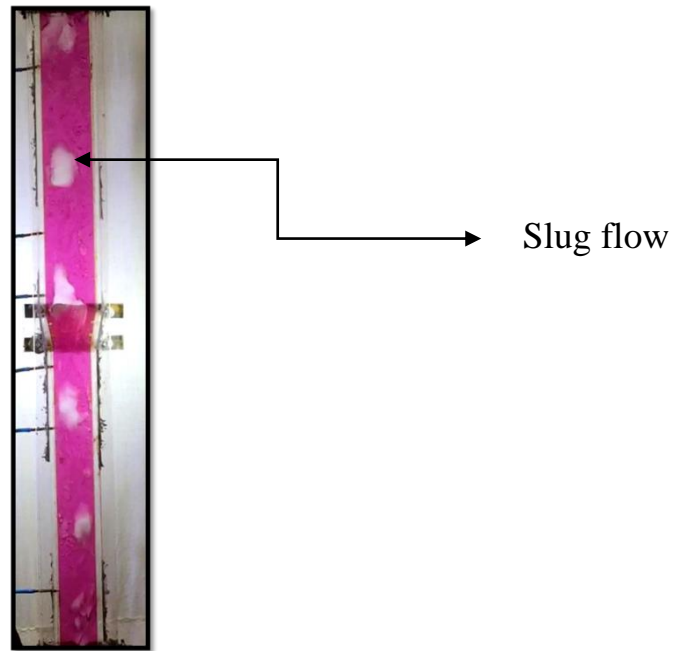


Figure (5.24): Flow pattern in vertical channel

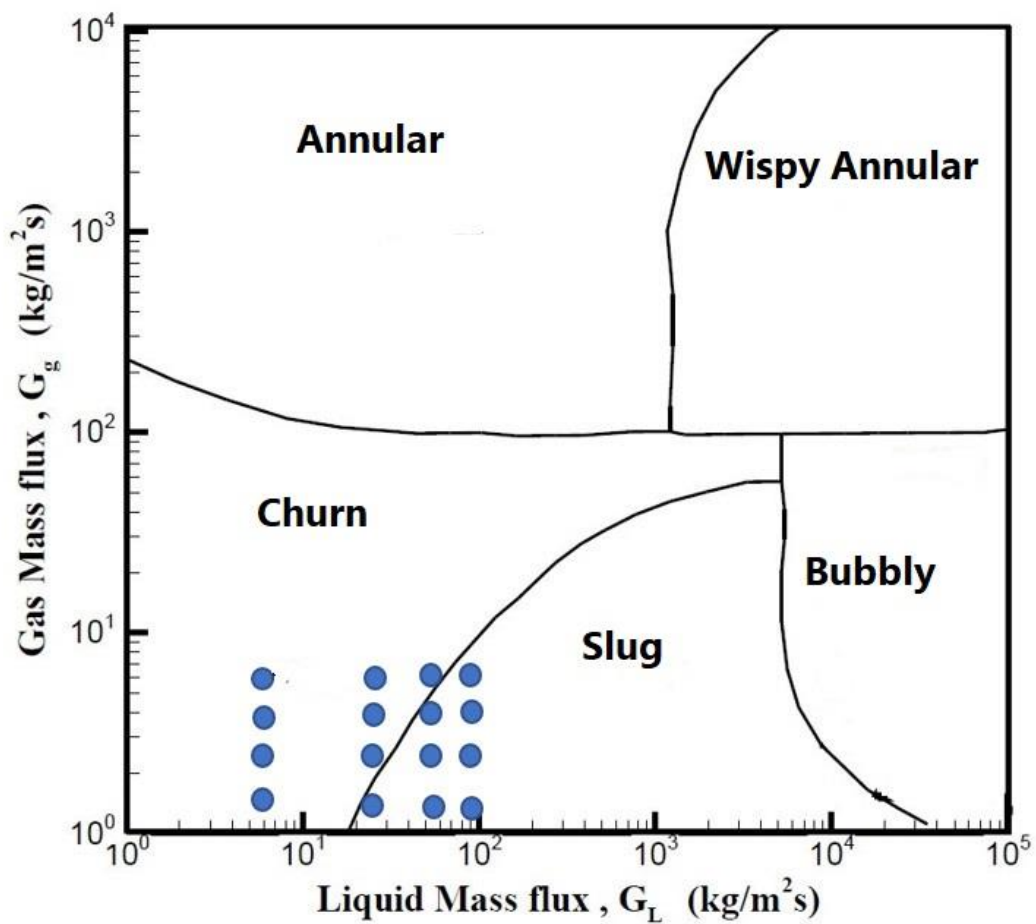


Figure (5.25): Flow pattern map of Hewitt and Roberts

[8]for vertical flow



Figure (5.26): flow pattern in inclined channel

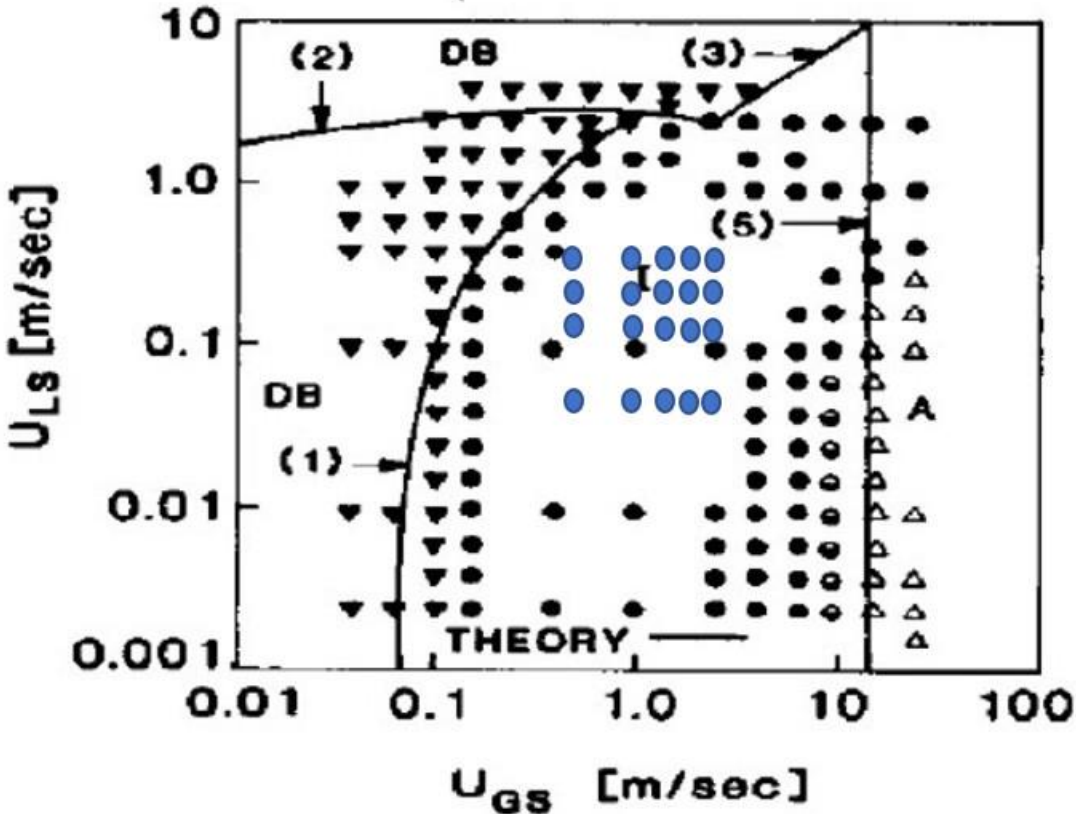


Figure (5.27) Flow pattern map Barnea[41] for inclined flow

The symbol in this flow patterns map is defined in figure (5.28)

□	STRATIFIED SMOOTH	(SS)	} STRATIFIED (S)
■	STRATIFIED WAVY	(SW)	
○	ELONGATED BUBBLE	(EB)	} INTERMITTENT (I)
●	SLUG	(SL)	
●	CHURN	(CH)	
△	ANNULAR, ANN./DISP	(AD)	} ANNULAR (A)
▲	WAVY ANNULAR	(AW)	
▼	DISPERSED BUBBLE	(DB)	

Figure (5.28)

The symbol represents ● the test cases in the present work According to the Table 4.2 for vertical flow pattern map and Table 4.1 for inclined flow.

5.3. Two-Phase Flow through the Convergence Section for Vertical and Inclined Position

5.3.1 Experimental Results

5.3.1. A. Effect of Water and Air Discharge on the Pressure Profile

The experimental results of the impact of increasing air and water discharge on the pressure profile can be shown in figures (5.29) to (5.32). It can be seen from these figures that the pressure in the testing channel decrease from the bottom to the top, especially in the convergence section. Also, It can be seen that the effect of increasing water or air discharge for the case of the convergent section is similar to that of divergent section. From the observation, it can be concluded that the pressure profile increased when the air or water discharge increased.

Figures (5.29) and (5.30), deal with the experimental results of the pressure profile for the vertical testing channel with convergence angle 10 and 15 degrees, respectively with different air discharge of (5.833,8.333,10.833,13.333 and 16.666) L/min and water discharge of (5,10,15,20) L/min. As the discharge of the water increase from (5) L/min to (20) L/min at the same location of pressure transducer and constant air discharge (0.35) m and (5.833) L/min, the value of the experimental pressure increase from 16.1 kpa to 18.5 kpa for convergence angle 10 degree, and from (15.9) kpa to 18.8 kpa for convergence angle 15 degree.

Figures (5.31) and (5.32) show the experimental results of the pressure profile for the inclined testing channel with convergence angle 10 and 15 degrees, respectively, with different air discharge (5.833,10.833 and 16.666) L/min and water discharge (5, 15,20) L/min. As the discharge of the water increase from 5 L/min to 20 L/min at the same location of pressure transducer and constant air discharge (0.35) m and (5.833) L/min, the value of the experimental pressure increase from 15.1 kpa to 16.8 kpa

for convergence angle 10 degree, and from 15.4 kpa to 17.3 for convergence angle 15 degree.

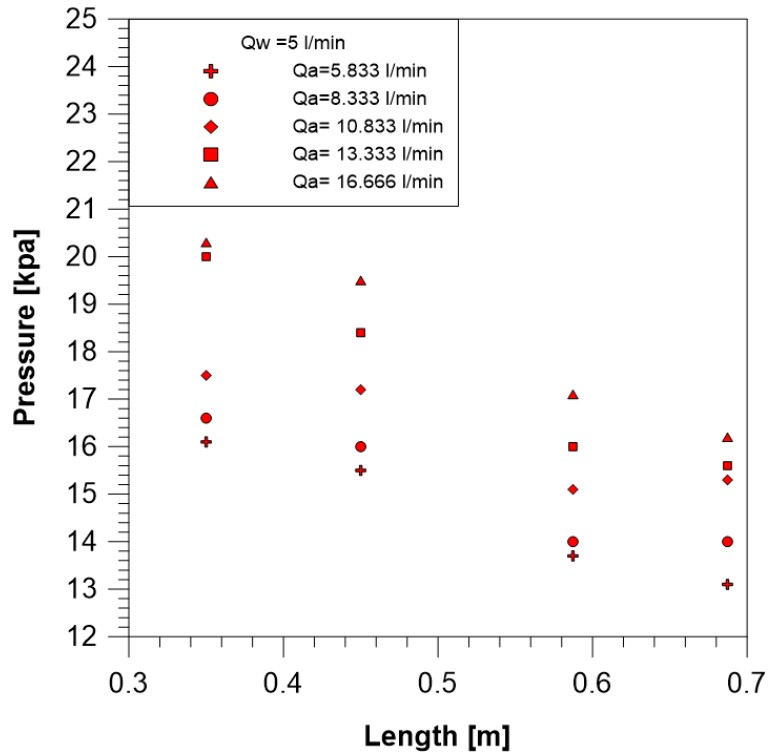


Figure (5.29 a)

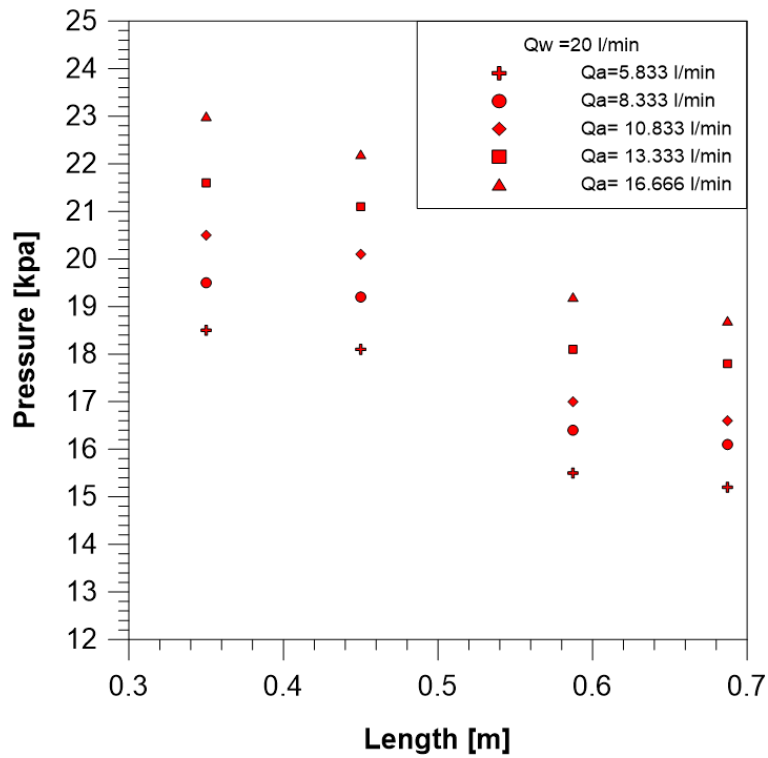


Figure (5.29 b)

Figure (5.29): Effect water discharge on Pressure profile for convergence angle 10 degree (vertical)

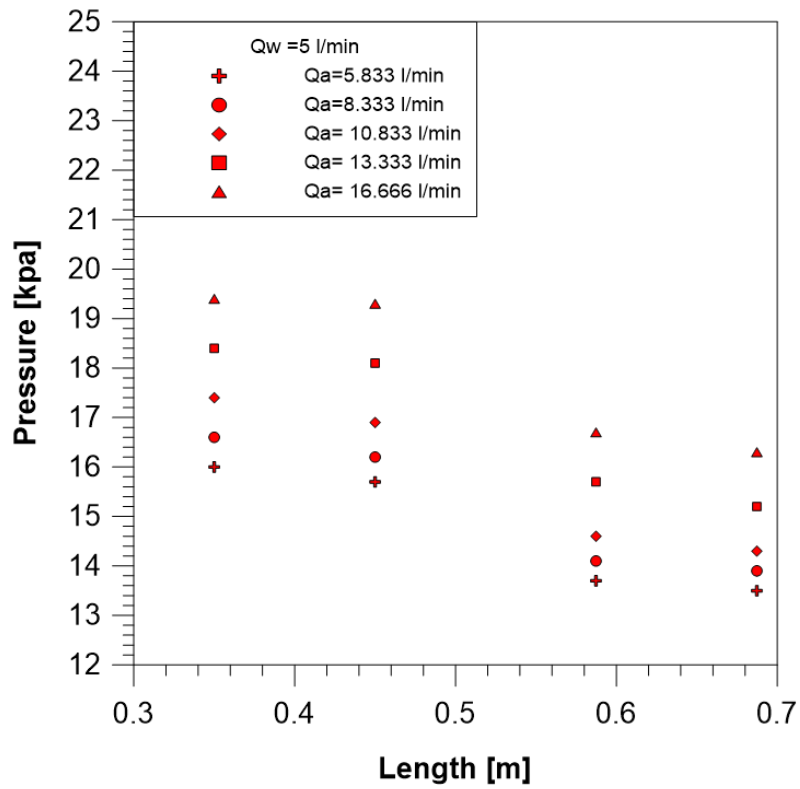


Figure (5.30 a)

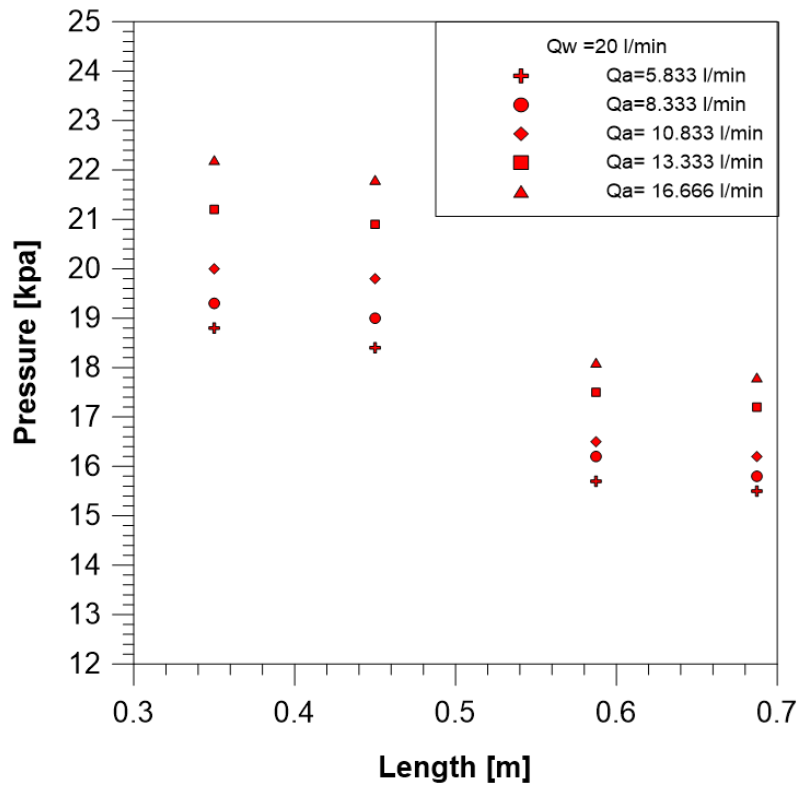


Figure (5.30 b)

Figure (5.30): Effect water discharge on Pressure profile for convergence angle 15 degree (vertical)

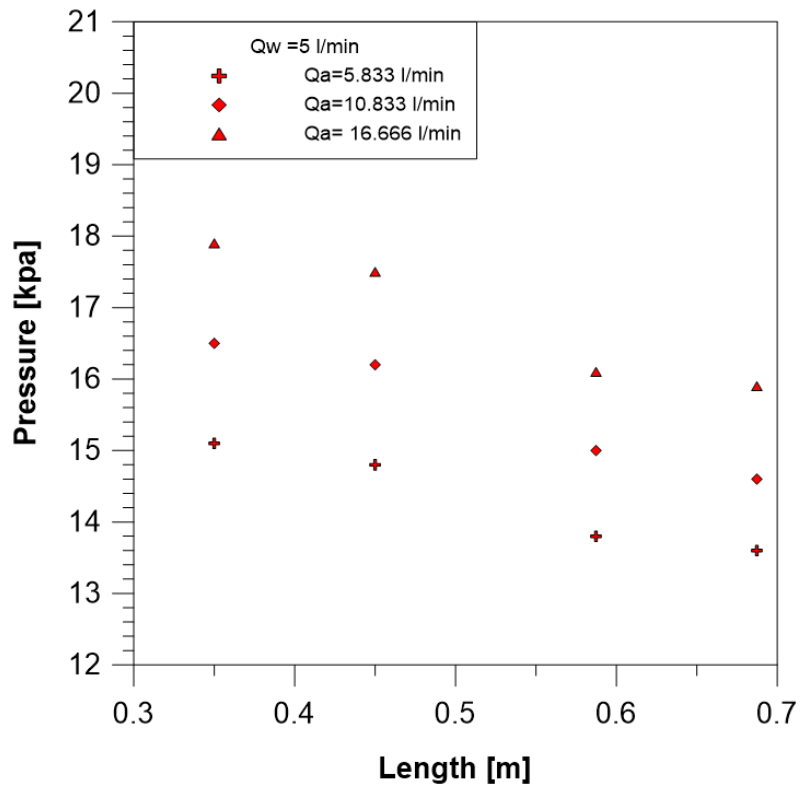


Figure (5.31 a)

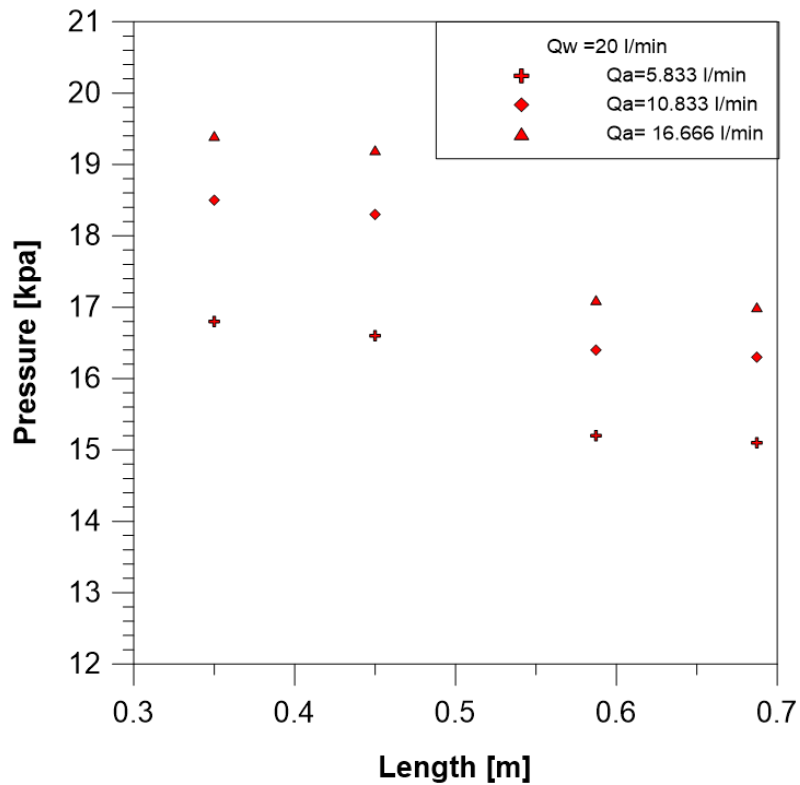


Figure (5.31 b)

Figure (5.31): Effect water discharge on Pressure profile for convergence angle 10 degree (inclined)

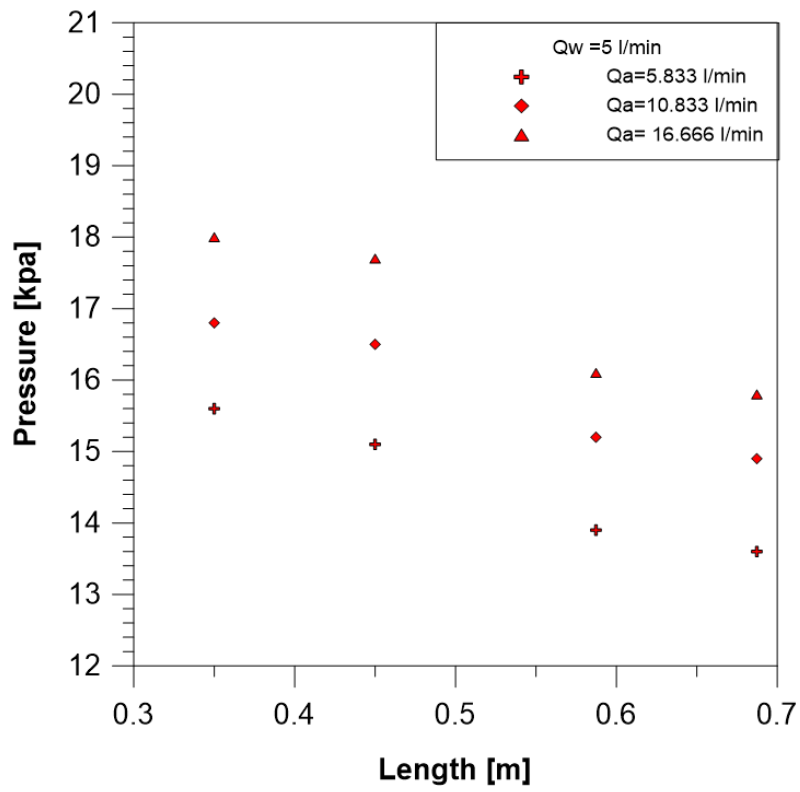


Figure (5.32 a)

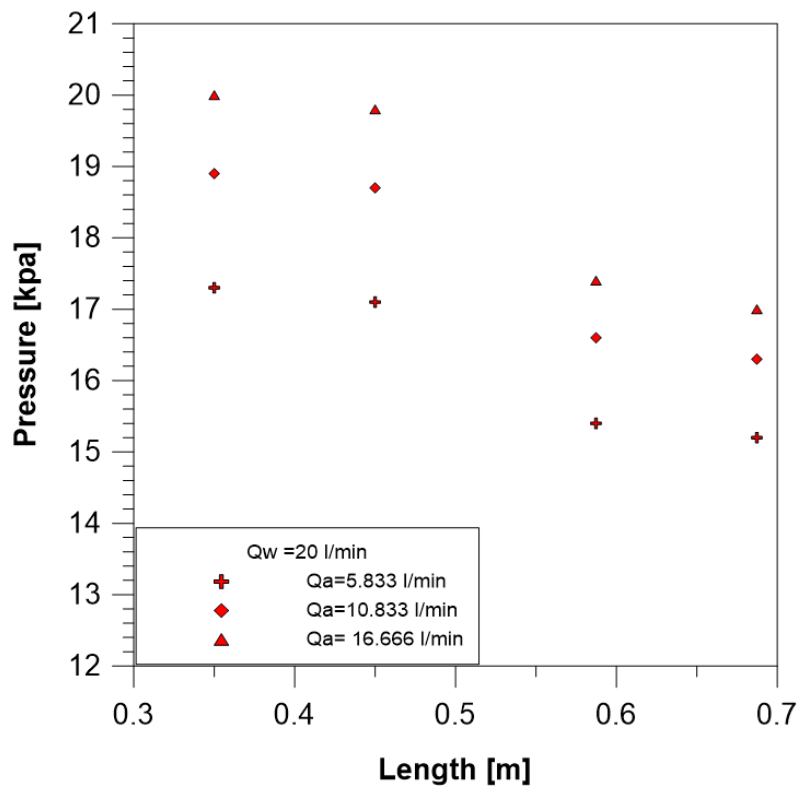


Figure (5.32 b)

Figure (5.32): Effect water discharge on Pressure profile for convergence angle 15 degree (inclined)

5.3.1. B. Effect of Water And Air Discharge And Convergence Angle on The Drop Pressure

The experimental results of the effect of increasing air and water discharge and effect of increasing of convergence angle on the drop pressure through the convergence section can be shown in Figure (5.33) to (5.36). It can be seen from these figures that the drop pressure increased by increasing the discharge rate of the air or water for both the 10 and 15 convergence angles. Also, it was observed that the effect of increasing the convergence angle on the pressure drop in the case of the convergence section was contrary to the effect of increasing the divergence angle on the recovery of pressure in the case of divergence section. So, the drop pressure for the convergence angle 15 is more than the drop pressure at the convergence angle 10 at the same air and water discharge rate because the eddies were more for the case of angle 15. However, the additional flow area contributed to the promotion of pressure drop and led to make the drop pressure more than the case of the convergence angle of 10 degrees.

Figures (5.33) and (5.34) show the values experimental drop pressure through the vertical convergence section for convergence angle 10 degrees and 15 respectively with different air discharge rate of (5.833,8.333,10.833,13.333 and 16.666) L/min and water discharge rate of (5,10,15,20) L/min. As the air discharge increased from (5.833 to 16.666) L/min at a constant water discharge (5) L/min, the drop value of the pressure increased from (1.8 kpa to 2.4 kpa) for convergence angle 10, and from (2 kpa to 2.6 kpa) for convergence angle 15.

Figures (5.35) and (5.36) show the experimental drop pressure through the inclined convergence section for convergence angle 10 and 15 degree, respectively with different air discharge (5.833, 10.833and 16.666) L/min and water discharge (5, 15,20) L/min. As the air discharge increased from (5.833 to 16.666) L/min at constant water

discharge (5 L/min), the value recovery pressure increase from (1kpa to 1.5 kpa) for convergence angle 10, and from (1.2 kpa to 1.6 kpa) for opening angle 15 degree.

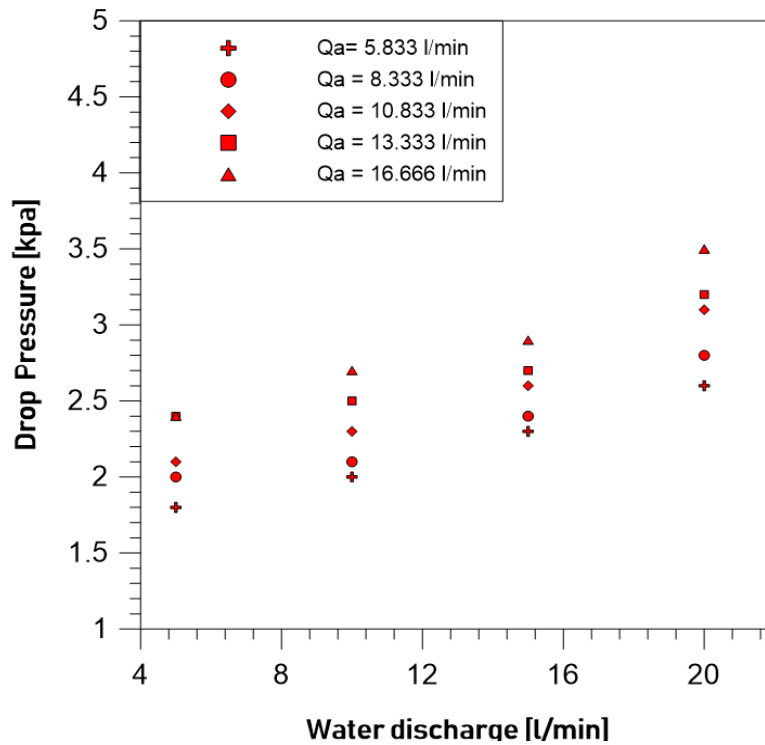


Figure (5.33): Drop pressure for different values of water Discharge at convergence angle 10 degree (vertical)

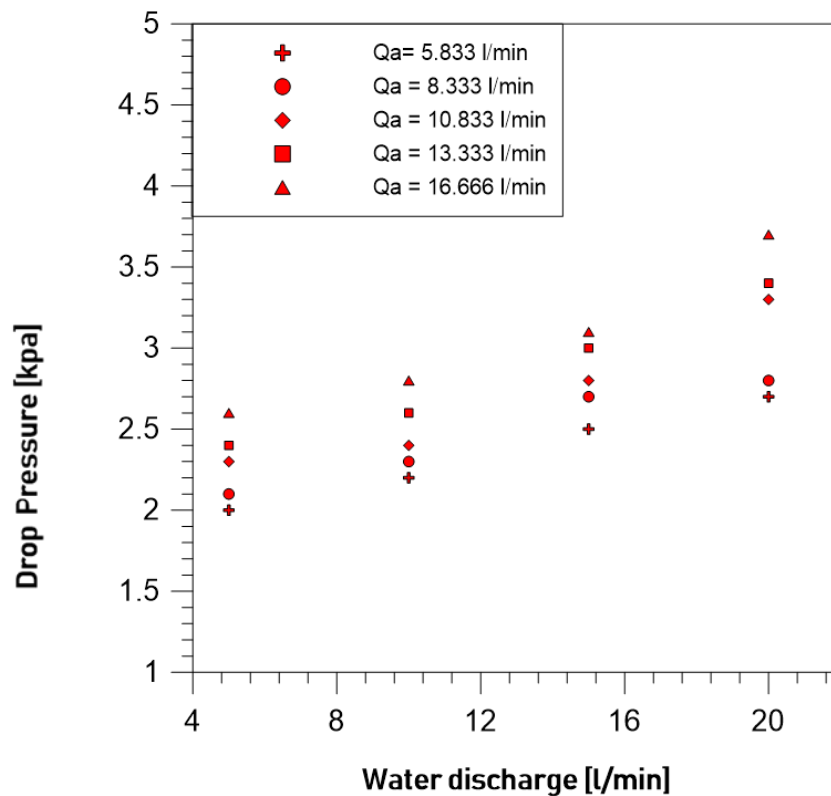


Figure (5.34): Drop pressure for different values of water Discharge at convergence angle 15 degree (vertical)

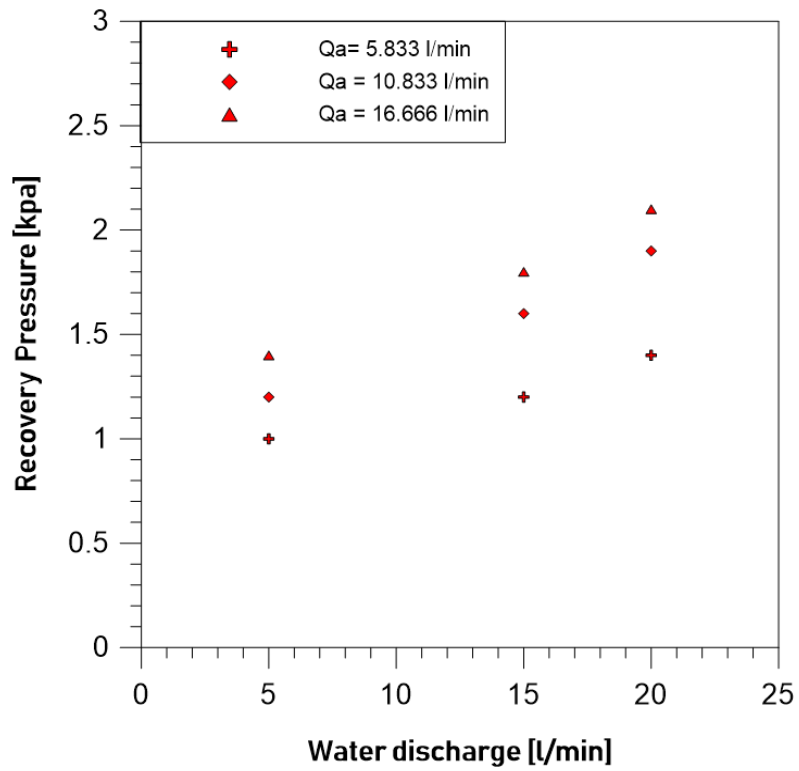


Figure (5.35): Drop pressure for different values of water discharge at convergence angle 10 degree (inclined)

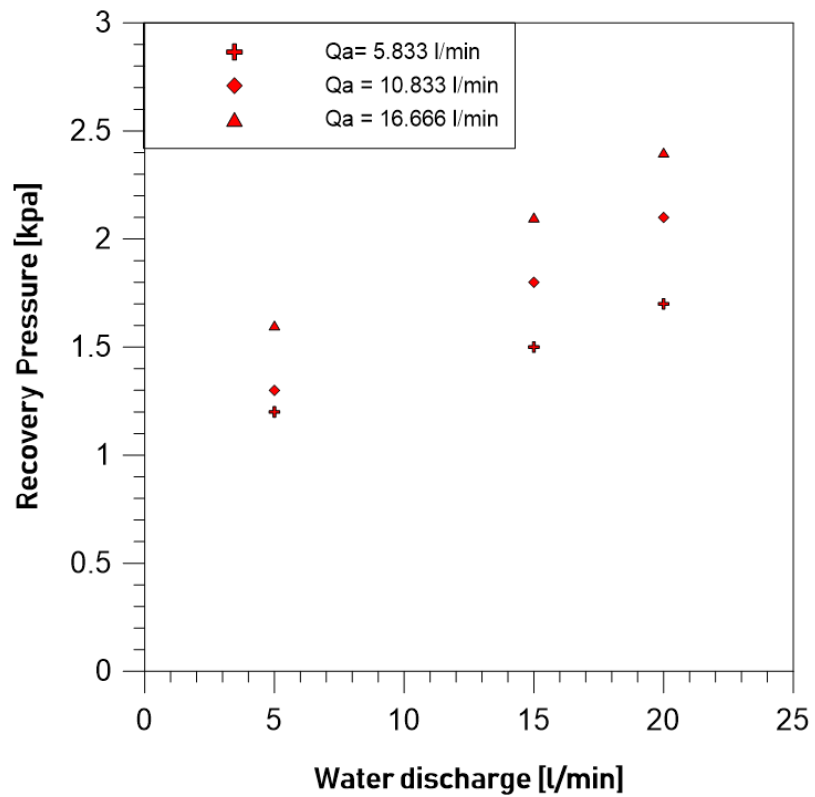


Figure (5.36): Drop pressure for different values of water discharge at convergence angle 15 degree (inclined)

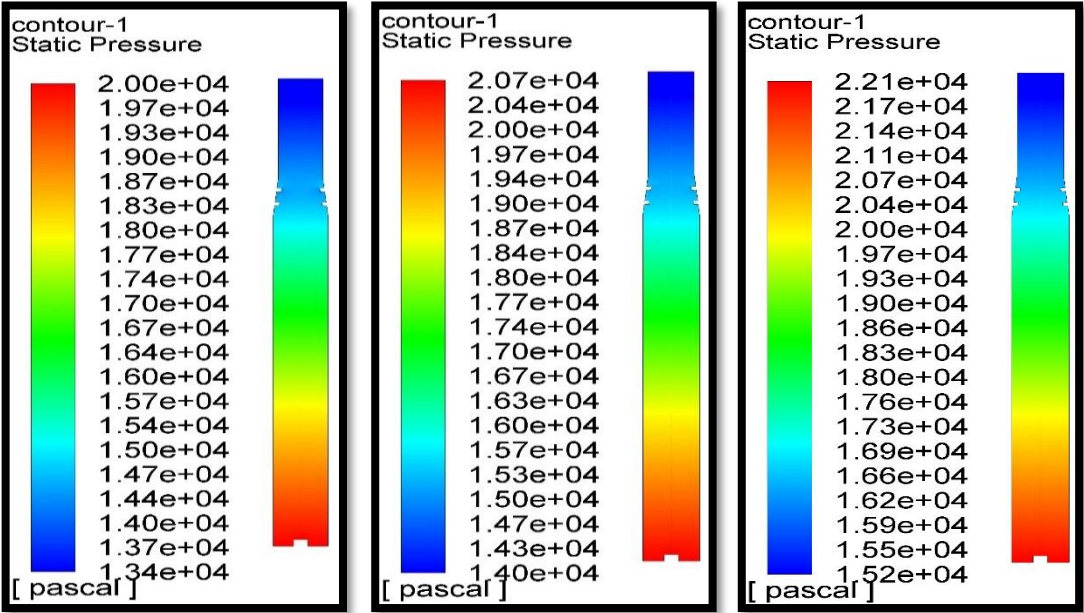
5.3.2. The Numerical Results

5.3.2. A. The Pressure Contour

The figures from (5.37) to (5.40) show the effect of air discharge on contours of pressure at various values of water discharge.

Figures (5.37) to (5.38), show the contours of pressure distribution for two-phase flow through the vertical ribs the convergence testing channel with convergence angle 10 degrees, at various values of water discharge of (5 and 20) L/min. Each figure has five values of air discharge (5.833, 8.333, 10.833, 13.333 and 16.666) L/min.

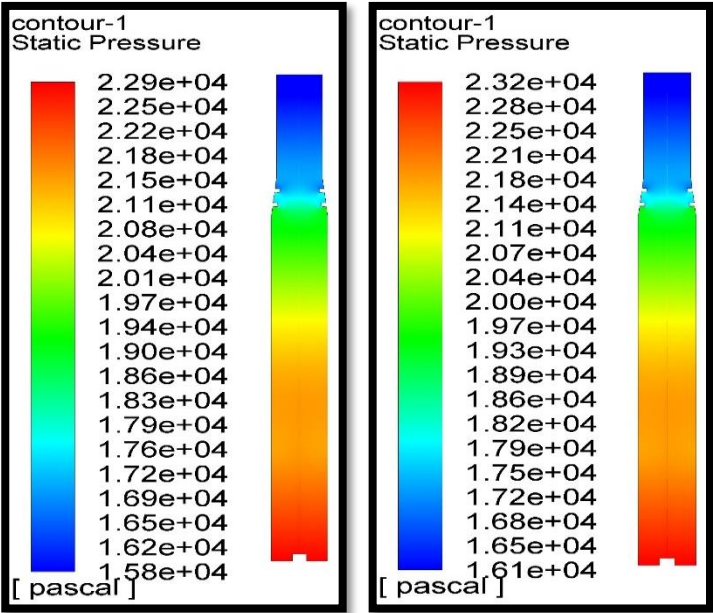
Figures (5.39) to (5.40) show the contours of pressure distribution for two-phase flow through the inclined ribs convergence testing channel with convergence angle 10 degrees, at various values of water discharge of (5, 15 and 20) L/min. Each figure has three values of air discharge (5.833, 10.833 and 16.666) L/min.



(a) $Q_{\text{air}} = 5.833$

(b) $Q_{\text{air}} = 8.333$

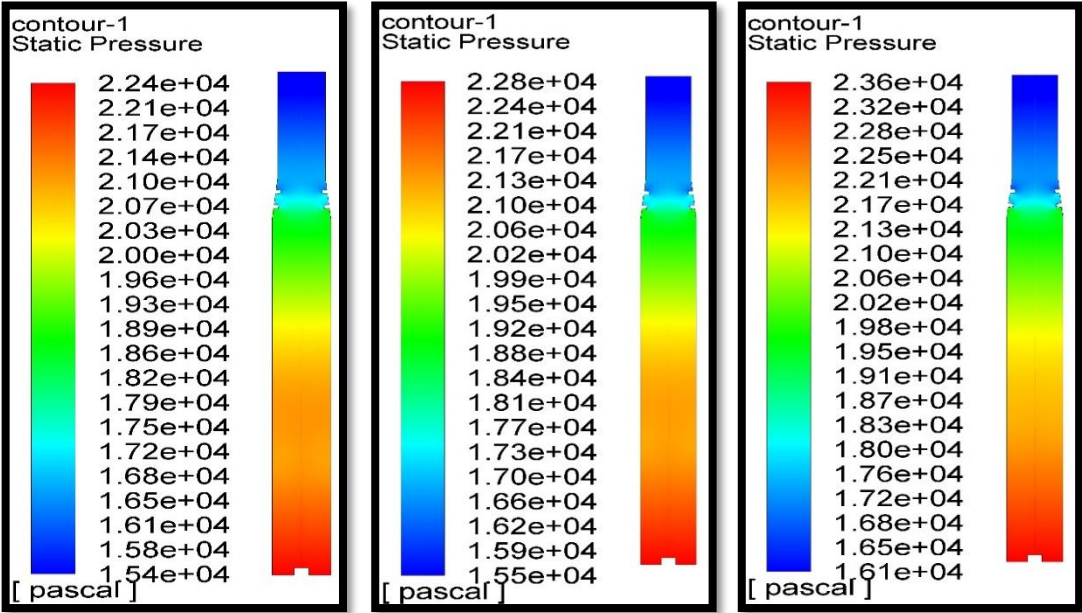
(c) $Q_{\text{air}} = 10.833$



(d) $Q_{\text{air}} = 13.333$

(e) $Q_{\text{air}} = 16.666$

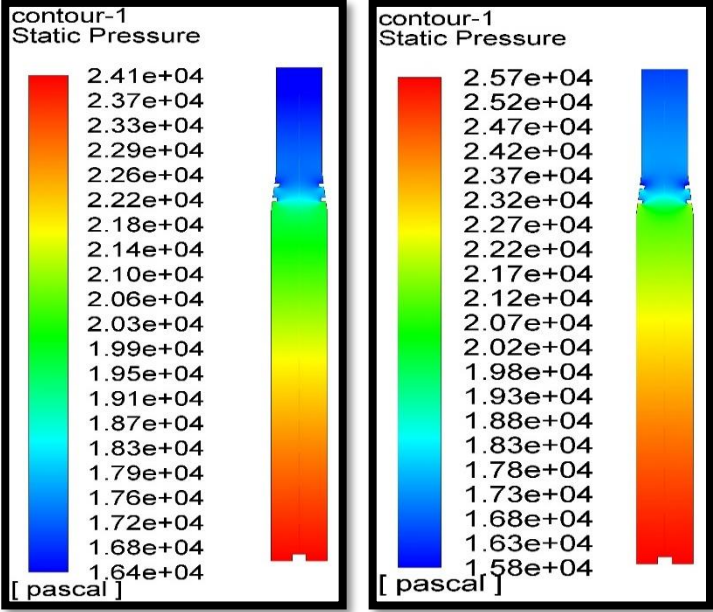
Figure (5.37): Effect of air discharge on pressure distribution at 5 L/min water discharge (convergence angle 10 degree)



(a) $Q_{air} = 5.833$

(b) $Q_{air} = 8.333$

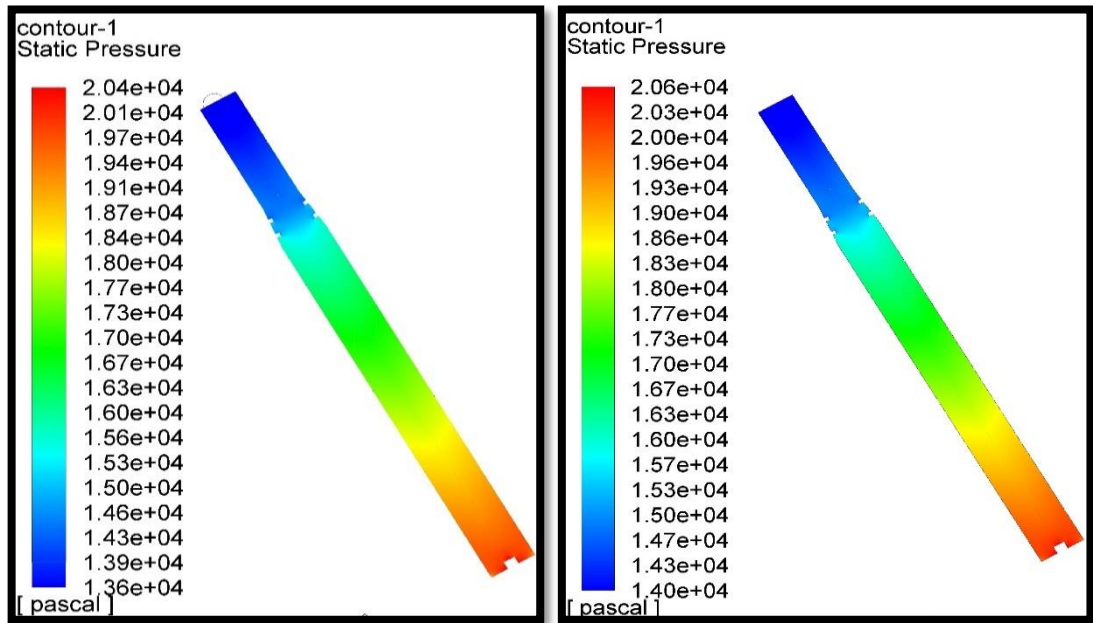
(c) $Q_{air} = 10.833$



(d) $Q_{air} = 13.333$

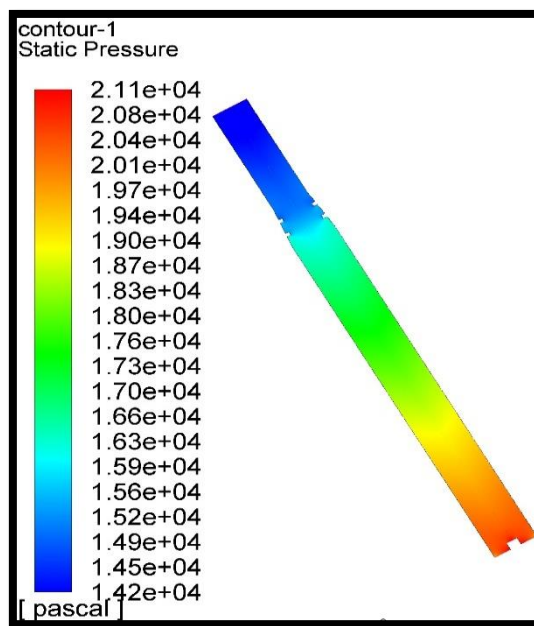
(e) $Q_{air} = 16.666$

Figure (5.38): Effect of air discharge on pressure distribution at 20 L/min water discharge (convergence angle 10 degree)



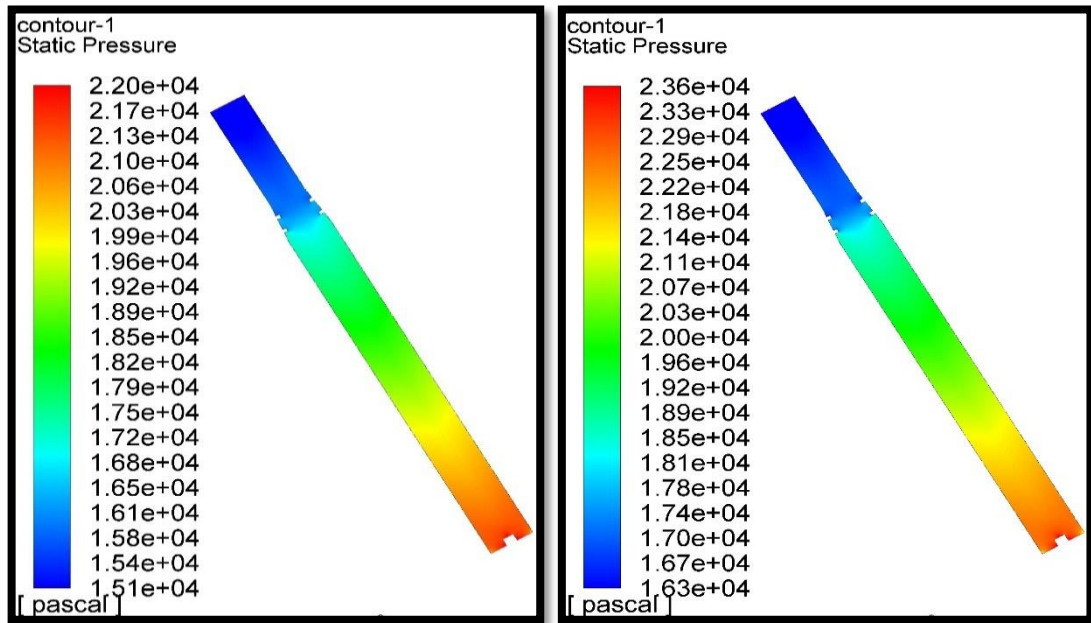
(a) $Q_{\text{air}} = 5.833$

(b) $Q_{\text{air}} = 10.833$



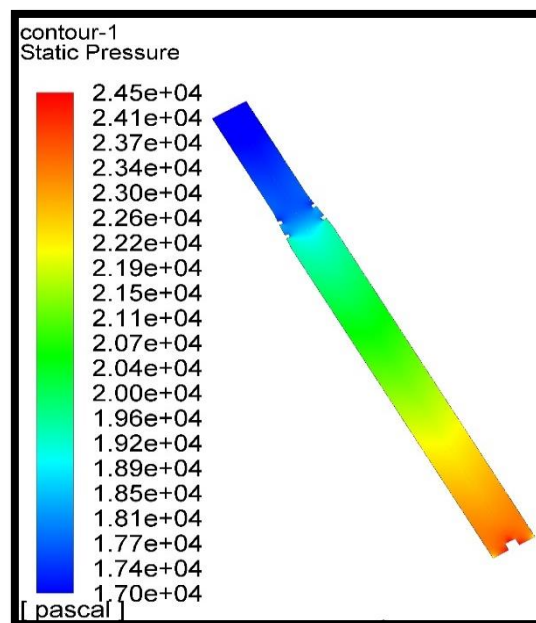
(c) $Q_{\text{air}} = 16.666$

Figure (5.39): Effect of air discharge on pressure distribution at 5 L/min water discharge (convergence angle 10 degree)



(a) $Q_{air} = 5.833$

(b) $Q_{air} = 10.833$

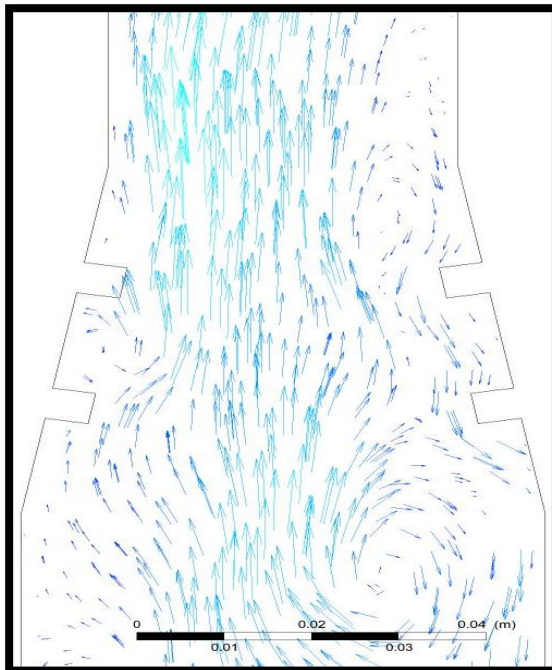


(c) $Q_{air} = 16.666$

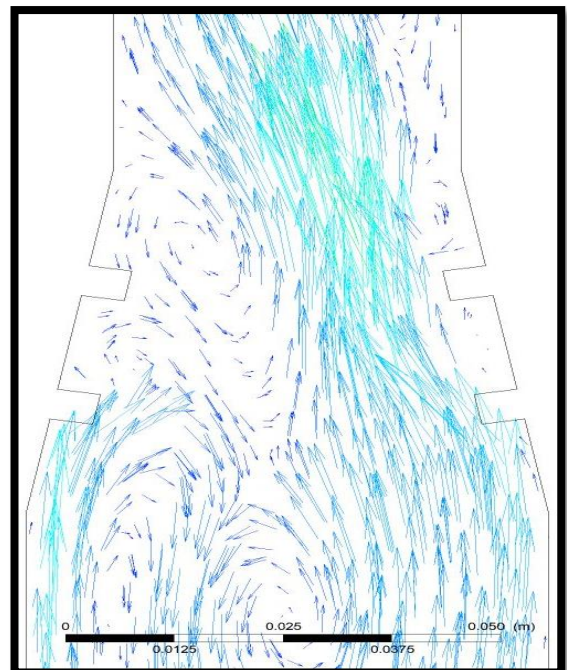
Figure (5.40): Effect of air discharge on pressure distribution at 20 L/min water discharge (convergence angle 10 degree)

5.3.2. B. The Velocity Vector

The figures (5.41) and (5.42) show the velocity vector. It is important to note that the generated vortexes are affected by the increased discharge of the air and water, which lead to increase the turbulence. Also, it is clear that the ribs have a role in changing the direction of velocity and thus generating further turbulence.

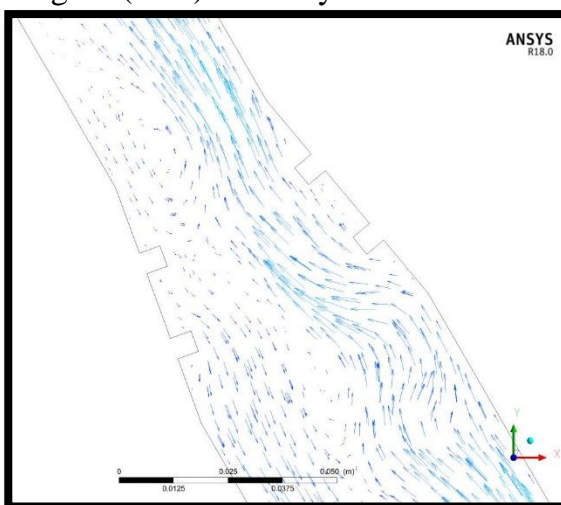


(a) $Q_{air}=5.833$ L/min

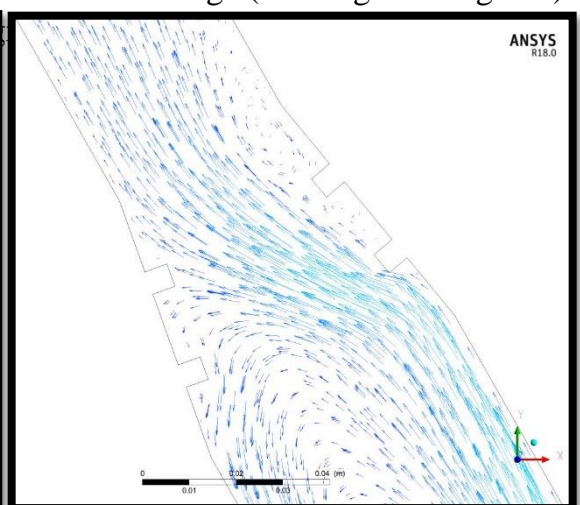


(b) $Q_{air}=16.666$ L/min

Figure (5.41): velocity vector at 5 L/min water discharge (convergence angle 10)



(a) $Q_{air}=5.833$ L/min



(b) $Q_{air}=16.666$ L/min

Figure (5.42): velocity vector at 5 L/min water discharge (convergence angle 10 degree)

5.3.3. Comparison Between Experimental And Numerical Results

5.3.3. A. Effect of Water And Air Discharge on The Pressure Profile

The figures (5.43) and (5.44) show comparisons between the experimental and numerical results. It can be observe that the behavior of the numerical results was similar to the experimental results. Also, it was observed that the values of experimental and numerical results were close and the maximum deviation was (9%).

Figure (5.43) demonstrates the comparison between the effect of increasing water discharge on the experimental and numerical results of the pressure profile at four different points along the vertical testing channel with convergence angle 10 degrees for various values of air discharges (5.833,8.333,10.833,13.333 and 16.666) L/min. Figure (5.44) shows the comparison between the effect of increasing water discharge on the experimental and numerical results of the pressure profile at four different points along the inclined testing channel with convergence angle 10 degrees for various values of air discharges (5.833, 10.833 and 16.666) L/min.

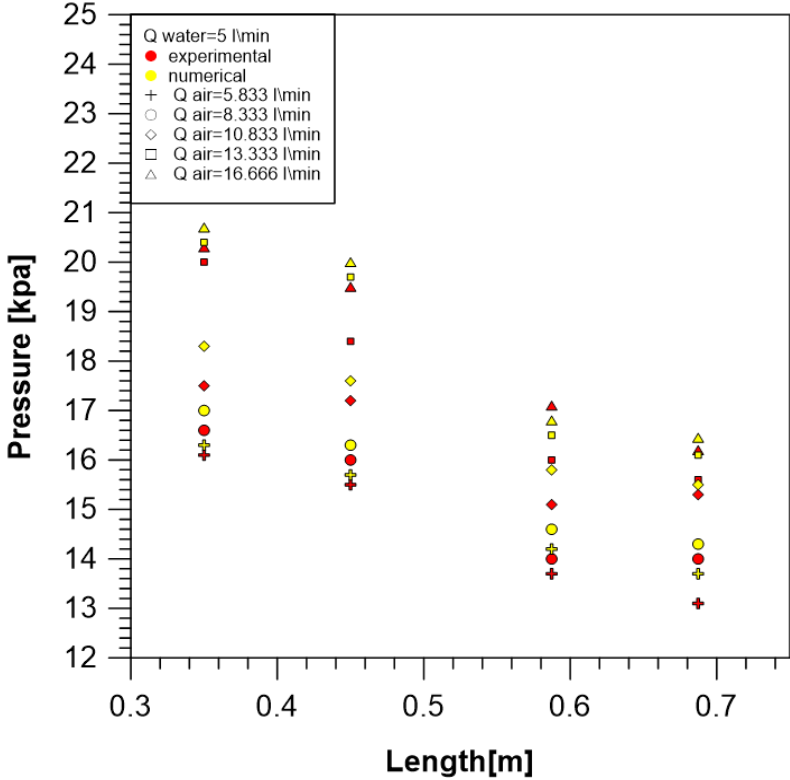


Figure (5.43a)

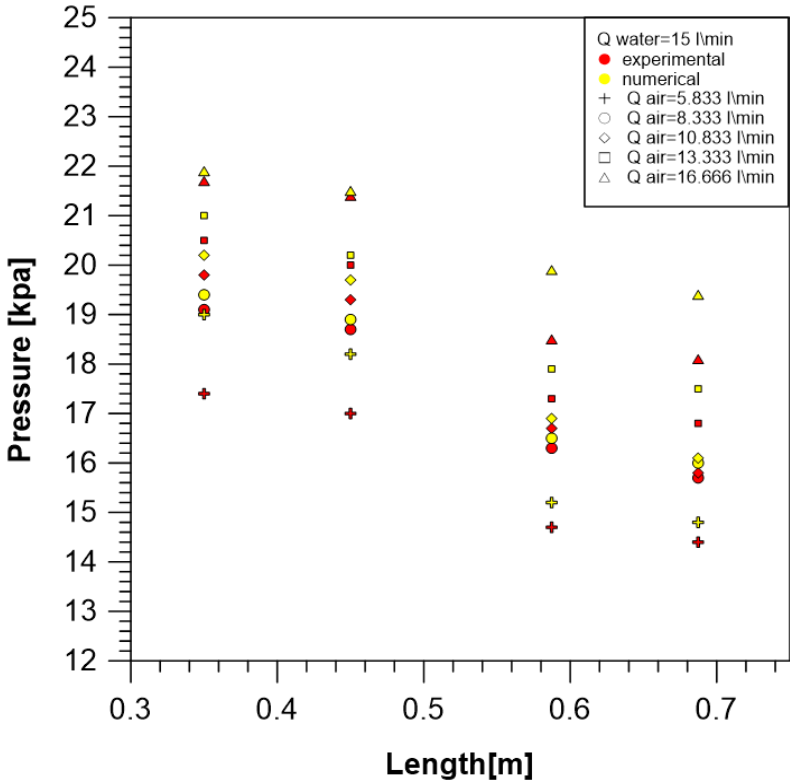


Figure (5.43b)

Figure (5.43): Compression between effect water discharge on experimental and numerical pressure profile for convergence angle 10 degree (vertical)

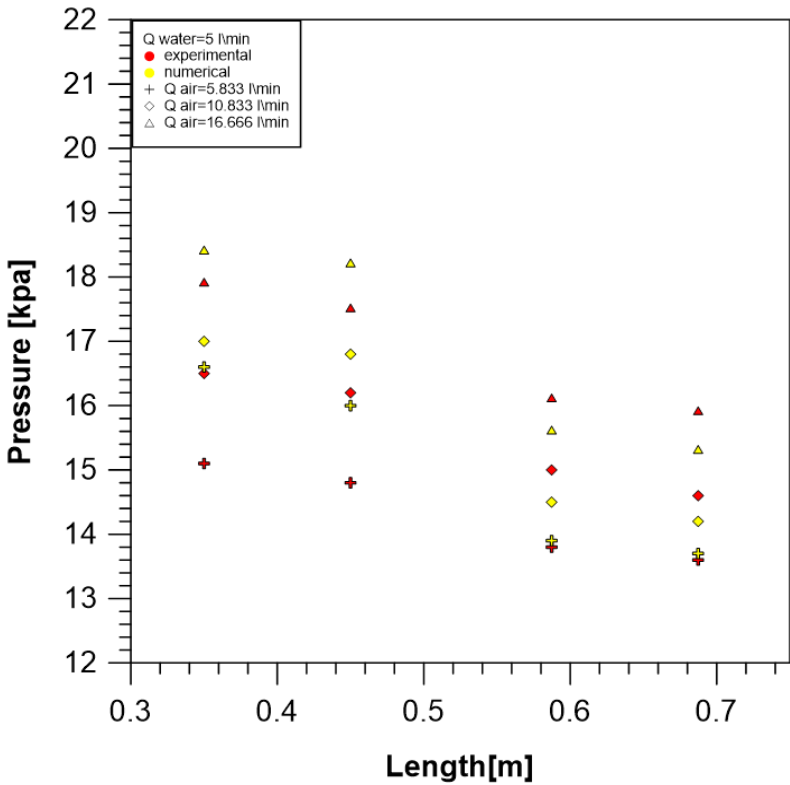


Figure (5.44a)

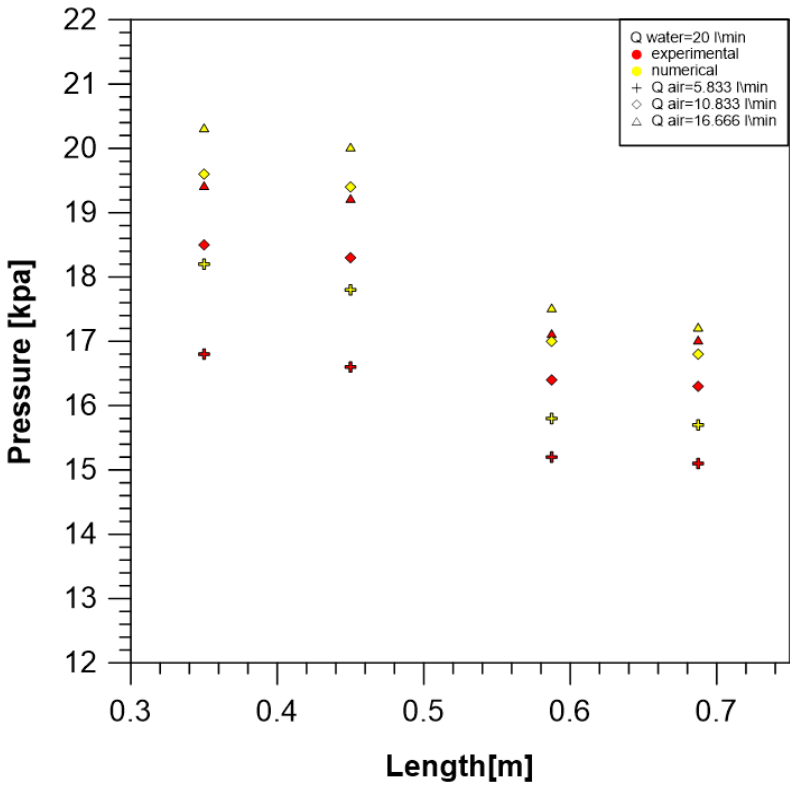


Figure (5.44b)

Figure (5.44): Compression between effect water discharge on experimental and numerical pressure profile for convergence angle 10 degree (inclined)

5.3.3. B. The influence of water and air discharge on the flow behavior

The figures from (5.45) to (5.48) show the experimental flow behavior through the photographs that were taken for ribs convergence section and numerical simulation. When a visually comparison made between the photos of air volume fraction that obtained from the experimental work and the images of air volume fraction that obtained from ANSYS 18, it was found a close similarity between them.

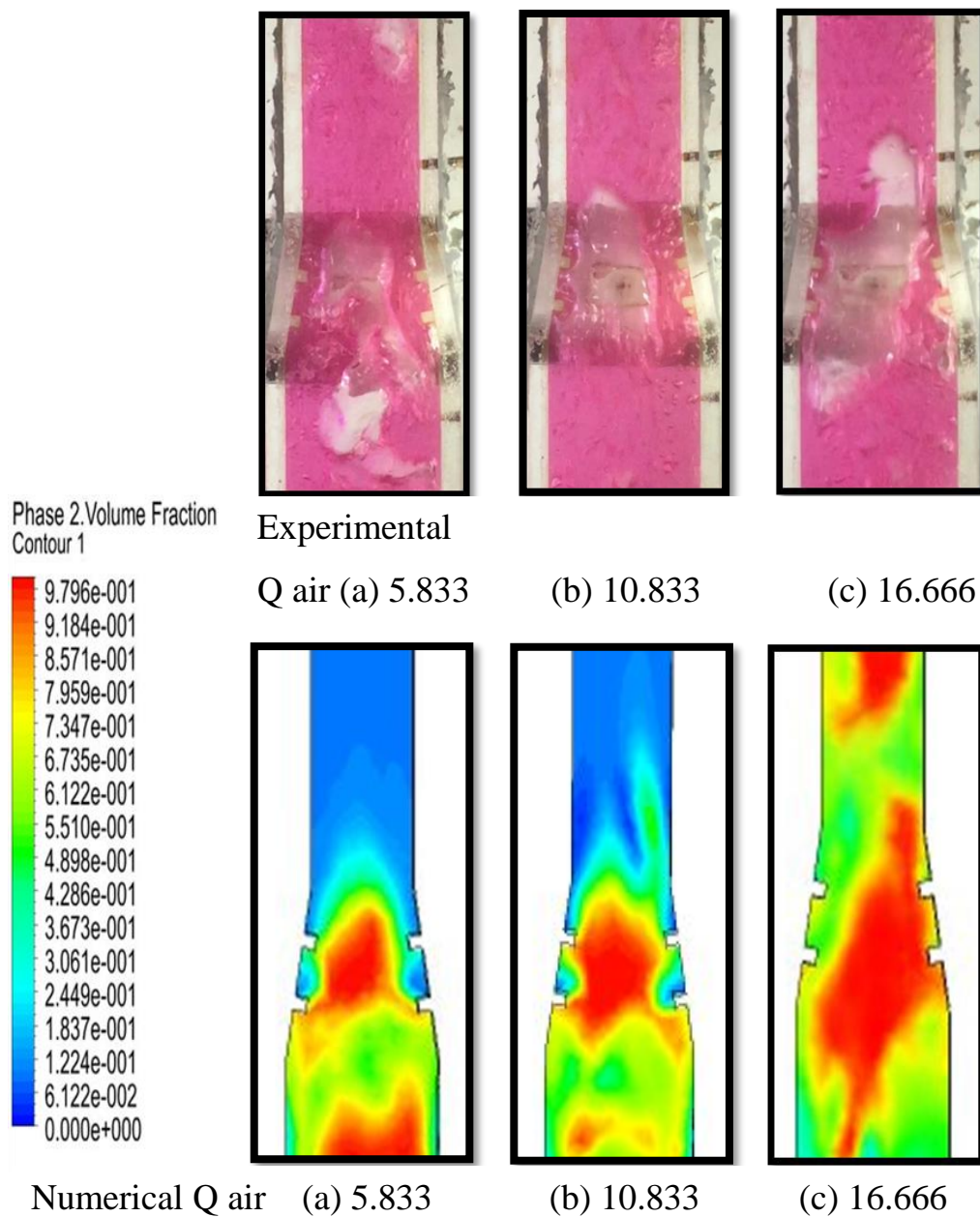
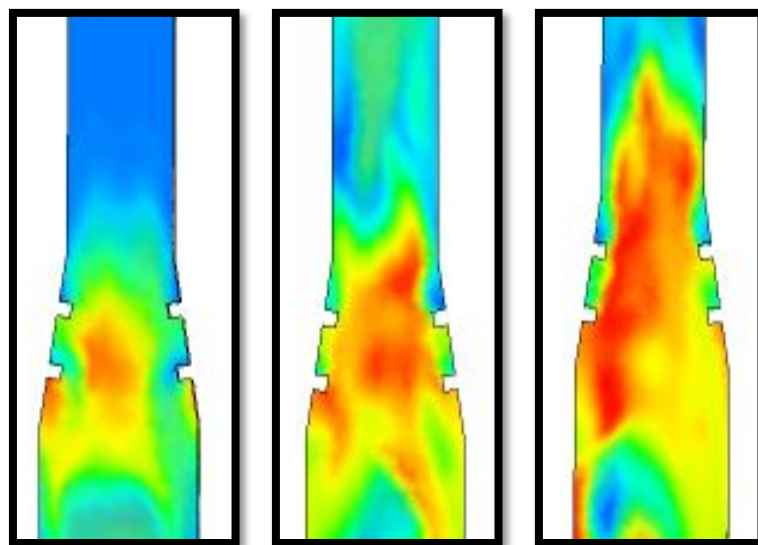
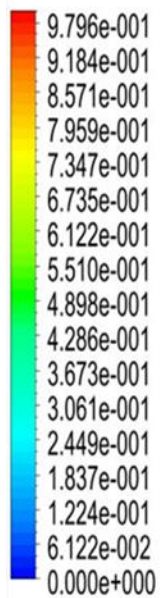


Figure (5.45) Comparison between the experimental and numerical effect of air discharge on the flow behavior at Q water =5 L/min



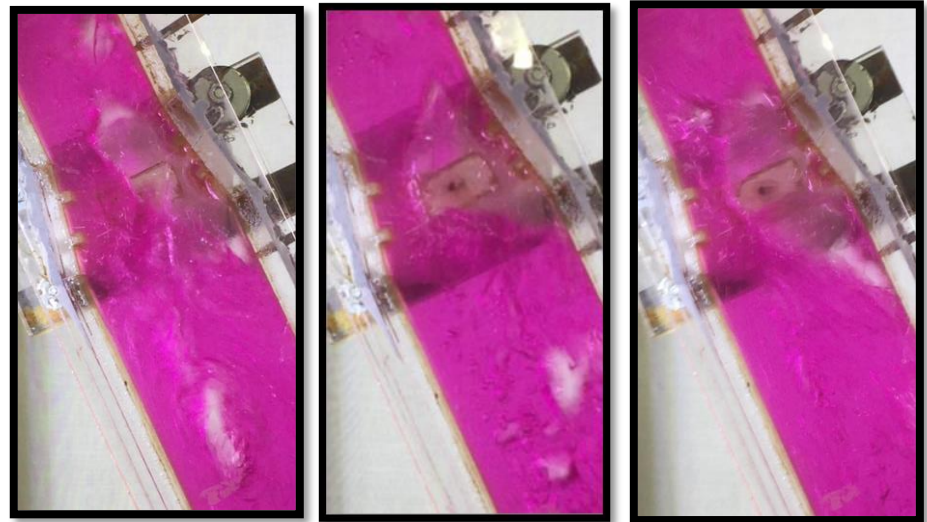
Experimental Q air (a) 5.833 (b) 10.833 (c) 16.666

Phase 2. Volume Fraction
Contour 1



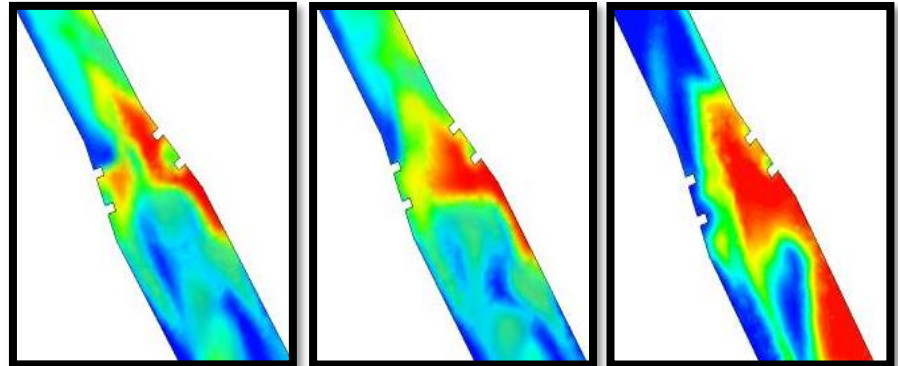
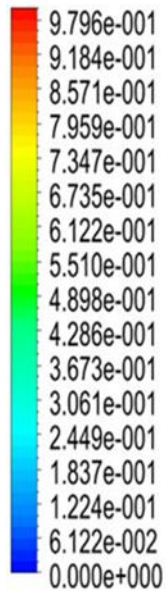
Numerical Q air (a) 5.833 (b) 10.833 (c) 16.666

Figure (5.46) Comparison between the experimental and numerical effect of air discharge on the flow behavior at $Q_{\text{water}} = 20 \text{ L/min}$



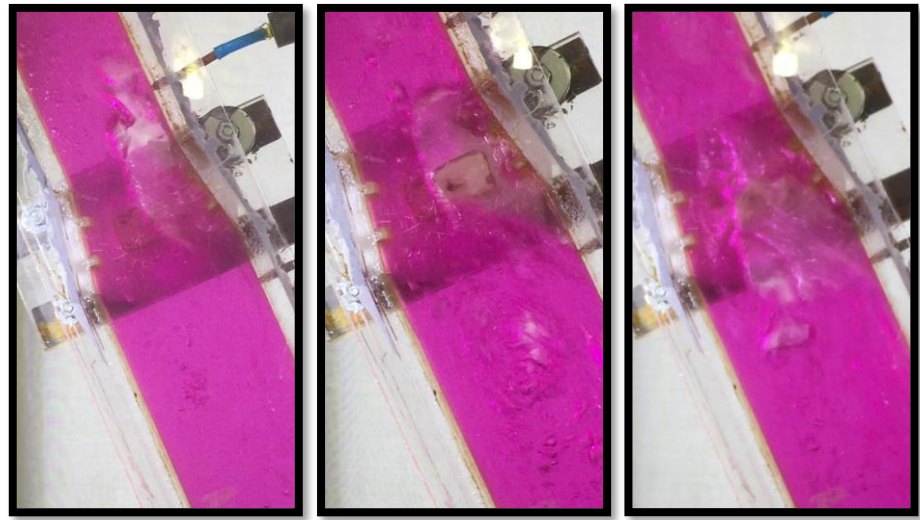
Experimental Q air (a) 5.833 (b) 10.833 (c) 16.666

Phase 2 Volume Fraction
Contour 1



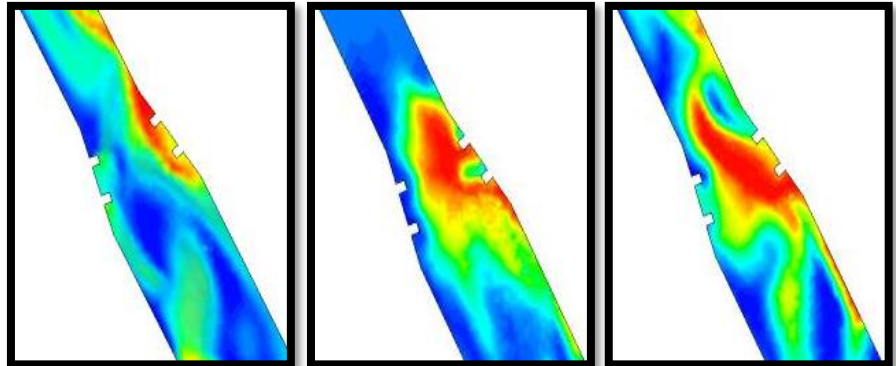
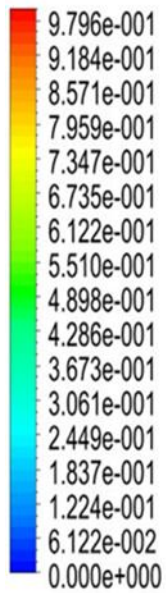
Numerical
Q air (a) 5.833 (b) 10.833 (c) 16.666

Figure (5.47) Comparison between the experimental and numerical effect of air discharge on the flow behavior at Q water =5 L/min



Experimental Q air (a) 5.833 (b) 10.833 (c) 16.666

Phase 2. Volume Fraction
Contour 1



Numerical

Q air (a) 5.833 (b) 10.833 (c) 16.666

Figure (5.48) Comparison between the experimental and numerical effect of air discharge on the flow behavior at Q water =20 L/min

5.4. Numerical Study of the Effect of Ribs on the Pressure Recovery

A numerical study was carried out to show the effect of ribs on the pressure recovery across the divergence section. A case was studied with ribs and without ribs as shown in figures (5.49) and (5.50).

Figure (5.71) represents the case of the flow through the divergence section with opening angle 10 and the air and water discharge were 5 L/min and 16.666 L/min with the absence of ribs. While figure (5.72) represents the flow within the same divergence section and same discharge of air and water with the presence of ribs. We noted that the values of the recovery of pressure across the divergence section without ribs are higher than the case with ribs. Where the pressure increased in the case without ribs from 17.2 kpa to 22 kpa. While in the case with ribs, the pressure increased from 17.3 kpa to 21.7 kpa because more vortexes occur as a result of the presence of ribs that led to reduce the pressure as shown in figures (5.51) and (5.52).

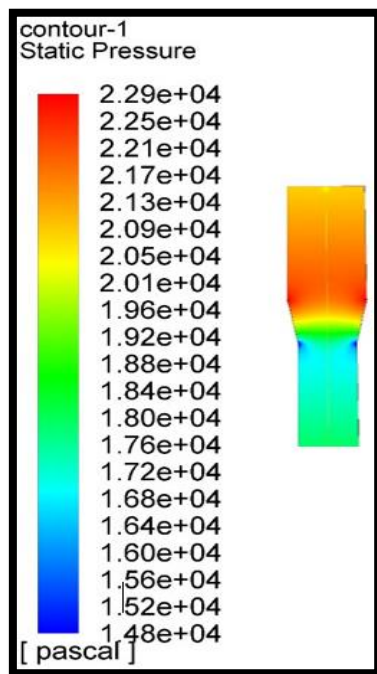


Figure (5.49)
Divergence section without ribs

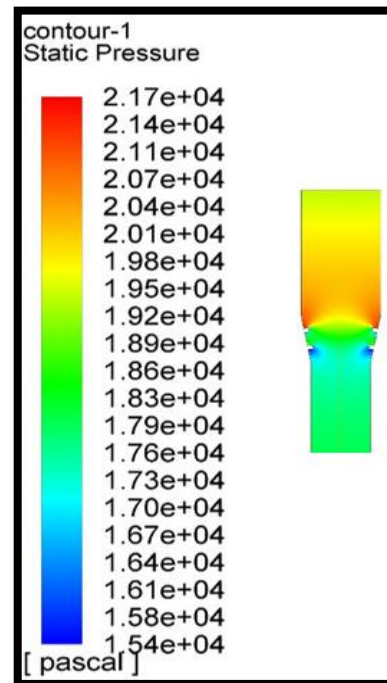


Figure (5.50)
Divergence section with ribs

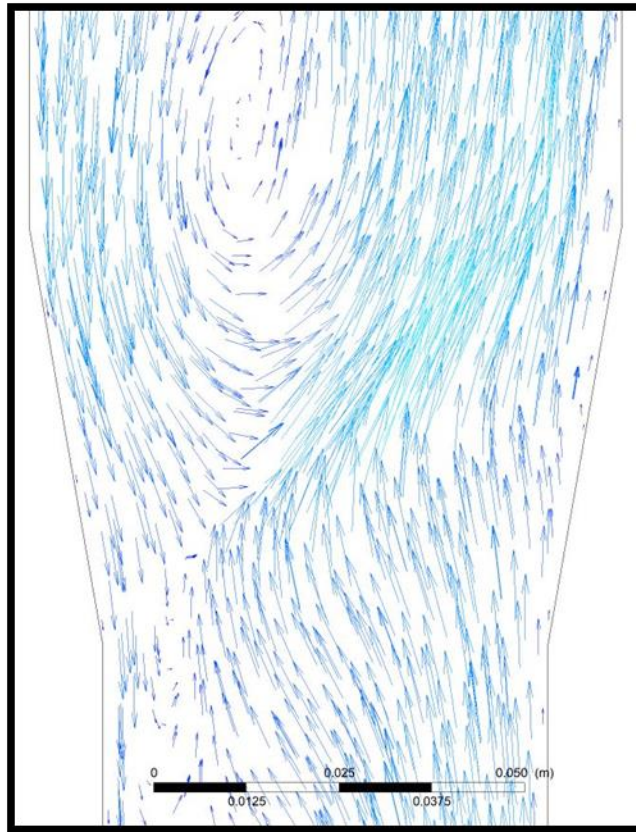


Figure (5.51): Velocity vector at divergence section without ribs

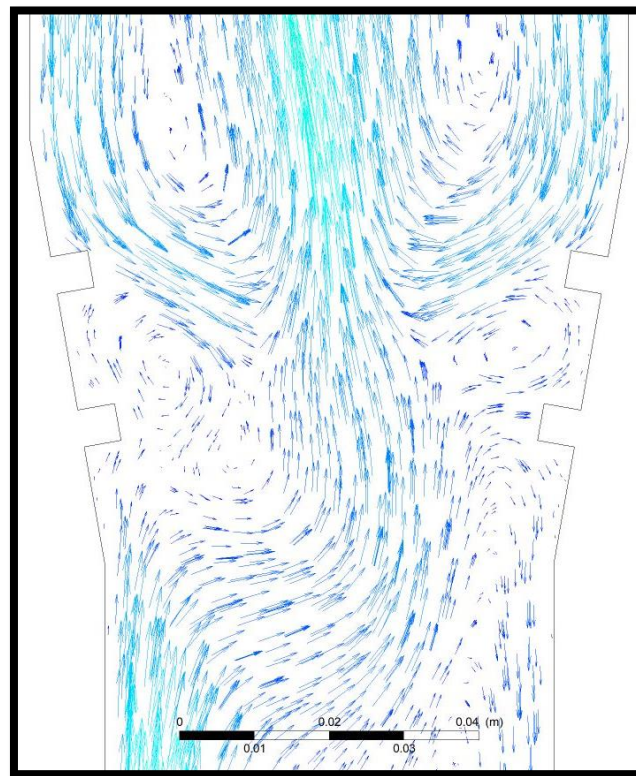


Figure (5.52): Velocity vector at divergence section without ribs

CHAPTER SIX

**CONCLUSIONS AND
SUGGESTION**

Conclusions and Suggestions

6.1 Conclusions

This work presented an experimental and numerical study of two-phase flow in the divergent\convergent rectangular duct. One hundred and sixteen experiments test were performed. The following conclusions can be drawn from this work:

1. The opening divergent angle has a direct proportional influence on the recovery pressure through the divergent section. While the convergent angle has an inversely proportional influence on the drop pressure through the convergent angle.
2. When air discharge increase, the volume and amount of bubbles increases. In addition, as the continuous air discharge increase, the flow turbulence increases so as the velocity of generating eddies.
3. The volume of bubbles decreases when water discharge increase. Also, as continuous water discharge increases, the flow became more turbulent and unstable and eddies became stronger.
4. The effect of increasing the water discharge on the turbulence is higher than the effect of increasing the air discharge because the water density is higher and, thus, its inertia force is greater.
5. The simulated model has given results similar to the experimental results with a maximum deviation of (9) %.
6. The ribs increase the flow disturbance, thus they affect the pressure recovery, so the pressure recovery value was reduced by 8.333%.

6.2 Suggestions for Future Works

For future work, the following suggestions are summarized:

1. Study the effect of using other types of fluid such as oil on the pressure and the behavior of flow.

2. Using a channel with sudden divergence and compare between them to show the influence on recovery pressure.
3. Direct the flow downward in a vertical and inclined direction and make a comparison between them to show the influence on pressure profile and flow behavior.
4. Using channel with a divergent/convergent section with three phases (solid-liquid-gas), and study the effect on the pressure profile and flow behavior.

References

References

References

- [1] A. J. Ghajar, "Non-boiling heat transfer in gas-liquid flow in pipes: a tutorial," *J. Brazilian Soc. Mech. Sci. Eng.*, vol. 27, no. 1, pp. 46–73, 2005.
- [2] V. G. Kourakos, P. Rambaud, S. Chabane, D. Pierrat, and J. M. Buchlin, "Two-phase flow modelling within expansion and contraction singularities," pp. 27–43, 2009.
- [3] Naji A. S., "Study of Two-phase Flow in Horizontal and Inclined Pipes," M.Sc Thesis, Al-Mustansireyah University, 2000.
- [4] M. R. Ansari and B. Arzandi, "Two-phase gas-liquid flow regimes for smooth and ribbed rectangular ducts," *Int. J. Multiph. Flow*, vol. 38, no. 1, pp. 118–125, 2012.
- [5] E. C. Rogero, "Experimental Investigation of Developing Plug and Slug Flows," M.Sc Thesis, University of München, 2009.
- [6] A. Oyewole, "STUDY OF FLOW PATTERNS AND VOID FRACTION IN INCLINED TWO PHASE FLOW," M.Sc Thesis, University of Ilorin, 2013.
- [7] D. Barnea, O. Shoham, Y. Taitel, and a. E. Dukler, "Flow pattern transition for gas-liquid flow in horizontal and inclined pipes. Comparison of experimental data with theory," *Int. J. Multiph. Flow*, vol. 6, no. 3, pp. 217–225, 1980.
- [8] G. F. Hewitt and D. N. Roberts, "Studies of Two-Phase Flow Patterns by Simultaneous X-Ray and Flash Photography," AERE-M 2159, HMSO, p. Medium: X; Size: Pages: 28, 1969.
- [9] Hernandez-Perez V. , Zangana M., Kaji R. and Azzopardi B.J., "Effect of Pipe Diameter on Pressure Drop in Vertical Two-Phase Flow," 7th Int. Conf. Multiph. Flow, 2010.
- [10] Thome J.R., *Wolverine Engineering Data Book*", a data book, Wolverine Tube Inc. Engineering Thermal innovation, Third Edit. 2010.
- [11] J. Xu, "Experimental study on gas-liquid two-phase flow regimes in rectangular channels with mini gaps," *Int. J. Heat Fluid Flow*, vol. 20, no. 4, pp. 422–428, 1999.
- [12] Noora Abdalwahid Hashim, "Experimental and Theoretical Investigation for Non-Boiling Two-Phase Flow in Vertical Pipe," M.Sc Thesis, University of Babylon, 2013.

References

- [13] Lockhart, R.W., and Martinelli, “Proposed Correlation of Data for Isothermal Two-Phase, Two-Component Flow in Pipes,” Chem. Eng. Prog. Symposium Ser., vol. 45, no. 1, pp. 39–48, 1949.
- [14] Müller-Steinhagen. H., Heck. K., “A Simple Friction Pressure Drop Correlation for Two-Phase Flow in Pipes,” J. Chem. Eng. Process, vol. 20, pp. 297–308, 1986.
- [15] S. Anupriya, S. Jayanti, “Experimental and modelling studies of gas–liquid vertical annular flow through a diverging section,” Int. J. Multiph. Flow, vol. 67, pp. 180–190, 2014.
- [16] A.Brankovic and I. G. Currie, “Turbulent Two-Phase Flow Through a Sudden Pipe Expansion: LDA Experiments and CFD Predictions,” Int. J. Comput. Fluid Dyn., no. 2013, pp. 37–41, 2007.
- [17] Y. Koichi, K., Kenji, “Flow patterns of gas-liquid two-phase flow in round tube with sudden expansion,” Proceeding ICONE10, USA, pp. 14–18, 2002.
- [18] A. Behzadi, R. I. Issa, and H. Rusche, “Modelling of dispersed bubble and droplet flow at high phase fractions,” Chem. Eng. Sci., vol. 59, no. 4, pp. 759–770, 2004.
- [19] I. M. Sakr, A. Balabel, K. Ibrahim, and S. El-kom, “Computations of Upward Water / Air Fluid Flow in,” vol. 4, pp. 193–213, 2013.
- [20] A. Ahmadpour, S. M. A. Noori Rahim Abadi, and R. Kouhikamali, “Numerical simulation of two-phase gas-liquid flow through gradual expansions/contractions,” Int. J. Multiph. Flow, vol. 79, pp. 31–49, 2016.
- [21] E. M. Abed and R. S. Al-turaihi, “Experimental Investigation of Two-Phase GAS- Liquid Slug Flow Inclined Pipe,” J. Babylon Univ., no. 5, pp. 1579–1591, 2013.
- [22] A. S. Naji, “Liquid Holdup Correlation for Inclined Two-Phase Stratified Flow in Pipes,” Kufa J. Eng., vol. 1, no. 1, pp. 1–15, 2009.
- [23] A. E. Taitel, Y., and Dukler, “A Theoretical Approach to the Lockhart-Martinelli Correlation for Stratified Flow,” Int. J. Multiph. Flow, vol. 2, pp. 591–595, 1976.
- [24] V. Kumar, “NUMERICAL STUDY OF OIL-WATER TWO PHASE FLOW IN HORIZONTAL & INCLINED TUBES,” M.Sc Thesis, Indian Institute of Technology, 2014.
- [25] F. Aloui and M. Souhar, “Experimental study of a two-phase bubbly

References

- flow in a flat duct symmetric sudden expansion - Part 1: Visualization, pressure and void fraction,” *Int. J. Multiph. Flow*, vol. 22, no. 4, pp. 651–665, 1996.
- [26] F.F. Abdelall, G. Hahn, S.M. Ghiaasiaan, S.I. Abdel-Khalik, S.S. Jeter, M. Yoda and G.W., “Pressure drop caused by abrupt flow area changes in small channels,” *Exp. Therm. Fluid Sci.*, vol. 29, no. 4, pp. 425–434, 2005.
- [27] A. Mugardich, “Studying the effect of mixing ratio on two phase flow in horizontal tube,” M.Sc Thesis, University Of Technology, 2007.
- [28] I. Y. Chen, M. C. Chu, J. S. Liaw, and C. C. Wang, “Two-phase flow characteristics across sudden contraction in small rectangular channels,” *Exp. Therm. Fluid Sci.*, vol. 32, no. 8, pp. 1609–1619, 2008.
- [29] C. C. Wang, C. Y. Tseng, and I. Y. Chen, “A new correlation and the review of two-phase flow pressure change across sudden expansion in small channels,” *Int. J. Heat Mass Transf.*, vol. 53, no. 19–20, pp. 4287–4295, 2010.
- [30] M. Ahmed, W. H., Ching, C. Y., and Shoukri, “Pressure recovery of two-phase flow across sudden expansions,” vol. 33, pp. 575–594, 2007.
- [31] W. H. Ahmed, C. Y. Ching, and M. Shoukri, “Development of two-phase flow downstream of a horizontal sudden expansion,” *Int. J. Heat Fluid Flow*, vol. 29, no. 1, pp. 194–206, 2008.
- [32] T. K. and M. I. Takashi OKE, “Flow Patterns of Gas-Liquid Two-phase Flow through an Abrupt Expansion in Millimeter-Scale Rectangular Channel,” *J. JSEM*, vol. 1, no. 2, pp. 131–139, 2011.
- [33] N. Eskin and E. Deniz, “Pressure Drop of Two-Phase Flow through Horizontal Channel with Smooth Expansion,” *Int. Refrigeration Air-Conditioning Conf.*, pp. 1–10, 2012.
- [34] S. K. Roul, M. K., and Dash, “Two-phase pressure drop caused by sudden flow area contraction /expansion in small circular pipes,” *Int. J. Num. Methods Fluids*, vol. 66, pp. 1420–1446, 2011.
- [35] T. Abadie, J. Aubin, D. Legendre, and C. Xuereb, “Hydrodynamics of gas-liquid Taylor flow in rectangular microchannels,” *Microfluid. Nanofluidics*, vol. 12, no. 1–4, pp. 355–369, 2012.
- [36] E. Deniz and N. Eskin, “Numerical analysis of adiabatic two-phase flow through enlarging channel,” *Proc. 24th Int. Conf. Effic. Cost*,

References

- Optim. Simul. Environ. Impact Energy Syst. ECOS 2011, 2011.
- [37] Richard S. Figliola and Donald E. Beasley, Theory and Design for Mechanical Measurements, Fifth Edit. Clemson University, 2011.
- [38] ANSYS, “ANSYS Fluent in ANSYS Workbench User's Guide”, ANSYS, Inc., Release 15.0, November 2013.
- [39] Bakker A., “Applied computational fluid dynamics, mesh generation”, Computational fluid dynamics lectures, 2002-2006.
- [40] Ansys 15.0 Help, Fluent Theory Guide, V.O.F Multiphase Model.
- [41] D. Barnea, O. Shoham and Y. Taitel, “GAS-LIQUID FLOW IN INCLINED TUBES: FLOW PATTERN TRANSITIONS FOR UPWARD FLOW,” Chem.Eng. Sci., vol. 40, pp. 131–134, 1985
- [42] Holman, J.P., and Gajda, W.J., “Experimental Methods for Engineers” , Text Book, McGraw-Hill Book Company, Fourth Edition, 1984.

APPENDIX A

Appendix A

Gas Flowmeter Calibration

Orifice meters are type of differential meters, all of which infer the rate of gas flow by measuring the pressure difference across a deliberately designed and installed flow disturbance. A standard designed orifice is used to calibrate the gas flow meter since it is easy to field-service and have no moving parts. An orifice meter is a conduit and a restriction to create a pressure drop. It consists of a straight length pipe of 50cm; inside it a central orifice of 14 mm inlet diameter and 45mm outlet diameter is located; which creates a pressure drop, thereby affecting the flow. The pressure deference entered in an equation to compute the air flow rate and compared it with the one measured by the flow meter[42].

$$\dot{V}_{\text{theory}} = V_2 A_2 = \frac{A_2}{\sqrt{1 - \frac{A_2}{A_1}}} \sqrt{\frac{2(\Delta P)_G}{\rho_G}} \quad \text{-----(1)}$$

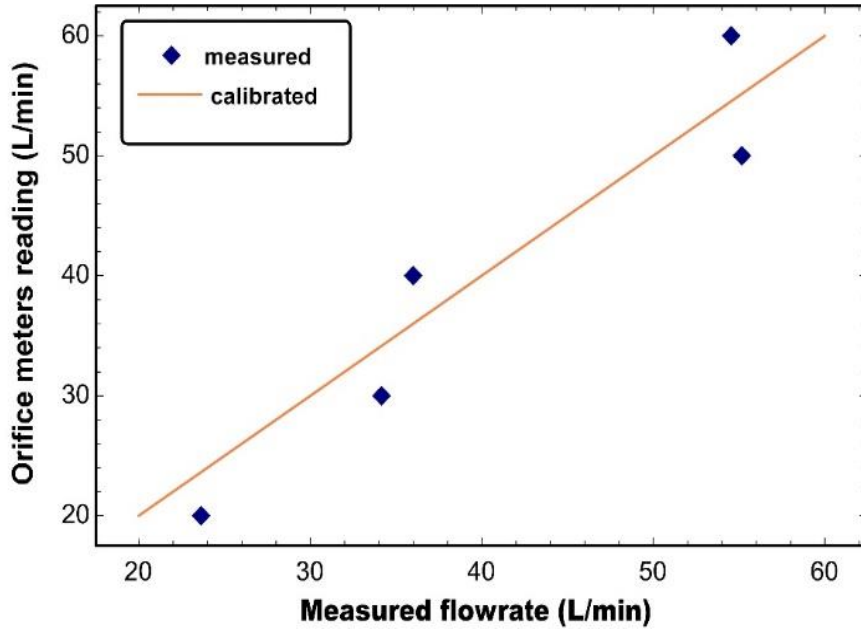
The computed error is $\pm 6\%$ which is giving the following gas flow meter calibration equation:

$$\dot{V}_{\text{flowmater}} = 0.96 V_{\text{orifice}} \quad \text{-----(2)}$$

Relation between orifice meter reading and that measured by gas flow meter was a polynomial equation used to correct the flowrate readings. as shown in figure below.

$$\dot{V}_{\text{calib}} = 49.416 - 3.0299\dot{V}_{\text{re}} + 0.1079\dot{V}_{\text{re}}^2 - 0.0009\dot{V}_{\text{re}}^3 \quad \text{-----(3)}$$

Appendix A



calibration of the gas flow meter

APPENDIX B

Appendix B

For the error analysis calculation, the pressure reading were repeated for four attempts for each sensor. The standard deviation and mean standard deviation were calculated as follows:

$$\sigma = \sqrt{\frac{\sum_1^n (x_i - \bar{x})^2}{n - 1}} \quad , \quad \sigma_m = \frac{\sigma}{\sqrt{n}}$$

Where σ is the standard deviation , σ_m is the mean standard deviation ,

x_i is the values of reading of pressure, \bar{x} is the mean of values of reading of pressure, n is the number of reading of pressure.

As the true value (x) was also calculated by

$$x = \bar{x} \pm \sigma_m$$

For pressure sensor (1) ,the pressure values were (14.7,14.4,14.1,15.1) kpa.

So ,the mean of this values is 14.57 kpa.

The the standard deviation is calculate by:

$$= \sqrt{\frac{(14.7-14.57)^2 + (14.4-14.57)^2 + (14.1-14.57)^2 + (15.1-14.57)^2}{4-1}}$$

$$=0.427$$

$$\sigma_m = \frac{0.427}{\sqrt{4}} = 0.213$$

And the true value (x) =14.57 \pm 0.213=14.783 , -14.357

$$\text{The percentage uncertainty} = \frac{14.783-14.57}{14.783} * 100\% = 1.44 \%$$

=

$$\frac{14.357-14.57}{14.357} * 100\% = -1.48 \%$$

Appendix B

As well as with other sensors. The Table below displays the shows the percentage uncertainty values of each of the four pressure sensors.

NO.Pressure sensors	Values of reading of pressure	X_m	σ	σ_m	X	percentage uncertainty %
P ₁	14.7 14.4 14.1 15.1	14.57	0.427	0.213	14.6 -14.3	1.44 -1.48
P ₂	14.2 14 13.8 14.7	14.17	0.386	0.193	14.3 -13.9	1.34 -1.38
P ₃	16 15.7 15.3 16.7	15.9	0.591	0.296	16.2 -15.6	1.85 -1.92
P ₄	15.6 15.1 14.6 15.8	15.27	0.537	0.268	15.538- 15	1.72 -1.8

الخلاصة

تم دراسة الجريان ثنائي الطور في قناة مستطيلة تحتوي على مقطع متباعد/متقارب يحتوي على مضلعات وتمت الدراسة بحالتين للجريان: جريان تصاعدي عمودي ومائل. تم استخدام الهواء والماء كمواد لتحقيق جريان ثنائي الطور. تم إجراء دراسة عملية وعددية لاختبار تأثير زيادة تصريف الهواء والماء على توزيع الضغط على طول قناة الاختبار وتأثيره على فرق الضغط عبر مقطع التباعد/التقارب وكذلك دراسة تأثير زيادة زاوية التباعد/التقارب على فرق الضغط عبر المقطع. كل البيانات العملية في هذه الدراسة تم الحصول عليها باستخدام محولة ضغط والمشاهدة البصرية باستخدام كاميرة فيديو. التصاريح المستخدمة للماء الداخل تتراوح من (5-20 L/min)، و تصاريح الهواء بين (5.833-16.666 L/min). تم استخدام قناتي اختبار بزوايا توسع/تقلص 10 و 15 درجة). بينت النتائج ان الضغط على طول القناة يزداد مع زيادة تصريف الهواء او الماء. بالنسبة للمقطع المتباعد نلاحظ انه عندما تزداد زاوية الانفتاح فأن قيمة استرجاع الضغط يقل بينما في حالة المقطع المتقارب فأن هبوط الضغط يزداد مع زيادة زاوية التقارب للمقطع. تم عمل محاكاة CFD لنموذج ثلاثي الابعاد باستخدام برنامج ANSYS FLUENT 18 الذي يعتمد على شرط حدود الدخول التي يتم اخذها من الجانب العملي والمحكومة بمعادلات Volume of Fluid (VOF) لنموذج اويلر للجريان متعدد الأطوار موديل الاضطراب هو RNG. الدراسة العددية أجريت لدراسة تأثير المضلعات على سلوك الجريان واسترجاع الضغط. في حالة عدم وجود المضلعات، لوحظ ان قيمة استرجاع الضغط عبر مقطع التوسع كان اعلى من حالة وجود المضلعات بنسبة (8.333%). لوحظ تطابق بين قيم النتائج العملية و النظرية للضغط و اعلى معدل انحراف كان (9 %)، كذلك لوحظ تشابه في سلوك الجريان بين الجانب العملي و النظري.



جمهورية العراق
وزارة التعليم العالي والبحث العلمي
جامعة كربلاء - كلية الهندسة
قسم الهندسة الميكانيكية

دراسة تجريبية وعددية لجريان ثنائي الطور في قناة توسعية/تقلصية مستطيله مضلعة

رسالة مقدمة الى كلية الهندسة - جامعة كربلاء كجزء من متطلبات نيل درجة ماجستير
علوم في الهندسة الميكانيكية

من لدن

علي عبد الائمة حسن

بأشراف

أ.م.د. عباس ساهي شريف

أ.د. رياض صباح الطريحي